OBSERVATIONS ON HEALING TISSUE: A COMBINED LIGHT AND ELECTRON MICROSCOPIC INVESTIGATION

By W. J. CLIFF

The Sir William Dunn School of Pathology, Oxford

(*Communicated by Sir Howard Florey, P.R.S.—Received 25 October 1962*)

[Plates 26 to 48]

CONTENTS

1. The process of healing in the rabbit ear chamber has been investigated in detail by correlating light microscopy, mainly *in vivo*, and electron microscopy.

2. During healing new vessels are formed from existing vessels by a process of sprouting and anastomosis, with subsequent remodelling of the loops so formed.

3. The fundamental process in the formation of vessels by sprouting is the mitotic division of existing endothelium, during which it retains its characteristic properties.

4. Blood vessel sprouts are composed of strands of tightly apposed cells formed in continuity with the walls of existing vessels. The subsequent canalization of such strands takes place extracellularly by a series of events largely as described by Billroth (1856).

5. The endothelium of recently formed vessels has a fine structure which distinguishes it clearly from that of more mature vessels. Certain features of this structure are compatible with a secretory activity by the endothelium during the formation of new vessels.

6. Evidence was obtained that in the course of differentiation of recently formed vessels fibroblast-like cells are incorporated into vessel walls to become adventitial cells, and that adventitial cells may undergo conversion to vascular smooth muscle cells.

7. Lymphatic endothelium exhibits properties during regeneration that confirm the specificity of this form of endothelium.

8. Cells with the characteristic fine structure of fibroblasts were frequently found in mitosis. The fibroblasts in the regions of active fibrogenesis had a highly developed cisternal form of endoplasmic reticulum. Vesicles and corresponding caveolae identifiable in such fibroblasts may provide a communication between the endoplasmic reticulum and the sites of fibrogenesis at the external surfaces of the cells.

9. Cells sharing characteristic features of fine structure formed a series which grouped together the monocyte, macrophage and foreign body giant cell.

10. Highly fibrillary intracytoplasmic tracts were found in both fibroblasts and macrophages. These tracts were equated with the fibroglial fibres of light microscopy.

Vol. 246. B. 733. (Price £2. 2*s*.; U.S. $6.30) 38 [Published 25 July 1963

11. 'Clear spaces' in advance of the growing fringe of blood vessels were temporary structures lined by a pavement of mesothelium-like cells.

12. No evidence was found of the formation of primitive mesenchymal tissue during healing in the mammal.

Introduction

This paper reports a morphological study of the process of healing in rabbit ear chambers (Sandison 1924; Clark, Kirby-Smith, Rex & Williams 1930) by both light and electron microscopy.

Experimental

'Half-lop' rabbits bred and maintained in the Sir William Dunn School of Pathology were used. The weights of the animals at the time of insertion of the ear chambers ranged from 2·6 to 3·5 kg. Before and after operation the rabbits were fed rabbit pellet diet No. 18 (Oxo Ltd) and were allowed water *ad libitum*.

Insertion of chambers. The ear chambers used resembled the castle-top chambers described by Sanders, Dodson & Florey (1954). The majority had a plain table with no removable pin. The bolts were of tantalum instead of zirconium. The technique for the insertion of the chambers was based on that described by Ebert, Florey & Pullinger (1939). No splints were used on the ears as they are not necessary with half-lop rabbits. Altogether 42 chambers were examined.

Examination of chambers. Each chamber was examined frequently in the living animal with the light microscope using bright field illumination and objectives ranging up to the $\frac{1}{12}$ in. oil immersion. Crossed polarized filters were employed to detect anisotropic collagen bundles. The ear was held on the microscope stage as described by Sanders *et al.* (1954).

Mensuration of repair tissue. The area of growth in each chamber was measured by taking photomicrographs at 2-day intervals (3-day intervals over week-ends). The area of repair tissue present at a particular time was calculated by tracing from the photomicrograph the outline of the tissue and then either transferring to squared paper and counting the squares, or transferring to paper of known weight per unit area and cutting out and weighing. In 14 chambers the thickness of repair tissue was measured by using the fine focus adjustment of the microscope (which had been calibrated previously) to obtain six values for the apparent depth of the tissue. From the mean of these six values the real depth was calculated by assuming that the refractive index of the repair tissue was similar to that of water, namely 1·33.

Injection of particles. In one rabbit colloidal graphite (Hydrokollag) was injected intravenously 13 min before chambers in both ears were fixed and removed. Four other rabbits were injected with 2·0 ml. of a thorium preparation (Thorotrast) intravenously once weekly to a total dose of 12 ml.

Fixation of tissue. The tissue in the chamber was fixed and removed with the animal under pentobarbitone sodium (Nembutal) anaesthesia. During the manipulations the ear chamber was held and transilluminated as for *in vivo* microscopy.

First the three nuts retaining the coverslip were gradually and evenly loosened and removed. Using the microscope for observation, a fine hypodermic needle attached to a

2·0 ml. syringe containing fixative solution was gently insinuated between the coverslip and the underlying tissue and its point advanced to lie near the repair tissue on the table of the chamber. Fixative was then gently injected until it was seen to flood completely over the table area, when the ear was immediately clamped near its base to stop all circulation. The lid was then removed, the tissue being gently irrigated with fixative solution to prevent drying. A small square of cartilage containing the circle of chamber tissue was then quickly dissected out and placed in the fixative.

The fixative solutions used were Helly's solution and mercuric-formaldehyde for light microscopy and osmium tetroxide solution buffered to pH 7·3 to 7·4 (Palade 1952) with added sucrose (Caulfield 1957) for electron microscopy. The osmium tetroxide solution was used at about 4 °C and when it was injected by syringe the operator's eyes were protected by goggles. Fixation for electron microscopy lasted for approximately 1 h at 4 °C.

Tissue for light microscopy was embedded in ester wax (Estax, Watford Chemical Co.), and sections were cut 4 to 5 micrometres (μm) thick. Tissue for electron microscopy was embedded in methacrylate (85 parts of *n*-butyl methacrylate to 15 parts of *n*-methyl methacrylate), in Araldite (Ciba Ltd, Duxford) after the long method of Glauert & Glauert (1958), and in an epoxy resin (Epikote resin 812, Shell Chemical Co.) after the method of Luft (1961). Polymerization was in all cases carried out by heating.

Preparation of electron micrographs. The orientation of the small blocks of tissue obtained from the ear chambers was of cardinal importance in the interpretation of the appearances of the sections cut from them.

At the 95 % ethanol stage of dehydration the tissue was placed on a small square of polyethylene sheet in 95 % ethanol in a Petri dish. All the ear cartilage was cut away, and using a small hand lens ($\times 10$) the disk of chamber tissue was cut whenever possible into six wedge-shaped blocks. These very small blocks were handled with a wide bore Pasteur pipette made from acid-cleaned glass.

When the blocks were embedded in polymerized plastic their patterns of vessels were examined with the hand lens and the particular segments that they represented were identified and marked on photomicrographs taken of the living tissue. The tip of the plastic block containing the tissue was then cut off by a sharp blow on the back of a scalpel held firmly in position. The tip containing the tissue was then trimmed, oriented and refixed to the plastic stem by a drop of the liquid plastic which was subsequently polymerized. Thus features of interest noted *in vivo* could be examined with the electron microscope.

In this way it was possible to know with certainty that the fringe of growing vessels was being examined and was in a particular orientation, or that a large venule, or an arteriole with plentiful smooth muscle in its wall, or a lymphatic vessel was present, and so on. The most satisfactory orientations were those in which the entire depth of the chamber tissue, as measured vertically across the space between the coverslip and the table, was presented in the block face so as to yield either cross or longitudinal sections of the vessels. In tracing growing sprouts from their proximal connexion to the most distal tips the longitudinal orientation was used.

Sections for electron micrscopy were cut with a glass knife on a Huxley microtome to give yellow or pale gold interference colours after spreading with chloroform vapour. They were mounted on copper grids, generally with a supporting film of Formvar.

Staining and photography. Stains used for light microscopy were haematoxylin and eosin, Heidenhain's iron haematoxylin, Mallory's trichrome, Mallory's aqueous acid fuchsin (Mallory 1903), McManus's periodic acid-Schiff stain, phosphotungstic acid-haematoxylin, Weigert's elastic stain and the Gordon & Sweet method for reticulin.

Enhanced contrast on electron microscopy was obtained (i) by treating methacrylate sections with lead hydroxide, (ii) by treating sections cut from Epon blocks with 2% aqueous uranyl acetate for ½ to 1 h, and (iii) by soaking blocks of tissue to be embedded in Araldite in a 1% solution of phosphotungstic acid in absolute alcohol for 1 h at the appropriate stage of dehydration.

Photomicrographs of the living ear chamber were taken on 35 mm film using the Leitz Mikas attachment.

Electron micrographs were taken on 35 mm film using the Philips EM 100 B electron microscope fitted with high resolution pole pieces and objective aperture.

Results

Mensuration

The curve of growth of the repair tissue obtained from this series of experiments was sigmoid (figure 1) and the specific growth curve was derived from this curve (figure 2).

The thickness of the ear chambers measured varied between 40 and 65 μm but it did not appear that any variation in growth rates could be attributed to differences in the thickness of the ear chamber space within this range.

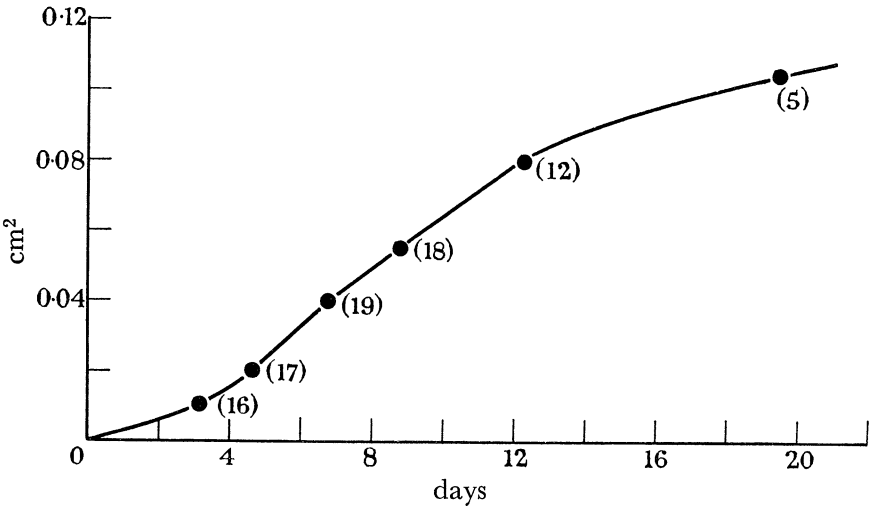

Figure 1. Average curve obtained for the growth of tissue (cm^2) into 4 mm castle-top chambers inserted into the ears of rabbits, plotted against time (days). The figures in brackets opposite each point on the curve indicate the number of ear chamber experiments used to obtain the co-ordinates for the point.

Qualitative observations

Light microscopy

In a narrow rim of tissue about ½ mm across, which was present in the most advanced region of the repair tissue, all the fundamental processes of healing could be observed. These were cellular proliferation and migration, new vessel formation, inflammation,

phagocytosis, new fibre (reticulin) formation and production of ground substance. Mitoses were most frequently seen in cells which are believed to be fibroblasts but they could also be found easily in adventitial cells and endothelial cells. Endothelial mitoses were seen proximal to the tips of the growing sprouts and not elsewhere.

In general the proliferating cells forming the repair tissue in this region were numerous and somewhat larger than mature cells. They had large nuclei and prominent nucleoli.

Regeneration of vessels

Two types of sprout arising *de novo* from existing blood vessels were identified. The commoner type will be referred to as the saccular type (figure 3, plate 26) and the less common one as the tapering type (figure 4, plate 26). Observations at high magnifications of the tapering type of sprout made it possible to conclude that there was a collapsed or 'potential' lumen in the tapering tip. During periods after the rabbit had received a fright or was struggling on the rabbit board blood corpuscles were sometimes seen being forced along the narrow tapering tips to join the general mêlée of extravascular cells within the surrounding fibrin clot. During such a process the corpuscles were considerably deformed. Figure 4 illustrates such barely resolvable lumina seen in a quiescent state.

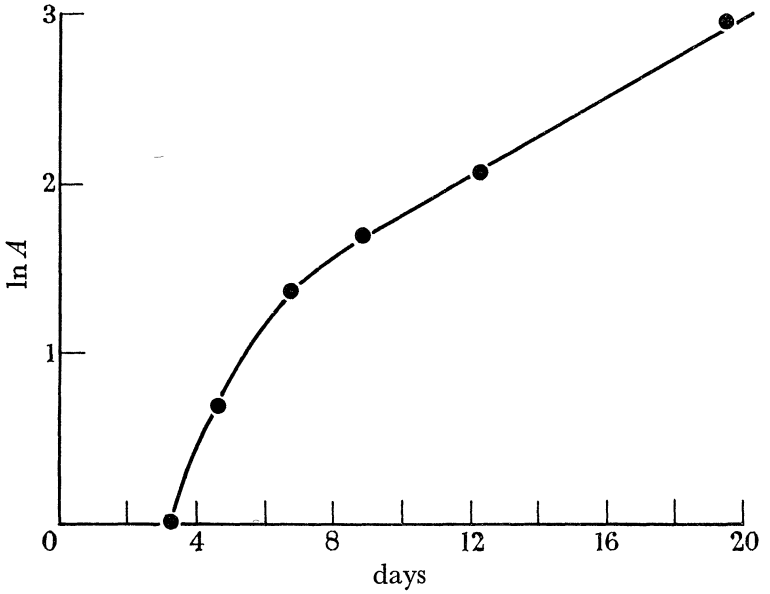

FIGURE 2. The specific growth curve derived from the average curve (figure 1). The ordinate (ln A) is plotted against time (days) as the abscissa. This expresses in the form of a graph the function $(dA/A)/t$ and reveals a progressive decrease in the regenerative power of the tissue invading the ear chamber.

It was observed *in vivo* that endothelial cells often projected into the lumina of newly formed vessels (figure 5, plate 27).

The subsequent anastomosis of sprouts to form loops and the modification of such loops according to Thoma's principles (1893) was observed.

Newly formed lymphatic vessels arose by budding from existing lymphatic vessels. In all cases observed they possessed saccular ends to their growing tips (figure 6, plate 27). When small segments of lymphatics became isolated they persisted and sometimes grew to re-establish connexion with the rest of the lymphatic system.

Growth of fibroblasts

Fibroblasts in mitotic division were frequently seen in fixed and stained preparations. They preceded the blood vessels growing into the chamber by 0·5 mm. In favourable circumstances it was possible to see *in vivo* that there was some finely fibrillary material near to the peripheral cytoplasm of these cells (figure 7, plate 28). By appropriate staining (Mallory 1903) of fixed preparations it was possible to identify plentiful 'fibroglial' fibrils in or near the peripheral cytoplasm of the fibroblasts (figure 8, plate 28).

The migrating fibroblasts were at first oriented radially (figure 7) but the orientation of the collagen fibres within the ear chamber (figure 9, plate 28) showed that there was a change to a circumferential orientation within the fibrous scar subsequently formed.

Reticular fibres were demonstrated by silver impregnation to be present where fibroblasts were invading the fibrin clot. These argyrophil fibres merged proximally with collagenous fibres. The extent of the zone occupied by argyrophil fibres, as measured from the point where fibroblast invasion of the central fibrin clot was occurring to the point where connective tissue fibres were identifiable as collagen, indicated that this zone required $2\frac{1}{2}$ days to be formed. In arriving at this value the average rate of formation of repair tissue as derived from figure 1 was used. From this it was deduced that during healing in the rabbit's ear the conversion of argyrophil fibres to collagenous fibres occupied a period of $2\frac{1}{2}$ days.

There was progressive reduction in the amount of fibroblast cell substance visible in sections and *in vivo* as fibrous tissue formed and matured in the scar.

Macrophages

These cells, together with the other highly amoeboid cells involved in the healing process, the granulocytes, were very numerous in advance of and within the growing fringe of repair tissue. With the formation and maturation of the fibrous scar tissue such cells became reduced in numbers. Macrophages were mostly found near the walls of blood vessels. Occasionally clusters of them surrounded foreign body giant cells, which in turn surrounded small foreign bodies (hair, fibre, talc crystals, etc.) within the chamber.

The reduction in the numbers of the polymorphonuclear leucocytes and of macrophages could be explained by the large numbers of such cells showing signs of death and disintegration in the region of the growing fringe.

Clear spaces

Clear spaces were identified in advance of the growing fringe at about the region of the zone of haemorrhage (figure 10, plate 29). These spaces were free from fibrin and were bounded by thin 'walls'. *In vivo* they were seen to contain moderate numbers of oscillating cells and much clear liquid. These structures could not be shown to have any connexion with existing blood or lymphatic vessels and they disappeared once the position they occupied was overtaken by the advance of the ingrowing repair tissue.

Electron microscopy

Endothelium of recently formed blood vessels

The endothelial cells of recently formed vessels possessed features of fine structure that clearly distinguished them from the endothelial cells of more mature vessels (figure 11,

plate 30). (1) They were thicker in relation to the size of the enclosed lumen (figure 12, plate 30). (2) The endoplasmic reticulum (Porter 1953) was plentiful and was composed of parallel interconnecting cisternae whose surface was studded with ribosomes (Palade 1955*a*) (figure 13, plate 31). (3) The cytoplasm could sometimes be seen to be divided into a highly fibrillary outer or 'cortical' region and a poorly fibrillary inner region (figure 14, plate 31). (4) There were numerous small dense granules within the ground substance of the cytoplasm (figure 13). (5) Typical mitochondria (Palade 1953*a*; Sjöstrand 1955) were numerous and at times they presented elongated profiles (figures 13, 14). (6) The nuclei were large and usually contained two distinct skein-like nucleoli (figures 20 and 22, plates 34 and 35).

Other features that distinguished recently formed vessels from mature 'normal' vessels were: (*a*) the adhesion of leucocytes to the endothelium and their emigration (figure 15, plate 37); (*b*) greater fragility, apparently related to conditions near the cell junctions, and resulting in haemorrhage (figure 16, plate 32).

Recently formed endothelium was found lying close to both fibrin (figure 17, plate 33) and collagen fibres (figure 12).

Formation of new vessels

The mechanism ultimately concerned in the production of new vessels was the mitotic division of the endothelial cells of the existing vessels (figure 18, plate 33). During mitosis the basement membrane of the vascular endothelium remains but is perforated by small projections from the basal surface of the endothelial cell while the cell junctions at each end of the dividing cell persist and appear more pronounced than usual. The orientation of the spindle is such (note centrosome, figure 18) that it would seem probable that the daughter cells formed would both be included in the endothelial lining of the vessel. Such cell divisions as this, as well as being the basis for growth by sprouting, are likely to contribute to the growth by intercalation that has been observed during the revascularization of wounds (Chalkey, Algire & Morris 1946).

The site of the endothelial mitosis identified by electron microscopy was situated somewhat proximal to the growing tip, as was to be expected from the findings of light microscopy on the healing of ear chambers (see above). These results emphasize that the further growth of an endothelial sprout is not accomplished by the mitotic division of the component cells of its tip but by the redistribution of new endothelial cellular elements formed by mitoses occurring somewhat proximal to the growing tip. It appears, therefore, that the sliding forward of cell substance from the sites of formation proximal to the growing tips to positions in the growing tips is a mechanism of fundamental importance in blood vessel sprout formation.

From consideration of many electron micrographs the suggestion is made that the following series of events takes place when new blood vessels are formed in an ear chamber.

(1) A cord or strand of closely apposed endothelial cells is formed in continuity with an existing vessel (figure 19, plate 34).

(2) Spaces develop between the apposed endothelial cells. At first these spaces are numerous and small (figure 20, plate 34); later they become fewer and larger (figures 21, 22, plate 35). In every region where the endothelial plasma membranes become

contiguous typical cell junctions are formed (Moore & Ruska 1957; Policard, Collet & Pregermain 1957; Bennett, Luft & Hampton 1959).

(3) The spaces between the endothelial cells forming the cord continue to enlarge and to coalesce until (*a*) a connexion is established with the lumen of the parent vessel (figures 21, 22), and (*b*) only one large space, the new lumen, is present between the endothelial cells.

These stages in fact overlapped considerably, large and small lumina being seen in a single section through a sprout (see figure 22).

The fundamental nature of the relationship between the endothelium and its basement membrane (Palade 1953*b*) was shown by the very early stage of new vessel formation at which the basement membrane developed. The basement membrane appeared to be built up by a process of condensation of fine fibrils formed in a region remote from the actual endothelial cell that was being invested (figure 17).

Electron micrographs of tapering sprouts (figure 19) and of saccular sprouts (figure 23, plate 48) showed certain differences. The endothelial cells of tapering sprouts sometimes possessed an incomplete basement membrane whilst those of saccular sprouts always had a complete basement membrane. Tapering sprouts had many extensively overlapping endothelial cells and only a rudimentary lumen, whilst saccular sprouts possessed a large, well-developed lumen.

Growth by intercalation

The further growth of a newly formed vessel occurred first by flattening and increase in the surface area of its existing endothelium, and secondly by the intercalation of more cells into its endothelial wall. In vessels situated proximally growth by intercalation was accomplished directly by mitotic division of the endothelium. In vessels situated distally (i.e. at and near to the growing fringe), where endothelial mitoses were not identified, the intercalation of additional cells occurred by a process similar to that of new vessel formation by sprouting. Figures 24 and 25, plates 36 and 37, illustrate the process of growth by intercalation where figure 24 is comparable to stages 1 and 2 of new vessel formation by sprouting and figure 25 is comparable to stages 2 and 3.

Anastomosis of sprouts

The process of anastomosis of sprouts can be broken down into a series of events similar to those occurring during the formation of new vessels by sprouting.

The region where two vascular sprouts have come into contact (figure 26, plate 37) is analogous to the solid cord of cells present at stage 1 of new vessel formation by sprouting. The appearance of spaces between the closely apposed endothelial cells and of numerous cell junctions (stage 2) was identified. It seems likely that this process progresses through a re-arrangement analogous to stage 3 of the formation of new vessels by sprouting (figure 27, plate 38).

Maturation of vessels

The first step in the maturation of a newly formed vessel was the incorporation of adventitial cells in the wall. Cells with some of the features of fibroblasts came to lie close to the outside of the endothelium (figure 28, plate 38) and became enclosed in a basement

membrane (figure 29, plate 39). At this stage these cells were very similar to endothelium both in fine structure and in their ability to store foreign material injected intravenously (figure 29).

In the course of development of arterioles/arteries cells were encountered which had taken up the circular orientation of vascular smooth muscle but which possessed some features similar to those of the adventitial type of cell (figure 30, plate 39). The walls of arterioles/arteries present in mature scar tissue formed in the rabbit ear chamber were shown to possess cells with the characteristic fine structure of smooth muscle cells (figure 31, plate 40) (Policard, Collet & Giltaire-Ralyte 1955; Caesar, Edwards & Ruska 1957; Pease & Molinari 1960).

Lymphatic vessels

Both recently formed (1 to 2 days old) (figure 32, plate 40) and mature (several months old) (figure 33, plate 41) lymphatic vessels were examined.

Features that distinguished the endothelium of these vessels from that of blood vessels were (1) a less marked difference in fine structure between recently formed and mature cells; (2) the extreme thinness of even recently formed cells (figure 32); (3) the presence of broad-based pointed projections from the basal surfaces of the cells (figure 32); (4) the highly developed phagocytic power of the cells (figure 34, plate 41; cf. figure 35, plate 42).

Fibroblasts

Cells recognized as fibroblasts were detected in the earliest stages of the formation of the scar tissue. They were mixed with macrophages, polymorphonuclear granulocytes and cell debris within the fibrin clot in advance of the invading fringe of blood vessels. The fibroblasts arose by mitotic division of existing cells of the same type (figure 36, plate 42).

A feature of the fibroblasts present in the region containing fibrin clot and cell debris, where the earliest invasion by repair tissue was occurring, was the presence within their cytoplasm of what appeared to be phagocytozed debris (figure 37, plate 43). In this region they also possessed well-developed tracts of finely fibrillary material coursing through their cytoplasm (figures 38*a*, *b*, plate 43). The length of such tracts was considerable and their width was about 0·4 to 0·5 μm, which meant that they could represent structures resolvable by the light microscope.

Membrane-bounded structures were identified in the fibroblasts engaged in fibre formation that were similar to the *caveolae intracellulares* of Yamada (1955) (figure 39, plate 44), with diameters of 55 to 60 (1 nm = 10^{-9} m). They appeared to possess contents of moderate electron density and were numerous where the plasma membranes were closely related to recently formed collagen fibrils. Vesicles with similar dimensions (*ca.* 55 nm) and with similarly electron-dense contents were identified within the cytoplasm of the fibroblasts, where they were dispersed singly, in clusters and in strings (figures 39, 40, plate 44). In figure 40 'budding' forms of these vesicles were identified as small evaginations of the membranes of the endoplasmic reticulum.

All fibrils that were recognizable as collagen were extracellular. In no instance were fibrils with the characteristics of collagen (Schmidt & Gross 1948) detected forming within cells or any parts of cells.

The incorporation of what appear to be fibroblasts into the walls of recently formed blood vessels during healing to become adventitial cells has been described above. An important feature of fine structure that distinguished the fibroblasts or fibrocytes from the adventitial cells that could apparently be derived from them was the universal absence of basement membranes related to the former and the universal presence of basement membranes related to the latter.

With maturation the fibroblasts persisted amongst the numerous bundles of collagen fibrils as fibrocytes (figure 41, plate 45). The fibrocytes were more attenuated than the fibroblasts and possessed less endoplasmic reticulum and fewer granules within their cytoplasm.

The wandering cells

Granulocytes were identified entering the healing tissue as the result both of haemorrhage from recently formed vesssels and of emigration through endothelial cell junctions. In some cases degenerate forms of these cells, the 'small round cells' of Clark, Clark & Rex (1936) were found within lymphatic vessels in close relation to the growing fringe (figure 42, plate 45), whilst necrotic cells of this type were frequently encountered related to the growing fringe (figure 36).

In normal mature repair tissue in the chambers no granulocytes were seen.

Lymphocytes were present in small numbers, together with occasional plasma cells. These, too, were absent from the mature scar tissue of the chambers.

Macrophage series. The cells of this series were considered to arise in the healing tissue from migrated blood-borne monocytes. An early stage in the migration of such a blood-borne monocyte is illustrated (figure 43, plate 46). It was possible to arrange a series of electron micrographs (figures 43 to 46, plates 46 and 47) to show a transition from the intravascular monocyte (figure 43) to the foreign body giant cell (figure 46). The highly developed phagocytic power of the cells of this series was demonstrated by the striking quantity of injected Thorotrast taken up and segregated (figure 44). The 'ruffled' pseudopodia which are very characteristic of this type of cell (Palade 1955*b*) are involved in phagocytosis of large particles such as an erythrocyte (figure 47, plate 48).

The plasma membranes of the macrophage can merge not only when elements of the ruffled border of one cell come into contact with one another but when elements of different macrophages touch (figure 45).

There was increasing prominence of the nucleolus during the course of the extravascular development from monocyte to giant cell (cf. figures 43 and 46). In the giant cell the nucleolus possessed a definite grid pattern, but even in this highly developed state no trace of a nucleolar membrane could be detected.

Apart from the 'ruffled' pseudopodia, features which helped to distinguish the macrophage series of cells from fibroblasts were (1) the prominence of the mitochondria amongst the various intracytoplasmic organelles and the oval profiles generally presented in sections by these structures (figures 44, 45); (2) the inconspicuous nature of the endoplasmic reticulum, which was composed mainly of tubular elements of both the rough and smooth varieties, with contents of low electron density; only occasionally did the endoplasmic reticulum of these cells show a tendency to take up a preferred orientation; (3) the

numerous pleomorphic, generally electron-dense, inclusions in the hyaloplasm (figure 47). A feature of interest within the cytoplasm of the macrophages was shared with the fibroblasts of the growing fringe. This was the presence of highly fibrillary tracts of considerable length and *ca.* 0·4 μm width within the cytoplasm (figure 45).

As the repair tissue matured cells of the macrophage series became less common and those that were occasionally seen were generally related to blood vessels (figure 30, plate 39).

Clear spaces

The transient 'clear spaces' described earlier were found to be lined by a continuous pavement of cells joined edge to edge (figure 48, plate 48). The cells lining these spaces did not appear to possess any basement membrane.

Discussion

The results of the mensuration experiments are in agreement with other work published on events in the rabbit ear chamber. The average curve of growth (figure 1) is similar both to the equivalent curve obtained from the mouse back chamber (Chalkey *et al.* 1946) and to a generalized form of growth curve (Medawar 1945). The specific growth curve indicates a progressive loss of the power of regeneration by the healing tissue. It is reasonable therefore to suppose that the regenerating tissue observed in the rabbit ear chamber has similar properties in respect of growth to other living tissues.

The average time for complete growth is 21 days (to the nearest day), which in a 4 mm chamber gives a rate of 0·19 mm per day for the ingrowth of tissue. This agrees well with the figure of 0·19 mm per day given for the rate of migration of fibroblasts into the rabbit ear chamber (Stearns 1939).

The lack of any relation between the thickness of the chamber and rate of growth agrees with the observations of Van den Brenk (1956), who varied the depth of his chambers from 100 to 200 μm with no appreciable effect on the growth rate.

Growth of blood vessels

The two types of blood vessel sprout that arise from existing vessels in the rabbit ear chamber have both been described previously, the 'fine pointed' sprouts by Clark, Clark & Abell (1933) and the 'saccular' sprouts by Abell (1946) and Williams (1959). From a comparison of the features of these types of sprout as seen in electron micrographs it is considered probable that the saccular sprout is a later stage in the process of formation of new vessels than the tapering sprout. The extensive projections formed by endothelial cells into the lumina of recently formed vessels have not been described previously.

The modification of the newly formed loops according to the principles enunciated by Thoma (1893) has been reported in the rabbit ear chamber (Clark 1936), as has the incorporation of extravascular cells which may be fibroblasts into the walls of newly formed vessels to become adventitial cells (Clark & Clark 1939) during the course of differentiation. The finding of cells possessing features of both adventitial cells and smooth muscle cells is taken to support the claim that adventitial cells may transform to smooth muscle cells in the walls of developing arterioles or small arteries (Clark & Clark 1940). The presence of typical smooth muscle cells in the walls of some of the vessels present in rabbit ear chamber

satisfied the requirements of Lutz & Fulton (1958) for an explanation of the vascular contractions, of both humoral (Sandison 1932; Clark & Clark 1940, 1943) and nervous (Clark, Clark & Williams 1934; Clark & Clark 1940) origin, that have been observed in these preparations.

The mitosis of endothelium within a vessel wall has not been described previously in terms of fine structure, although the mitoses in an endotheliosarcoma have been so described (Porter 1955).

The features listed as characteristic of the endothelium of recently formed vessels differentiate it from mature endothelium, which has been extensively described elsewhere (Palade 1953*b*; Buck 1958: Policard & Collet 1958; Bennett *et al.* 1959; Fawcett 1959). Among these features the greater thickness of the endothelium relative to the lumen of the vessel was noted *in vivo* (figure 4, plate 26) as well as in electron micrographs.

The type of endoplasmic reticulum encountered in the endothelium of forming and of recently formed vessels has been seen also in cultured foetal endothelium (Palade & Porter 1954). An extensively developed endoplasmic reticular system lined by rough-surfaced membranes, such as is found in these cells, has been associated with the elaboration of protein-rich secretions in general (Palade & Porter 1954) and in the exocrine pancreatic gland cell in particular (Weiss 1953). The Golgi substance, which is thought to play an important intermediary role in the secretory process, as for instance in the exocrine pancreatic gland cell (Caro 1961), can also be identified by electron microscopy (Dalton & Felix 1954) in this endothelium (figures 13, 20 and 22, plates 31, 34 and 35). These systems of paired membranes, which are evidence of ability to secrete, and the plentiful mitochondria, which are evidence that metabolic energy is available for secretion (Schneider 1959), together furnish good evidence for some secretory activity by the endothelial cells of forming and recently formed blood vessels. It is postulated that the endothelial cells play a secretory role in the production of the liquid-filled spaces, which are the earliest stage in the development of the new vascular lumen, that have been detected in the electron microscopic examination of new vessel formation by sprouting. Such activity on the part of the endothelium of forming and recently formed blood vessels could also explain the production of 'plasma' by developing vessels in the yolk sac of the embryonic chick (Sabin 1921).

The division of the cytoplasm of the endothelium of recently formed vessels into a highly fibrillary cortical and a poorly fibrillary inner zone may be evidence for the existence of a highly gelled cortical region of these endothelial cells, such as was observed *in vivo* by Clark & Clark (1939). A consideration of the structure of gels in general (Frey-Wyssling 1953) is compatible with such an interpretation of the electron micrographic finding. A similar interpretation of the significance of densely fibrillary cytoplasmic regions has been made by Porter (1955).

The numerous small dense granules within the cytoplasm of the endothelium of recently formed and forming vessels are taken as further evidence of the proliferation of these cells during healing (Porter & Thompson 1947; Porter 1953; Palade 1955*a*).

The fine details of the margination and migration of leucocytes in the vessels of healing tissue are largely the same as those described in acute inflammation (Marchesi & Florey 1960; Marchesi 1961). However, leucocyte migration in the venules, as reported in those

papers, is not possible in healing tissue as many of the vessels from which leucocyte emigration is occurring have not differentiated sufficiently to be identified as arterioles, capillaries or venules. It is considered, nevertheless, that these phenomena are manifestations of the inflammatory component of the healing reaction (Wright 1958).

The fragility of recently formed vessels (Clark 1936), which is responsible for the characteristic zone of haemorrhage seen *in vivo* in ear chambers (Ebert *et al.* 1939), is traceable in the electron micrographs to conditions in the regions of endothelial cell junctions. Micrographs such as figure 16, plate 32, are interpreted as showing a tendency for junctions of recently formed vessels to separate in response to slight changes in the pressure differences across the vessel wall which would produce no haemorrhage from more mature vessels.

The highly developed phagocytic power of the endothelium of recently formed vessels is evidence of a quantitative rather than a qualitative difference between such endothelium and that of mature vessels, for mature endothelium has been found to be phagocytic (Buck 1958). There is no reason to consider that the phagocytic power possessed by endothelium of vessels in healing wounds indicates the re-emergence of a generalized characteristic of embryonic endothelium suggested by Beard & Beard (1927).

The close relationship seen between recently formed and forming vessels and fibrin strands suggests that the fibrin network acts as a scaffolding for the formation of blood vessel sprouts (Chalkey *et al.* 1946) as well as for the migration of other elements of the repair tissue (Weiss & Garber 1952; Weiss 1959). There is no evidence from the electron micrographs that recently formed vessels have fibrinolytic activity as observed *in vivo* (Clark *et al.* 1933; Clark & Clark 1939), but the presence of highly developed endoplasmic reticulum in the endothelium would be compatible with the production of enzymes such as fibrinolysins.

The very close topographical relationship that may exist between recently formed vessels and recently formed collagen fibrils is not considered to be evidence for the possible production of such fibrils by the endothelium (Corner 1920), though it suggests that this fibrillary scaffolding also is an aid to the formation and ingrowth of the blood vessel sprouts. The presence of newly formed collagen fibrils (reticulin) in the chambers can always be explained by the mediation of fibroblasts, which is in accord with current views on collagen fibrillogenesis (Porter 1951; Porter & Pappas 1959; Karrer 1960; Peach, Williams & Chapman 1961; Chapman 1961).

The probable series of events that occurs during the formation of new vessels by sprouting, as it can be deduced from the observations reported in this paper, has already been outlined. In general terms there is an intercellular canalization of cords of endothelial cells formed in continuity with existing vessels. Billroth (1856), in describing 'primary' vessel formation in granulation tissue, recognized the earliest vessel as a solid cylinder composed of closely apposed cells which developed a lumen through the formation of spaces between the plasma membranes of contiguous cells. Again in 'secondary' vessel formation, also encountered in granulation tissue, cells extended spindle-shaped processes which lay close together and alined in their long axes, with a central canal between them (Billroth 1856). Common factors in these two methods of vessel formation were first that the first recognizable antecedent of the lumen arose extracellularly and second that the cells

contributing to the new vessel maintained their individuality and did not at any time form a syncytium. These basic concepts were confirmed by observation of the formation of vessels in life in the developing chick (Thoma 1893; Lewis 1925–26). So also the present studies with the electron microscope have failed to confirm theories that postulated the formation of the lumen by intracellular vacuole formation and the existence of a syncytium of cells in the growing tip (Clark & Clark 1939). The latter finding is in harmony with current views that question the existence of true syncytia in animal somatic tissues (Caesar *et al.* 1957).

It is postulated from the present observations that the basic processes responsible for the formation of new vessels by sprouting are also those responsible for the further growth of the vessel and for the anastomosis of sprouts.

It has not been possible to identify in the healing tissue of the ear chamber the structure known as a protocapillary (Kisch 1957) which was described as showing in transverse section a single endothelial cell disposed around a lumen with its ends joined by a single cell junction.

An interesting relationship emerged from a study of the relative numbers of endothelial cells and endothelial cell junctions present in a vessel wall. In a mature vessel where n was the number of endothelial cells the number of cell junctions present was also n, as for example in figure 11, plate 30, where 4 endothelial cells and 4 junctions are present. However, in the case of vessels in the process of growing, other than by the process of direct intercalation by mitosis, there exists for a period (stage 2 to end of stage 3) an arrangement of the n endothelial cells involved such that there are $n+m$ cell junctions, where n and m are positive integers. Figure 20, plate 34, illustrates this latter 'immature' or 'unstable' relation where $n = 2$ and $n+m = 5$. This tendency of endothelial cells to adhere to one another has been described as a fundamental property associated with their embryological differentiation (Sabin 1921).

The appearances during the formation of the endothelial basement membrane are not readily compatible with the view that this structure may be solely the product of the endothelium itself (Fawcett 1959).

The differences observed between lymphatic and blood vessel endothelium confirm the conclusion reached from *in vivo* observations (Clark & Clark 1937) that the two forms of endothelium show complete specificity.

Relationships of cell types

Investigators of wound healing in the past have frequently claimed the participation of some form of multipotent stem cell, e.g. the polyblast (Maximov 1916, 1917*a*; Foot 1921; Arey 1936), or some multipotent mesenchmyal cell (Foot 1921; Arey 1936; Hadfield 1951), in the production of the various cell types finally found in repair tissue. Current opinion tends to oppose the idea that such multipotent cells take part in the healing of tissues in adult mammals (Cameron 1952; Wright 1958). In the electron micrographs studied in these experiments no evidence has been found to suggest the presence of any multipotent mesenchymal cells comparable to those for which descriptions of fine structure are available (Hay 1958; Godman & Porter 1960). The sources of the various cell types identified throughout healing could be adequately traced to pre-existing adult cell types.

It has been possible to find evidence supporting only some of the interconversions between cells of mesenchymal origin which have been claimed to occur and which are relevant to this discussion as for example, the claimed conversion of endothelium to fibroblast (Maximov 1916, 1917*b*), endothelium to fibroblast and macrophage (Foot 1921, 1925), fibroblast-like cell to macrophage (Porter 1951), mononuclear to fibroblast-like cell (Carrel & Ebeling 1922), connective tissue cell to mesothelium (Clarke 1914), monocyte to macrophage, epithelioid cell and giant cell (Lewis 1925–26), monocyte to macrophage (Ebert & Florey 1939), fibroblast to vascular adventitial cell (Clark & Clark 1939) and vascular adventitial cell to vascular smooth muscle cell (Clark & Clark 1940).

The fibroblast

The origin of the fibroblasts, which for the most part persisted as fibrocytes in the mature scar, was through the proliferation by mitotic division of existing fibroblasts. The endoplasmic reticulum is a positive aid in identifying the fibroblast in mitosis, for during mitosis it persists in a moderately dispersed state and has many features in common with the endoplasmic reticulum of the interphase fibroblast (Palade & Porter 1954; Palade 1955*a*) and little in common with the endoplasmic reticulum of cells of the macrophage series (Palade 1955*b*, *c*).

The fibroblast participating in healing is concerned largely with the production of collagen fibrils, first by secreting tropocollagen (Jackson 1957; Jackson, Flickinger & Dunphy 1960) and secondly by supplying at its cell surface sites for the elaboration of the morphologically discernible fibrils of collagen newly formed from tropocollagen (Porter 1951; Jackson 1953; Porter & Pappas 1959; Karrer 1960). The highly developed *RNA*-studded cisternae of the endoplasmic reticulum (Palade 1955*a*) of the fibroblast type of cell were considered to be the sites of tropocollagen synthesis by Karrer (1960) and Cameron (1961). This agrees with the current concepts of the role of such a form of the endoplasmic reticulum in the synthesis of proteins for secretion (Weiss 1953; Porter 1953; Palade & Porter 1954).

A pathway must exist by which the tropocollagen in the cisternae of the endoplasmic reticulum can leave the membrane-bounded confines wherein it has been synthesized and so be secreted into the extracellular space, if the current views on protein secretion and collagen fibrogenesis are correct. Direct continuity between the membranes of the endoplasmic reticulum and the plasma membrane, with the formation of a small opening connecting the interior of the endoplasmic reticulum to the extracellular space, has been observed in sarcoma cells (Epstein 1957) and embryonic fibroblasts (Karrer 1960). However, such observations are rare and Karrer mentioned a second method whereby secretion of the contents of the endoplasmic reticulum into the extracellular space could occur. This was by pinching off and extrusion from the fibroblast *in toto* of dilated cisternal elements of the endoplasmic reticulum. It is suggested that the system of vesicles seen in these preparations, about 55 nm in diameter and connected both with the membranes of the endoplasmic reticulum and with the plasma membrane near sites of fibrogenesis, and also lying free in the cytoplasm, represents a similar mechanism, though it differs from that demonstrated by Karrer in the size of the portions of endoplasmic reticulum pinched off before extrusion from the cell. Such a method for the transport of newly synthesized

tropocollagen from the cisternal spaces of the endoplasmic reticulum to the exterior of the cell is in harmony with the pinocytic vesicle theory of membrane permeability (Palade 1956), and with concepts of the dynamic properties of the endoplasmic reticulum, based on a study of its morphology (Palade & Porter 1954; Hodge 1956). Vesicle formation from the endoplasmic reticulum during secretion has also been described in the pancreatic exocrine gland cell (Weiss 1953). It is postulated therefore that the system of membrane-bounded intracytoplasmic vesicles (about 55 nm in diameter), the 'budding forms' of these from the endoplasmic reticulum, and the caveolae intracellulares of similar size detected within the fibroblasts in healing tissue, represent a possible pathway of secretion for tropocollagen synthesized in the endoplasmic reticulum.

The monocyte–macrophage series

The micrographs illustrated as linking the monocyte, macrophage and giant cell into a single series are presented as corroboration of the work of Lewis (1925–26), Lewis (1926) and Ebert & Florey (1939). The monocytes in the rabbit ear chamber conformed to descriptions already made of the fine structure of these cells (Palade & Porter 1954; Palade 1955*c*). They showed evidence of traversing the walls of blood vessels by migration through endothelial cell junctions (Marchesi & Florey 1960).

The macrophages conformed in their fine structure to descriptions available (Palade & Porter 1954; Palade 1955*b*). The foreign body giant cells shared features of fine structure with the osteoclast (Gonzales & Karnovsky 1961). Two of these, namely the highly developed system of 'ruffled' pseudopodia and the numerous mitochondria, are probably related to the common role of these cells in the ingestion and subsequent digestion of extracellular material.

The findings in relation to the fibroblast–fibrocyte series and the monocyte–macrophage series indicate that these two series of cells have individual origins and individual parts to play in the healing process and in populating the final scar tissue. No evidence was found to support any of the claims for interconversions between these two series. Occasional points of similarity between cells of the two series could be explained in terms of interaction between cell and environment producing temporary morphological changes. Under such a heading may be placed (1) the apparent phagocytosis of debris by fibroblasts, which might be no more than a result of the locomotion of these cells, and (2) the tracts of highly fibrillar material present within cells of both types which were considered to represent in terms of fine structure the fibroglial or 'stress' fibrils detected in both cell types by light microscopy (Porter 1951) and were probably produced by a process of 'micellar crystallization' (Holfreter 1947).

While the work recorded in this paper was being prepared for publication Ross & Benditt (1961) published observations made with the light and electron microscope on the healing of linear skin incisions in guinea pigs. Their conclusions differed from some of those in the present work in (1) supporting the possible origin of fibroblasts in the course of healing from either 'polyblasts', lymphocytes or blood-borne monocytes, (2) the interpretation given of the fibroglial fibres in terms of fine structure, and (3) the recognition of certain intracytoplasmic inclusions of macrophages which they considered to be characteristic. A system of small vesicles and caveolae within fibroblasts, as noted in the present

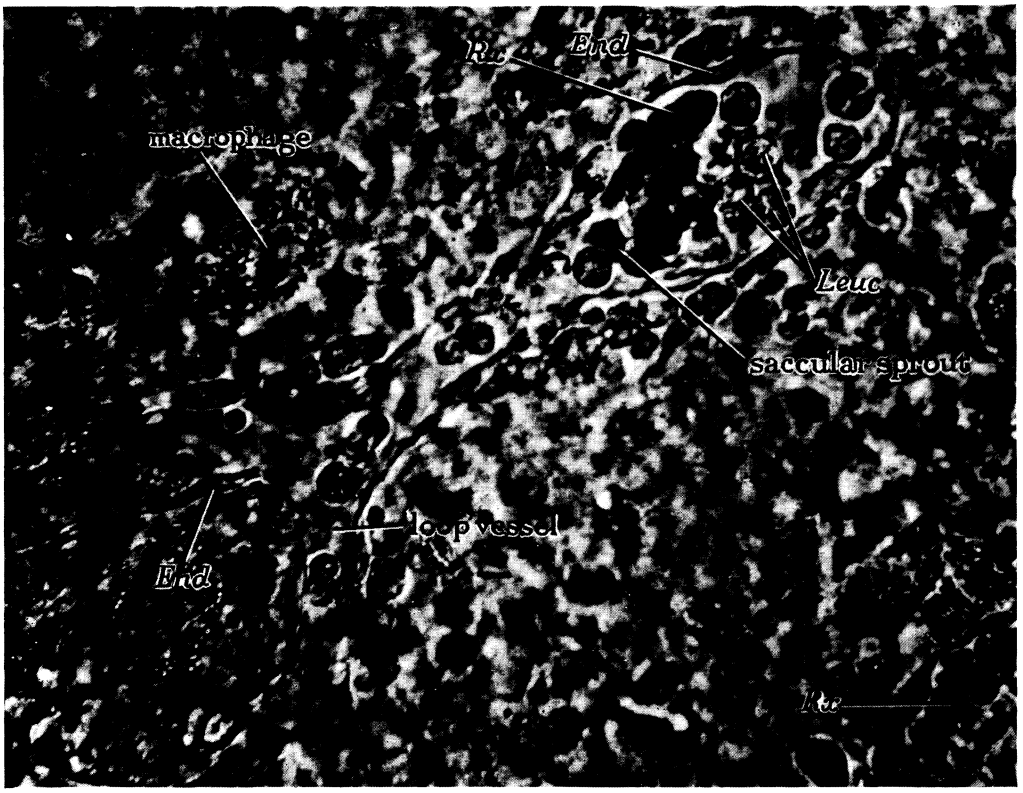

3

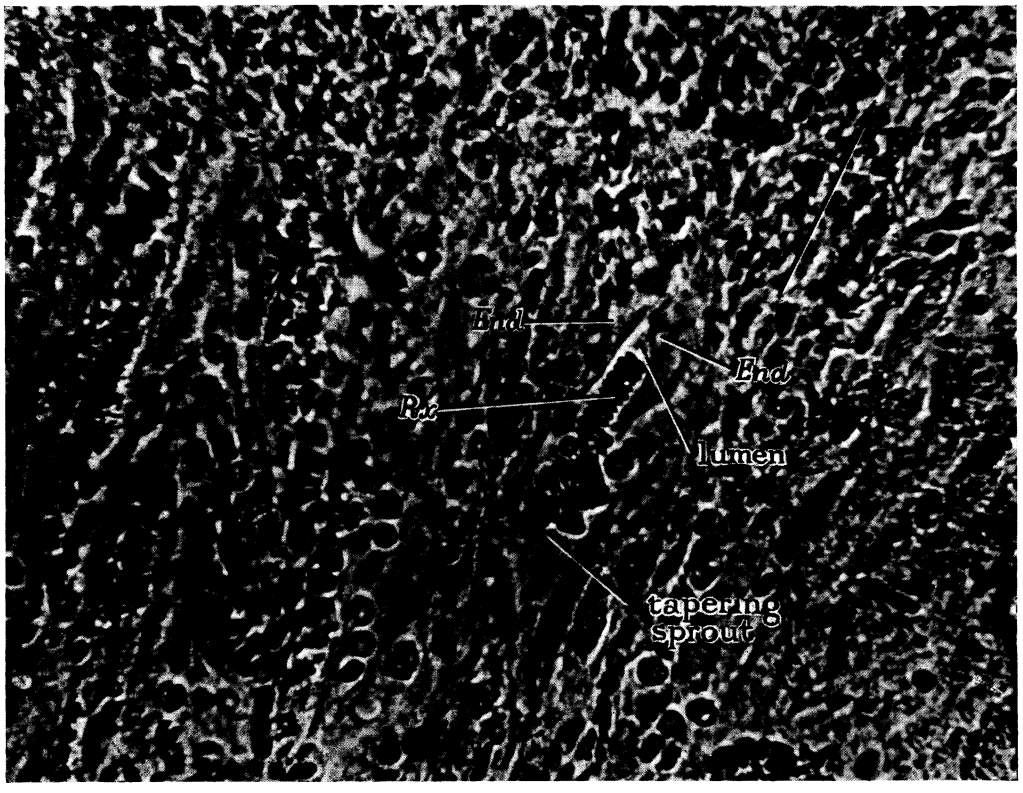

4

Except where indicated otherwise the figures are electron micrographs.

FIGURE 3. Photomicrograph of a saccular sprout *in vivo*. The endothelial lining (*End*) of the sprout and of its parent 'loop' vessel is clearly seen. The lumen of the sprout contains rouleaux of erythrocytes (*Rx*); similar formations are present within a vascular lumen in the lower right corner. There are large numbers of leucocytes (*Leuc*) in the lumen of the sprout. A macrophage containing numerous granular inclusions is indicated near the growing fringe. Objective, 1/7 in. (oil immersion) (× 747).

FIGURE 4. Photomicrograph of a part of the growing fringe. The plump endothelial lining (*End*) of a tapering sprout encloses a lumen which tapers to unresolvable dimensions as it is traced distally between the endothelial cells. *Rx*, Rouleaux of erythrocytes within the lumen of the sprout. The arrow indicates the direction of advance of the growing fringe. Objective, 4 mm apochromat (× 577).

(*Facing p.* 320)

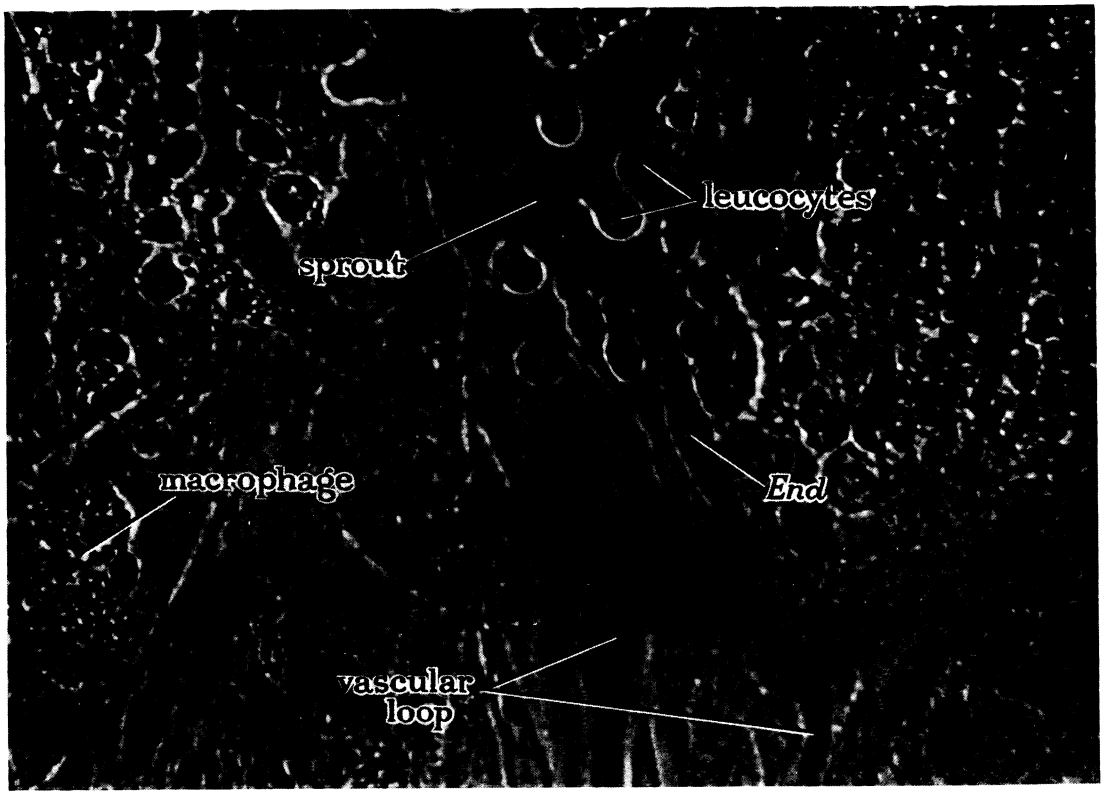

5

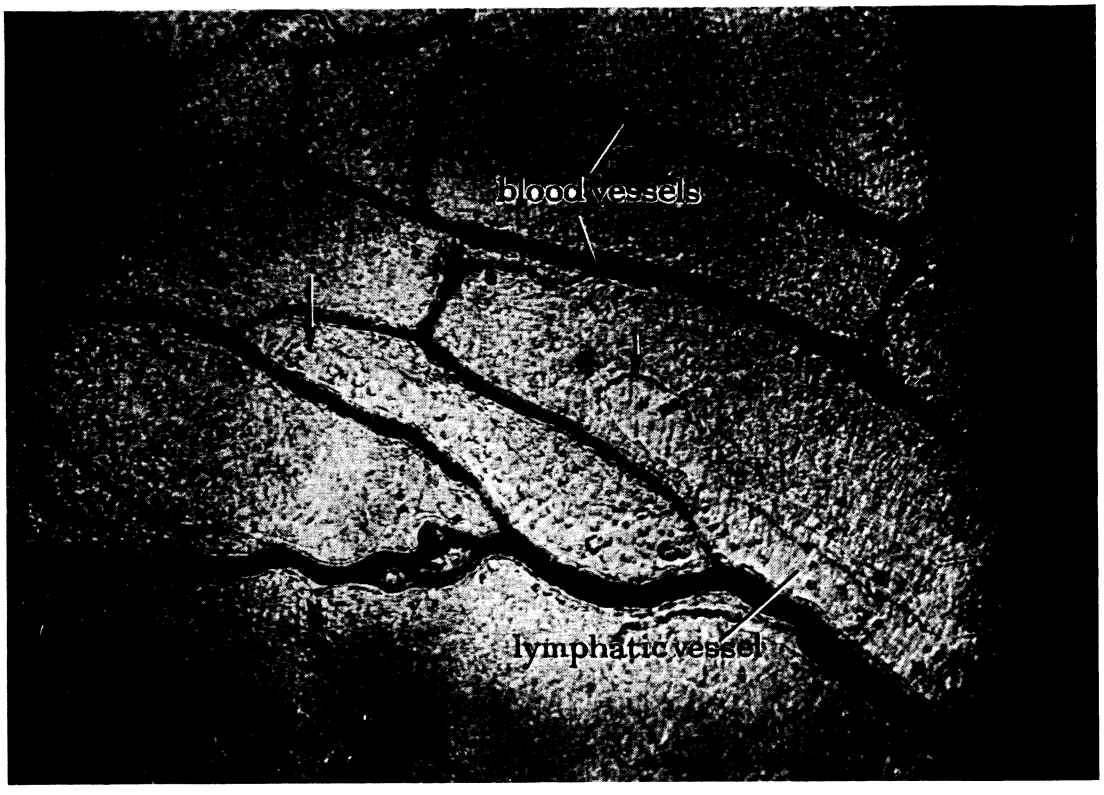

6

FIGURE 5. Photomicrograph of the growing fringe. A vascular loop with active circulation is giving rise to a sprout. The endothelial wall of the sprout is clearly seen (*End*) and one endothelial cell has a long pointed process extending into the lumen of the sprout (arrow). Objective, 1/7 in. (oil immersion) (× 747).

FIGURE 6. Photomicrograph of scar tissue in a rabbit ear chamber. The black shadow curving across the right side of the micrograph is the edge of the table of the chamber. A rich network of blood vessels is present and a lymphatic vessel is invading the ear chamber tissue along the lines of existing blood vessels. The saccular ends of the two branches of this lymphatic are indicated by arrows (× 146).

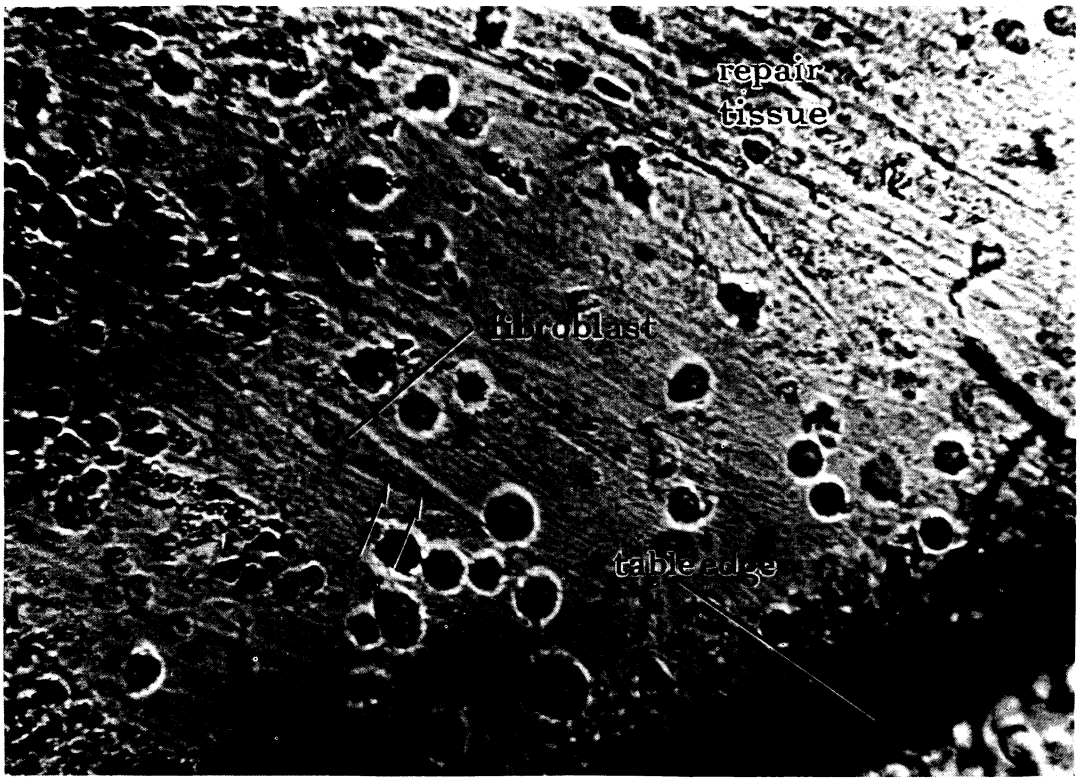

7

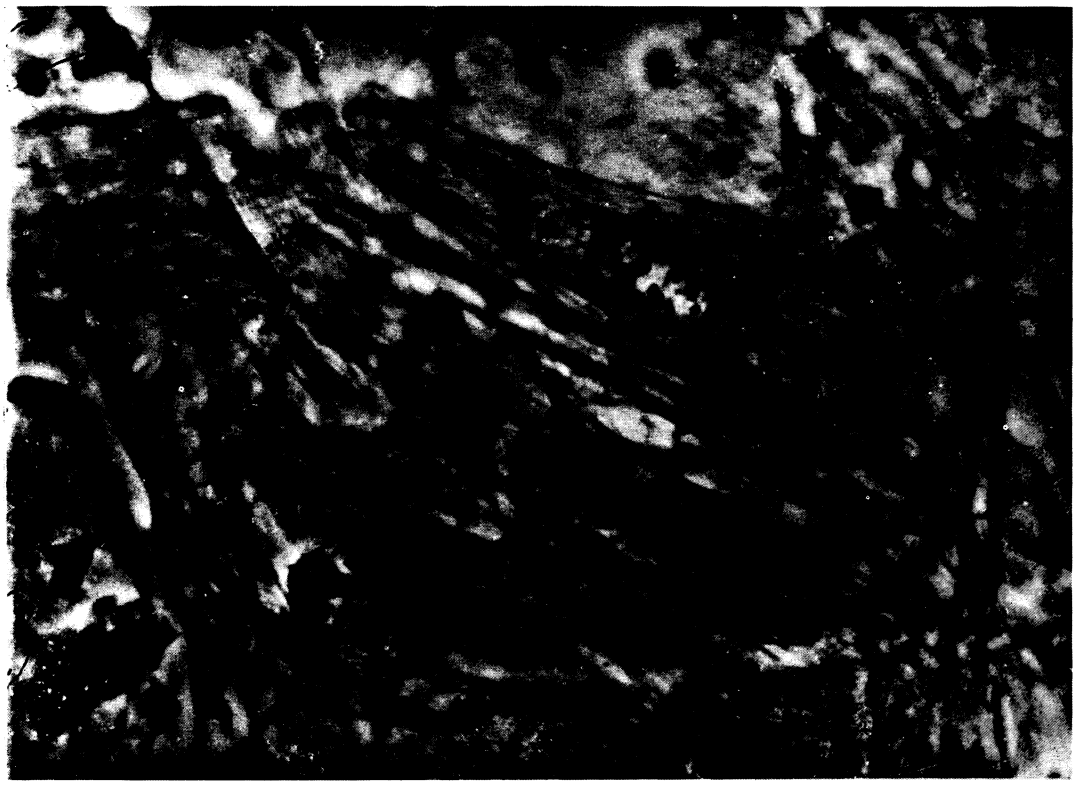

8

FIGURE 7. Photomicrograph of early repair tissue near the edge of the table. An isolated fibroblast is indicated with very fine fibrils apparently in or over its cytoplasm (arrows). Objective, 4 mm apochromat (× 577).

FIGURE 8. Photomicrograph of a section from a healing ear chamber to illustrate fibroglial fibres within fibroblasts. Fixation, mercuric-formol; stain, acid fuchsin (Mallory). Objective, 1/12 in. (oil immersion); filter, Wratten B 2 (green) (× 1333).

9

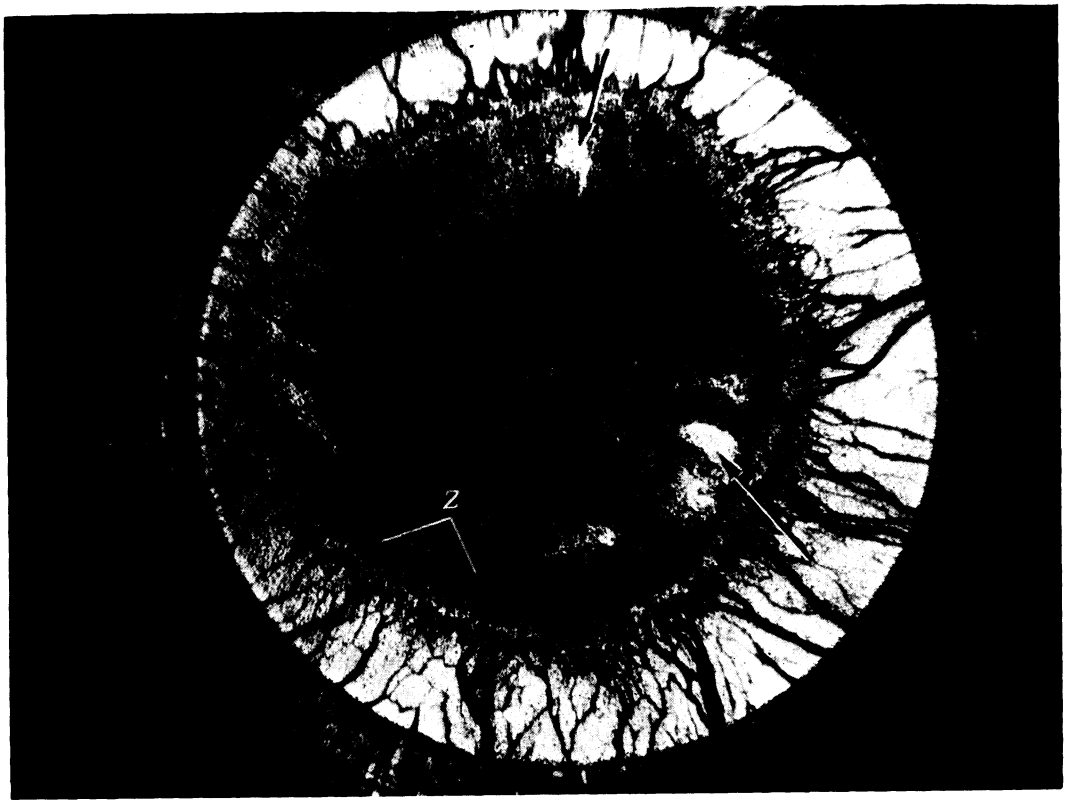

10

FIGURE 9. Photomicrograph of part of an ear chamber that had been fully healed for 3 weeks. Abundant collagen fibres with circular orientation are shown by examination with polarized light. Objective, × 10; filters, crossed polaroid (× 146).

FIGURE 10. Photomicrograph of a rabbit ear chamber showing fairly even invasion by the highly vascular growing fringe. This corresponds well to the illustrations prepared by Billroth (1856) of the vascular pattern of granulation tissue. Several clear spaces are visible distal to the growing fringe, two of which are indicated by arrows. These clear spaces are largely within the zone of haemorrhage (Z). Objective, Zeiss A; filter, Wratten B 2 (green) (× 27).

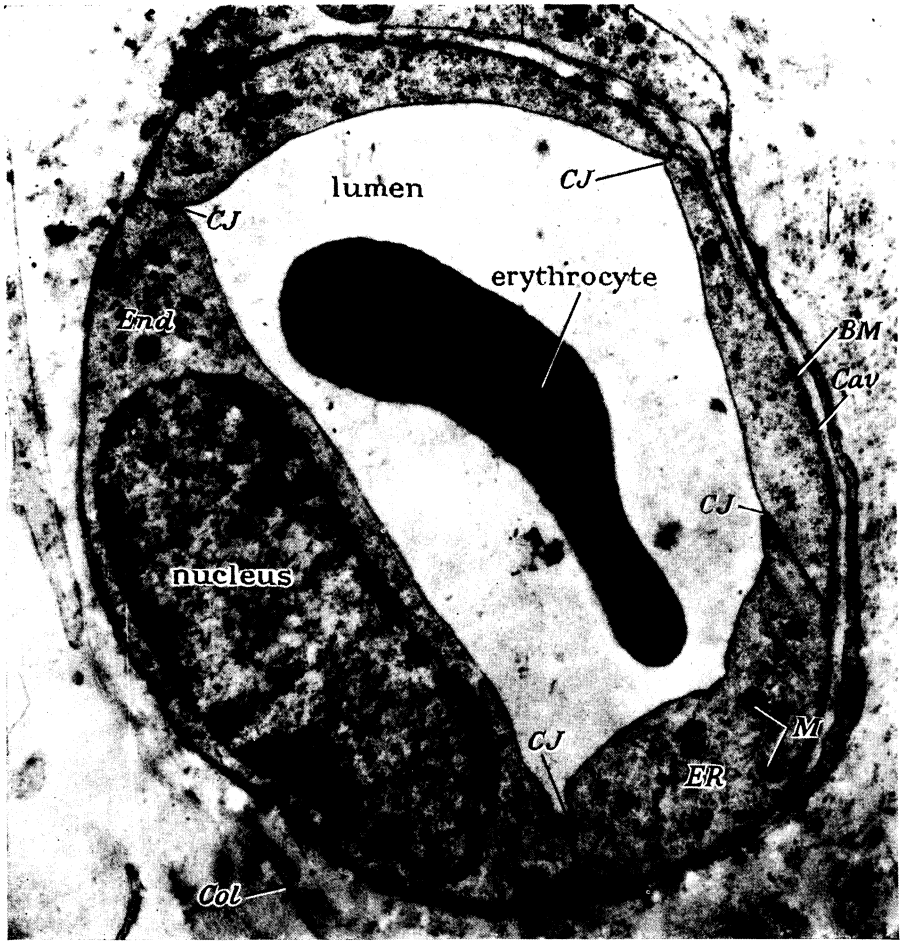

FIGURE 11. Mature blood capillary. The endothelial lining (*End*) is formed by 4 cells with 4 cell junctions (*CJ*). There are numerous caveolae intracellulares (*Cav*), an inconspicuous endoplasmic reticulum (*ER*), and mitochondria (*M*). *BM*, Basement membrane; *Col*, collagen. Epikote 812, uranyl acetate (× 13500).

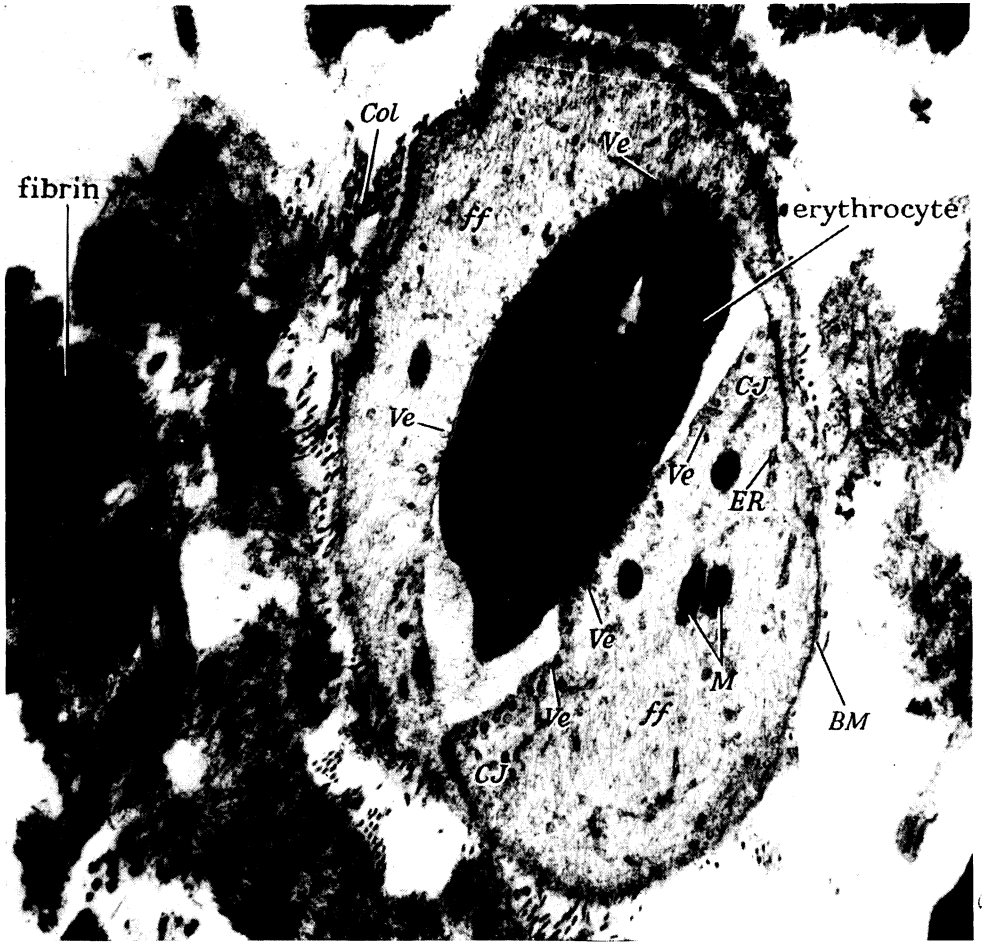

FIGURE 12. Recently formed vessel with narrow lumen, the greatest diameter being 4·5 μm. The endothelium is plump in relation to the lumen (as in figure 4). This vessel is penetrating the fibrin clot. *BM*, Basement membrane; *Col*, collagen; *CJ*, cell junction; *ER*, endoplsamic reticulum; *ff*, fibrillary region of cytoplasm; *M*, mitochondria; *Ve*, vesicles. Phosphotungstic acid; Araldite (× 17000).

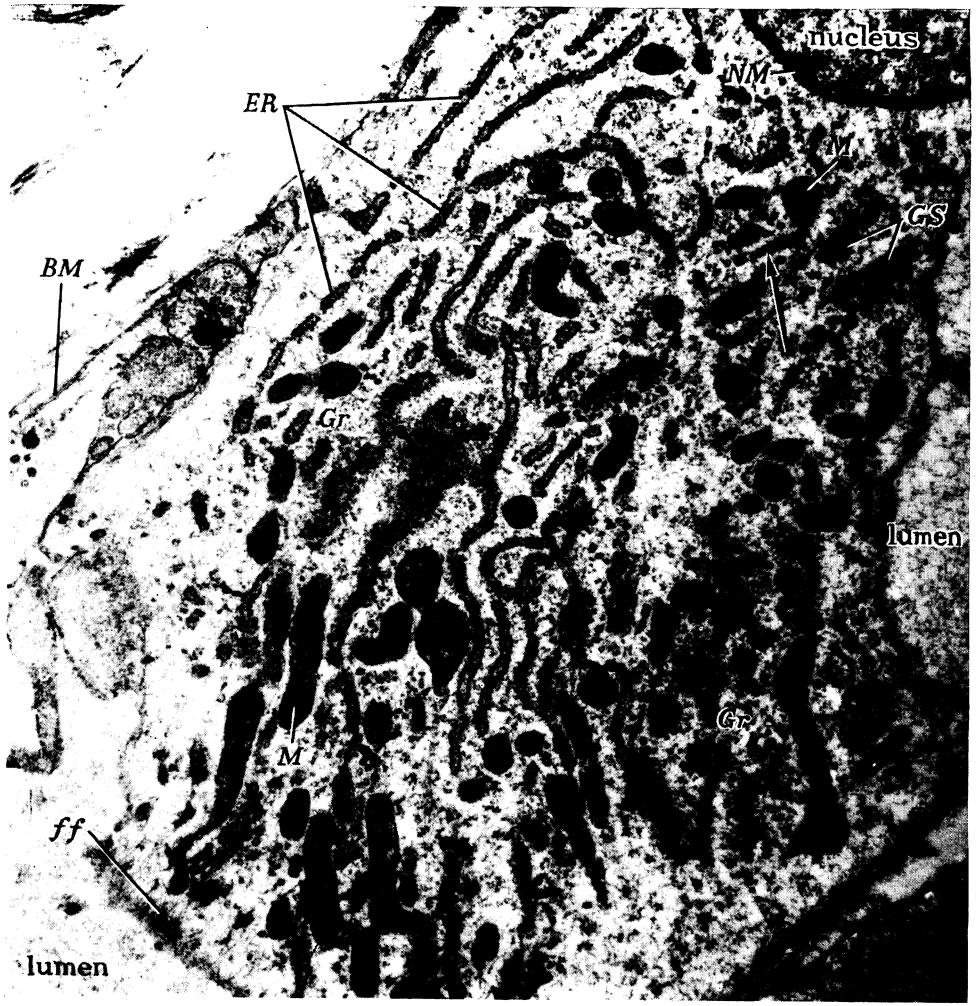

FIGURE 13. Endothelium from the distal part of a vessel that was invading fibrin clot. It contains numerous elements of endoplasmic reticulum (*ER*) between the paired membranes of which is moderately electron-dense material. The lacunes of the endoplasmic reticulum are about 680 Å wide and are studded with numerous dense ribosomes (*RNP* granules) which in one region (arrow) show a linear disposition. Closely apposed smooth surfaced pairs of membranes together with groups of small vesicles are part of the Golgi substance (*GS*). Numerous elongated mitochondria (*M*) with plentiful transverse cristae are present. The hyaloplasm contains much finely fibrous (*ff*) and granular material (*Gr*). *BM*, Basement membrane; *NM*, nuclear membrane. Phosphotungstic acid; Araldite (× 18000).

FIGURE 14. Endothelium of a recently formed vessel. A radicle of a greatly distorted erythrocyte is insinuated at a cell junction (*CJ*). This endothelium possesses much endoplasmic reticulum (*ER*) and numerous mitochondria (*M*). A region of highly fibrillary cytoplasm about 0·2 μ wide (*ff*) forms a distinct peripheral zone in one endothelial cell; in certain parts (e.g. at *X*) the fine fibrils are condensed to form small dark bodies. Note numerous small vesicles (indicated by arrows) within the fibroblast. *Col*, collagen. Phosphotungstic acid; Araldite (× 18000).

FIGURE 15. Immature venule and branch. Three granulocytes (*Grc* 1, 2 and 3) are related to the vessel wall. *Grc* 1 is passing through the endothelial lining (*End*) of the venule. This granulocyte has not penetrated the basement membrane which may be identified in relation to it (*BM*). *Grc* 2 has penetrated the endothelium (perhaps at arrow) and lies between it and the perivascular sheath. *Col*, Collagen; *CJ*, cell junction; *N*, nucleus. Phosphotungstic acid; Araldite (× 4 000).

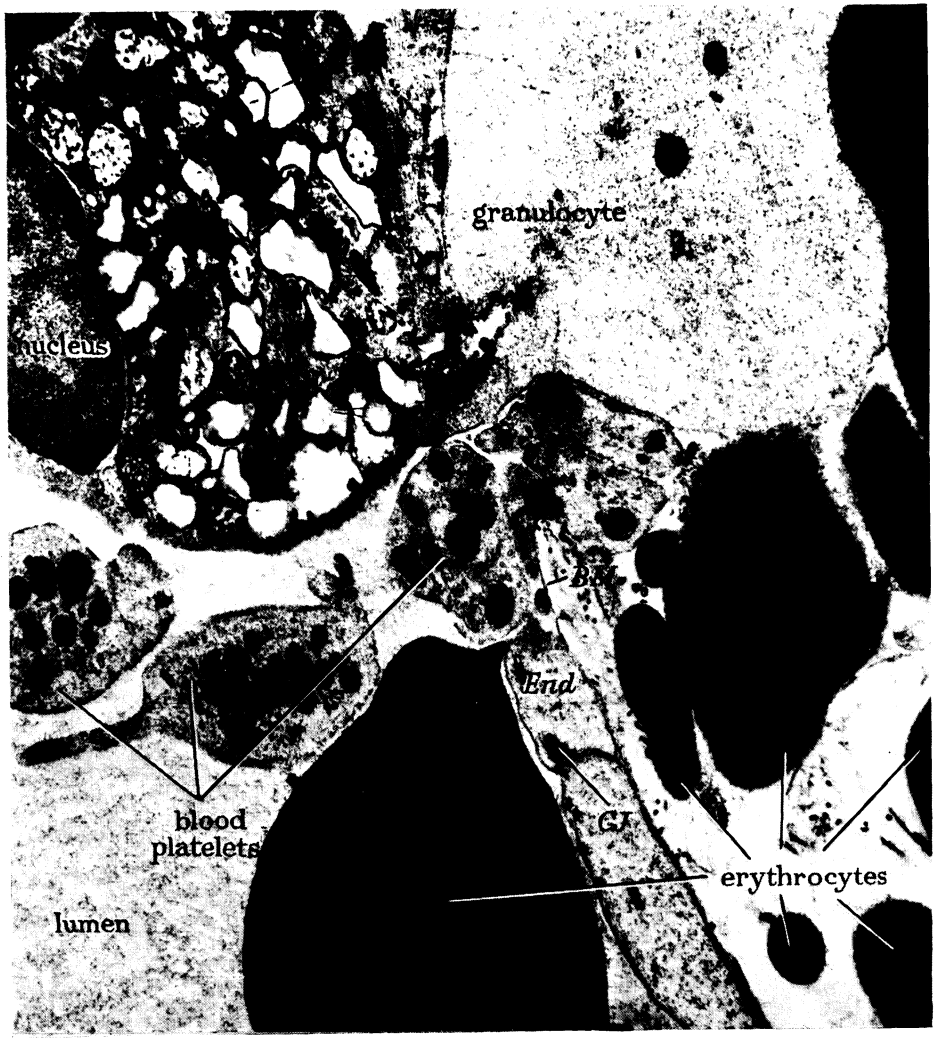

FIGURE 16. Wall of an immature vessel with a granulocyte, an erythrocyte and blood platelets passing through the endothelium (*End*) near a cell junction (*CJ*) into the extravascular space. The basement membrane (*BM*) is being traversed by the granulocyte and platelets, but it is still present across the lower part of the gap (as seen in the figure) and appears to be partly obstructing the passage of the various formed elements of the blood. Phosphotungstic acid; Araldite (× 16 500).

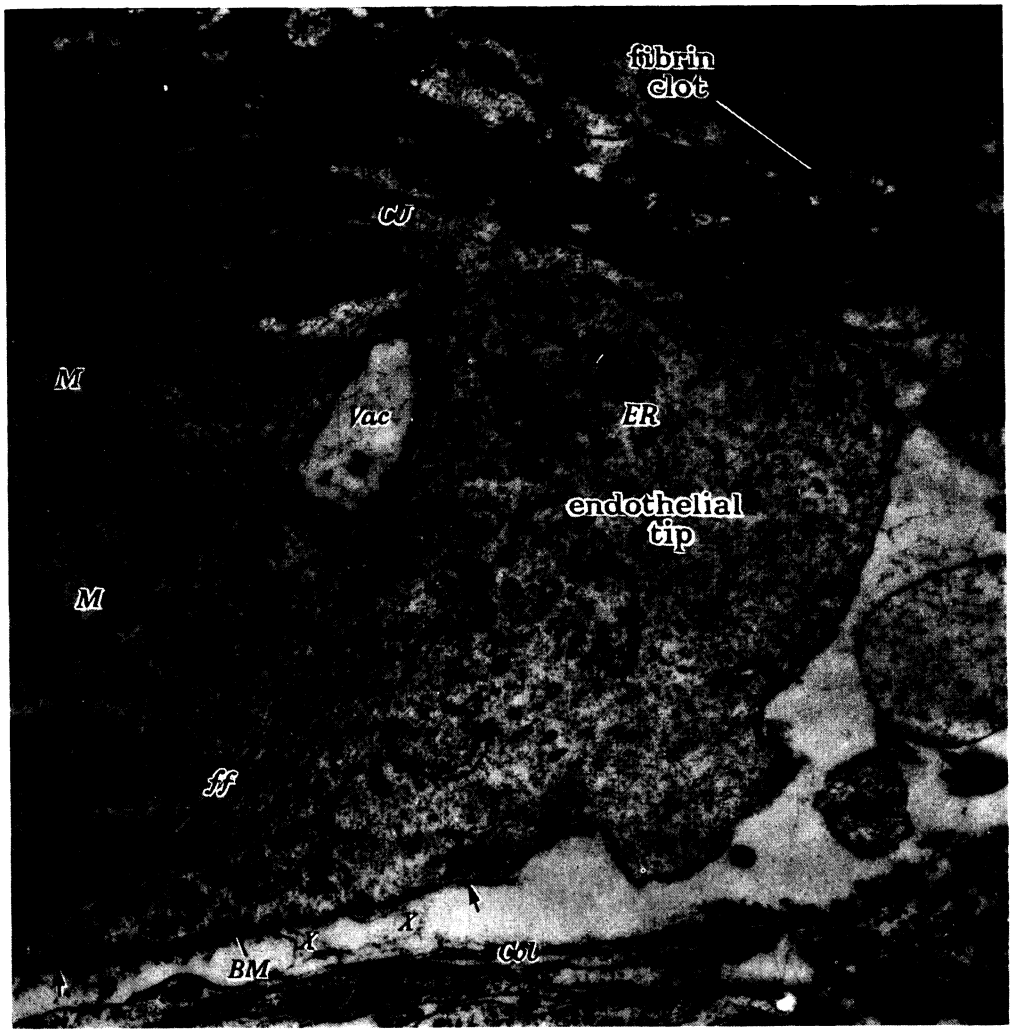

FIGURE 17. Endothelial tip of a vessel invading the fibrin clot. The extent of the basement membrane (*BM*) is indicated by arrows. This incomplete basement membrane has a frayed appearance, and at *XX* the frayed portion can be traced towards a region where very early collagen fibrils (*Col*) are present. *CJ*, Endothelial cell junction; *ER*, endoplasmic reticulum; *ff*, finely fibrillar region of cytoplasm; *M*, mitochondria; *Vac*, vacuole. Phosphotungstic acid; Araldite (×18000).

FIGURE 18. Mitosis of an endothelial cell situated just proximal to tip of a young vessel. Arrow indicates projection from the basal surface of the cell; *CJ*, cell junction; *End*, endothelium; *M*, mitochondria. Phosphotungstic acid; Araldite (×5500).

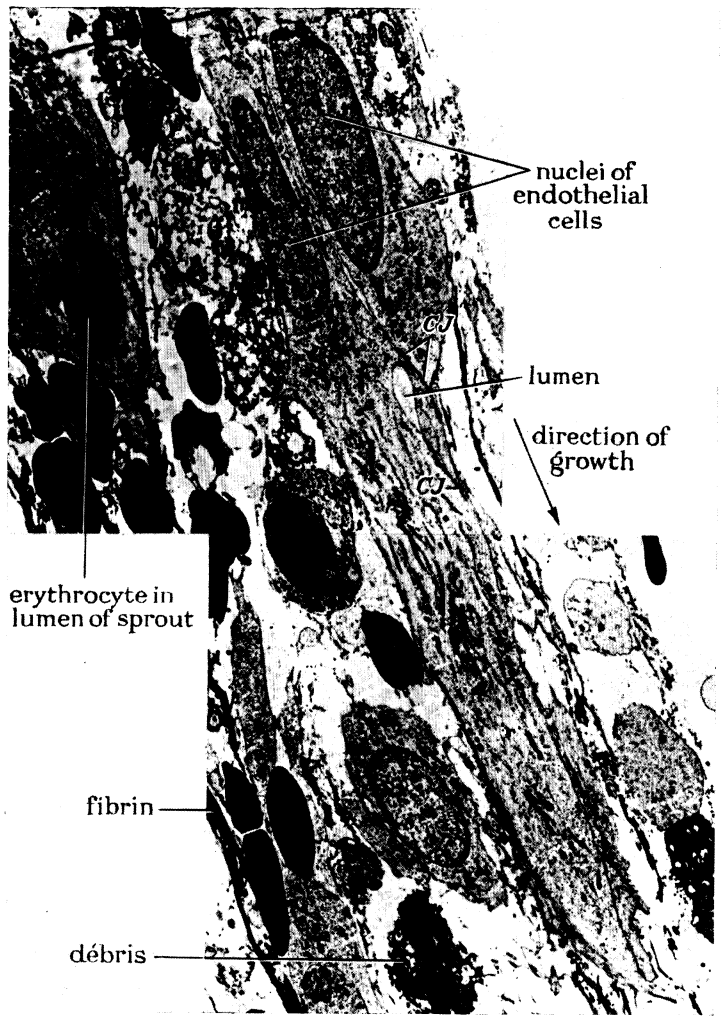

FIGURE 19. A cord of apposed endothelial cells is invading region of fibrin clot and débris in the direction indicated by the arrow. A slit-like lumen is present between two cells of the cord. Typical endothelial cell junctions are present (*CJ*). On the left is another sprout with a single red cell in its lumen. Phosphotungstic acid; Araldite (× 4000).

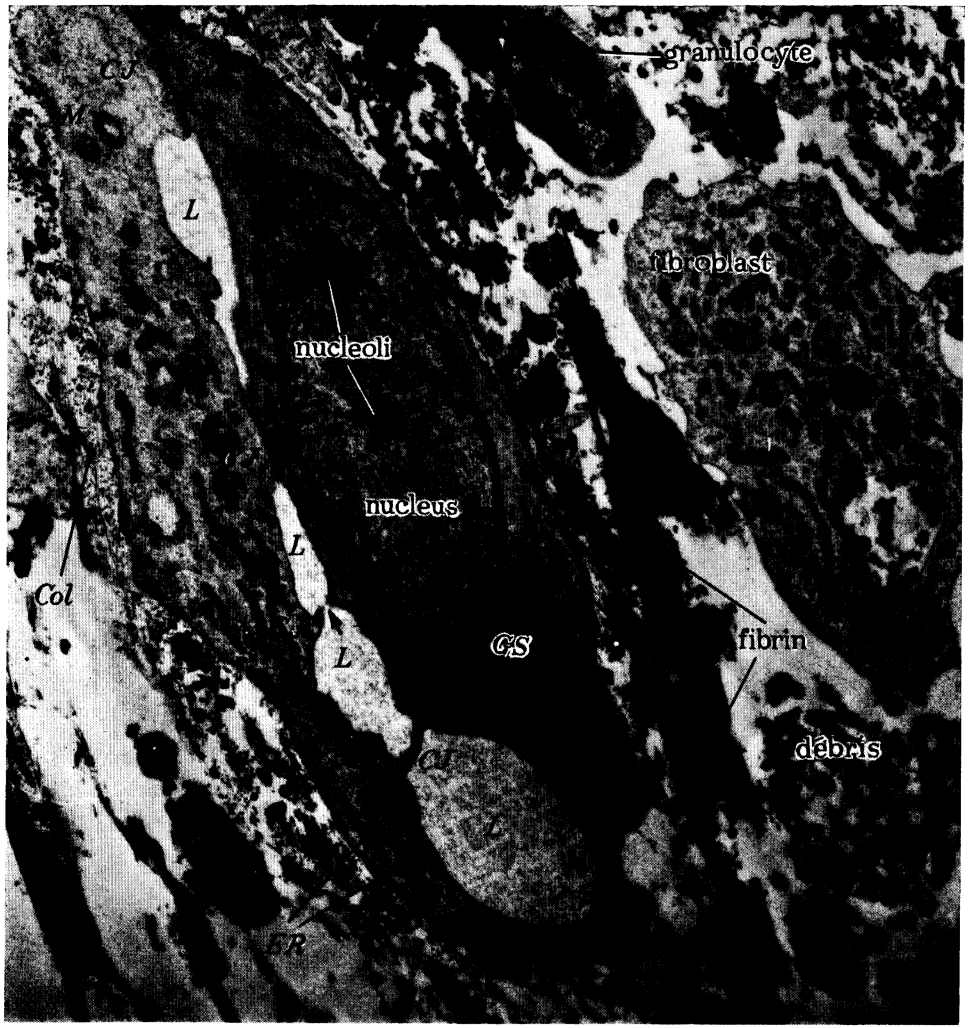

FIGURE 20. Endothelial sprout penetrating fibrin clot, with four small spaces (*L*) present between two endothelial cells. At arrow a narrow septum between two of the spaces is perforated. *Col*, Collagen; *CJ*, endothelial cell junctions (5); *ER*, endoplasmic reticulum; *GS*, Golgi substance; *M*, mitochondria. Phosphotungstic acid; Araldite (× 8500).

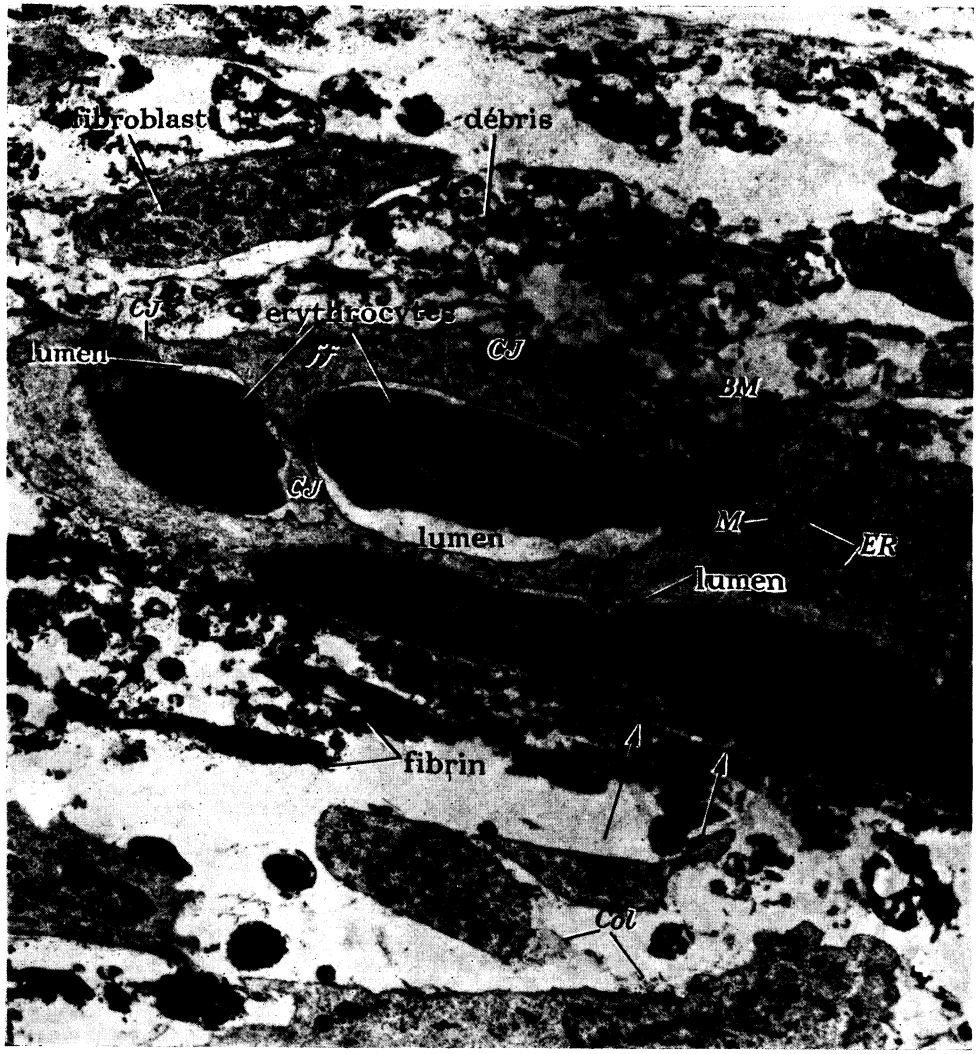

FIGURE 21. Endothelial sprout invading fibrin clot. In three places a lumen containing erythrocytes can be seen. Apparent defects in the wall of the lowest lumen are indicated by arrows. The two upper lumina are contained by the same two endothelial cells, which share 3 cell junctions (*CJ*). *BM*, Basement membrane; *Col*, collagen; *ER*, endoplasmic reticulum; *ff*, fibrillar region of cytoplasm; *M*, mitochondria. Phosphotungstic acid; Araldite (× 6000).

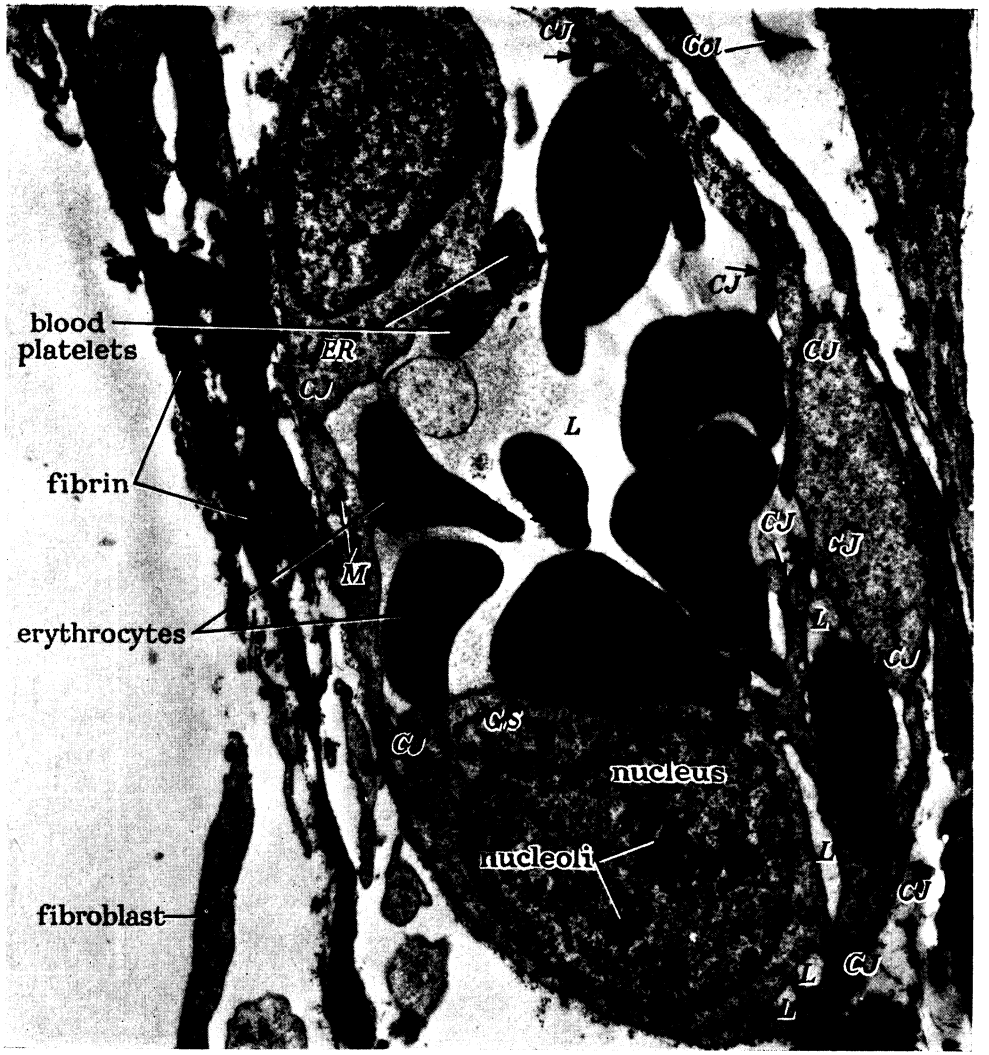

FIGURE 22. Endothelial sprout invading fibrin clot. Lumina (*L*) can be seen in five places one being much larger than the others. Cell junctions (*CJ*) are numerous and the three indicated by arrows are probably at sites where there were previously septa across the largest lumen. The four smaller lumina were probably destined to enlarge and coalesce, by loss of septa and separation of junctions, until one continuous lumen remained, bounded by the endothelial cells shown here. *Col*, collagen; *ER*, endoplasmic reticulum; *GS*, Golgi substance; *M*, mitochondria. Phosphotungstic acid; Araldite (× 8000).

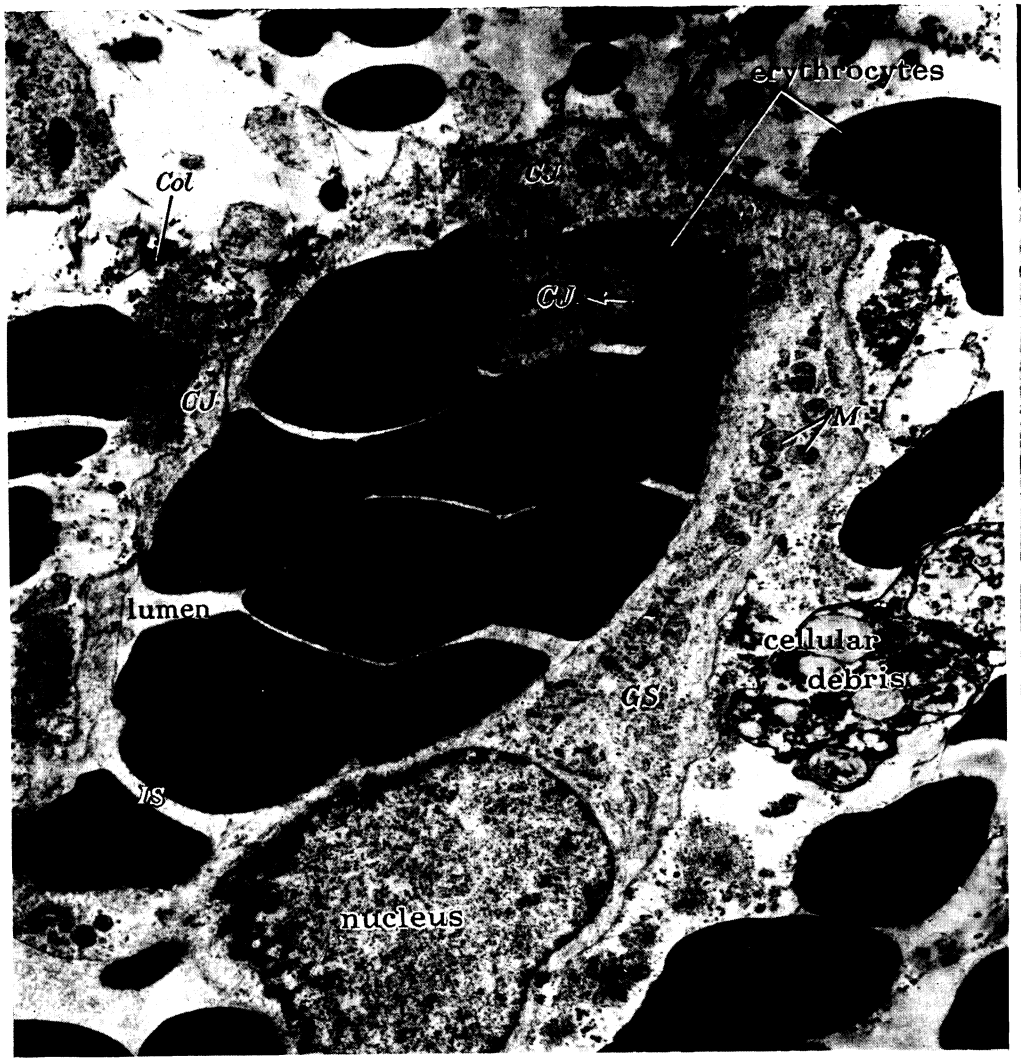

FIGURE 23. A saccular sprout. A similar vessel *in vivo* is shown in figure 3, plate 26. *Col*, Collagen; *CJ*, endothelial cell junction; *GS*, Golgi substance; *IS*, projection of endothelial cell spanning lumen of sprout; arrow indicates small luminal slit; *M*, mitochondria. Phosphotungstic acid; Araldite (× 8500).

FIGURE 24. Early stage in the intercalation of a cell (with labelled nucleus) into the endothelial wall of a vessel with lumen (*L*) containing erythrocytes. Three smaller lumina are marked (*L*) and there are several small slits (indicated by arrows) developing in relation to the nucleated endothelial cell. By enlargement of these spaces, with the accompanying disappearance of septa and cell junction (*CJ*), a stage such as that illustrated in figure 21, plate 35 would be reached. *Col*, Collagen; *ER*, endoplasmic reticulum; *M*, mitochondrion. Phosphotungstic acid; Araldite (× 9000).

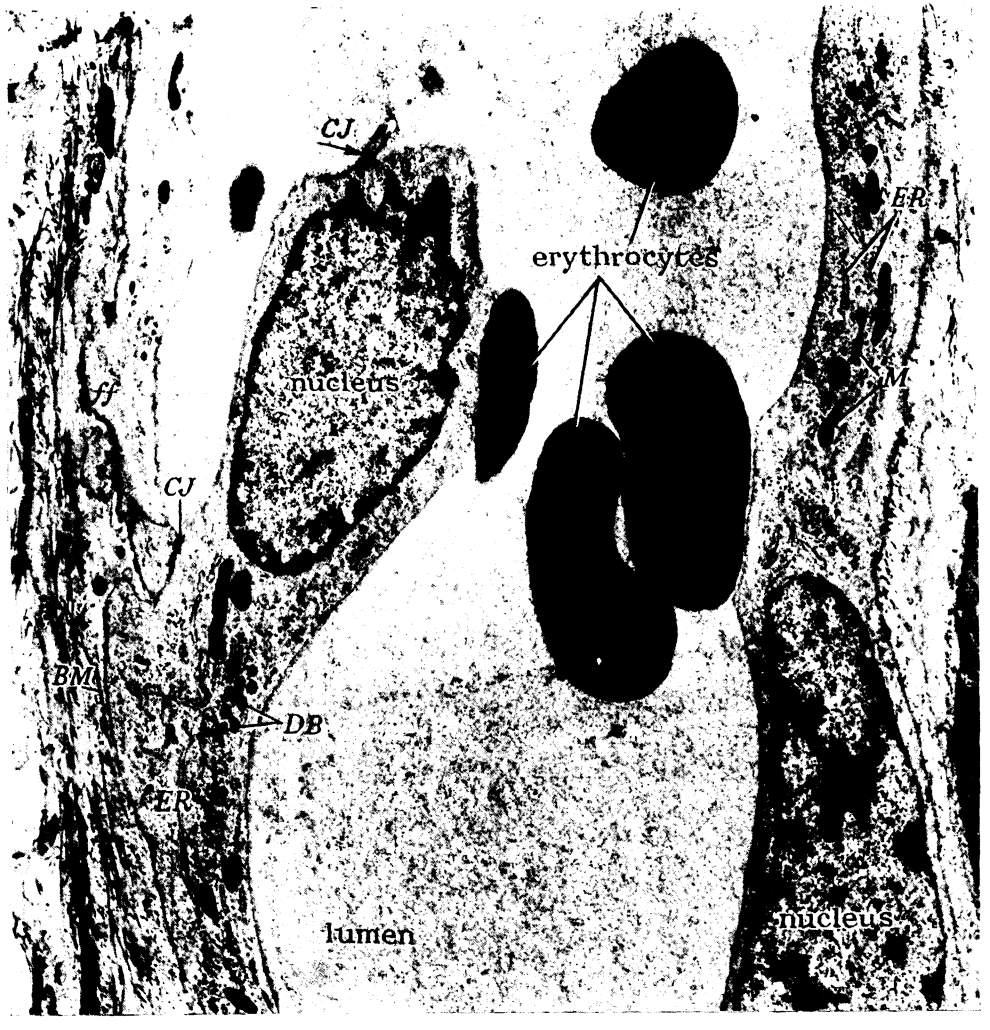

FIGURE 25. Late stage of the process of intercalation of an endothelial cell into the wall of a vessel with patent lumen (cf. figure 5, plate 27). Arrow indicates a cell junction (*CJ*) recently deprived of connexions, associated with an endothelial projection that had previously acted as septum dividing the lumen. *BM*, Basement membrane; *Col*, collagen; *DB*, dense cytoplasmic inclusion bodies; *ER*, endoplasmic reticulum; *ff*, fibrillary region of cytoplasm; *M*, mitochondria. Phosphotungstic acid; Araldite (× 8000).

FIGURE 26. A region where two endothelial sprouts (*Sp* I, *Sp* II) within the fibrin clot have united by cell junctions (*CJ*). The lumen of sprout II is filled with tightly packed erythrocytes, whilst the lumen of sprout I is a mere slit (*L*) within the cord of closely apposed cells. *ER*, Endoplasmic reticulum; *ff*, fibrillary region of cytoplasm; *GS*, Golgi substance; *M*, mitochondria. Phosphotungstic acid; Araldite (× 8000).

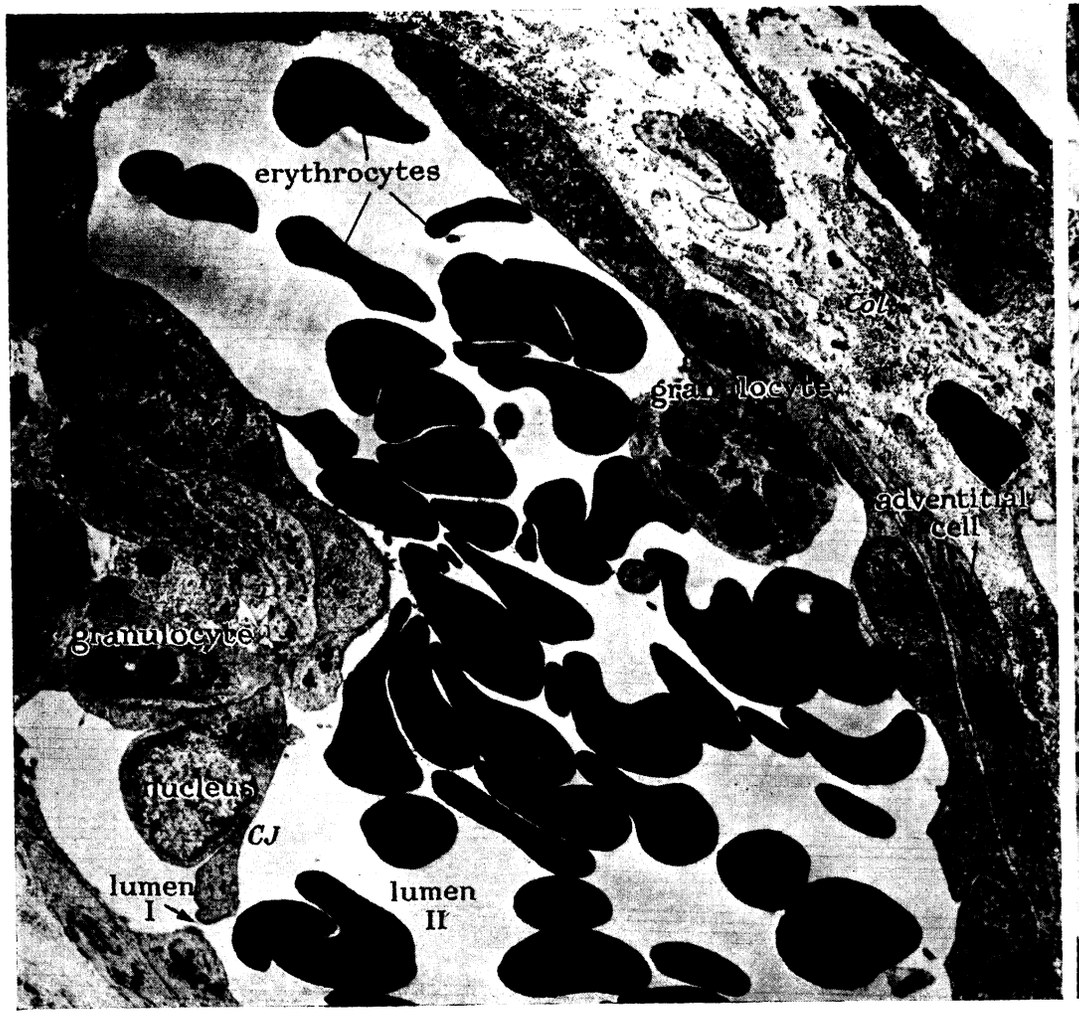

FIGURE 27. Immature vessels. The two lumina present (I and II) are connected by a small channel (arrow) produced by the separation of the cells forming the dividing septum. *Col*, Collagen. Phosphotungstic acid; Araldite (× 4000).

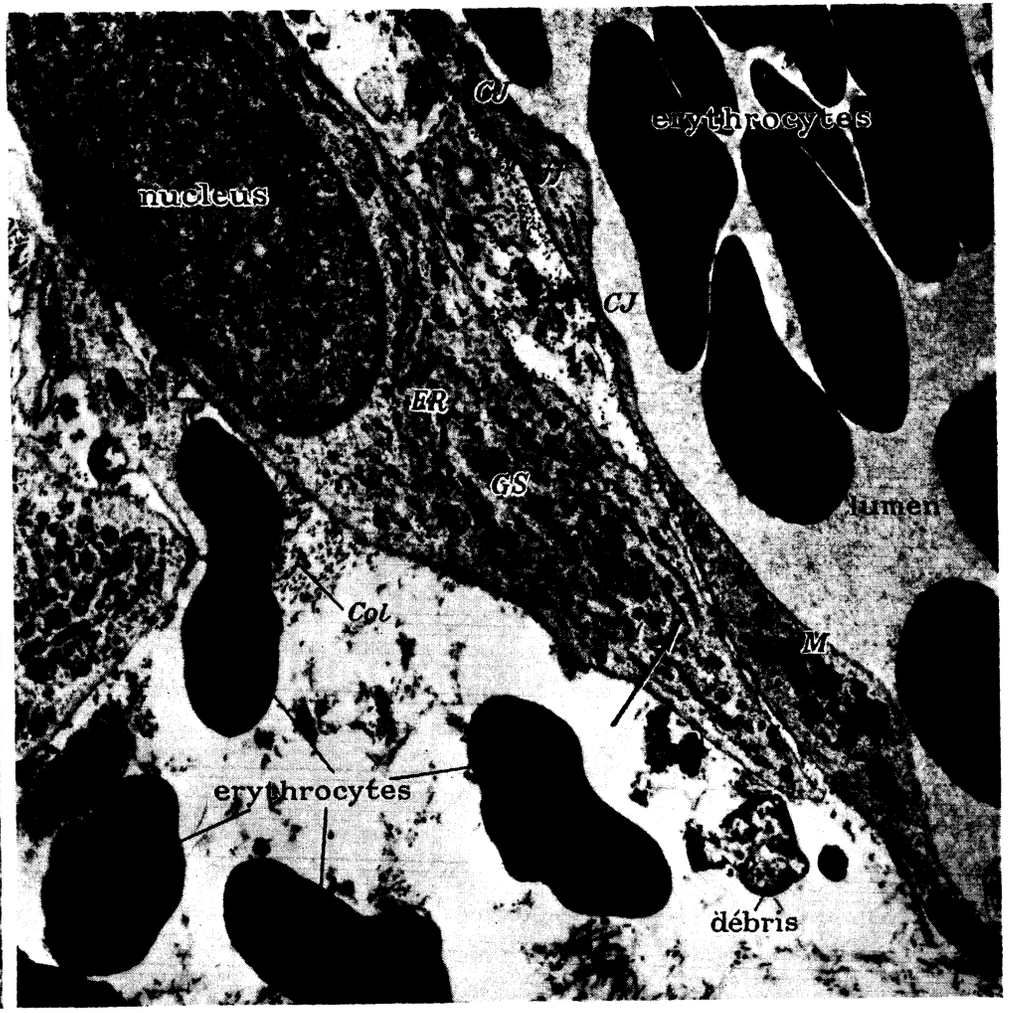

FIGURE 28. Large fibroblast-like cell (with nucleus) lying in close relation through one tapered extremity (arrow) to the thin endothelial lining of a vessel with a wide lumen. *Col*, Collagen; *CJ*, cell junction; *ER*, endoplasmic reticulum; *ff*, fibrillary region of cytoplasm; *GS*, Golgi substance; *M*, mitochondria. Phosphotungstic acid; Araldite (× 8750).

FIGURE 29. Adventitial cell lying in close relation to the endothelium of a vessel. The adventitial cell possesses a basement membrane (*BM*) and contains stored granules of Thorotrast (*TG*) in several sharply localized masses. *Col*, Collagen; *CJ*, cell junction; *ER*, endoplasmic reticulum; *ff*, fibrillary region of cytoplasm; *M*, mitochondria. Phosphotungstic acid; Araldite (× 17 500).

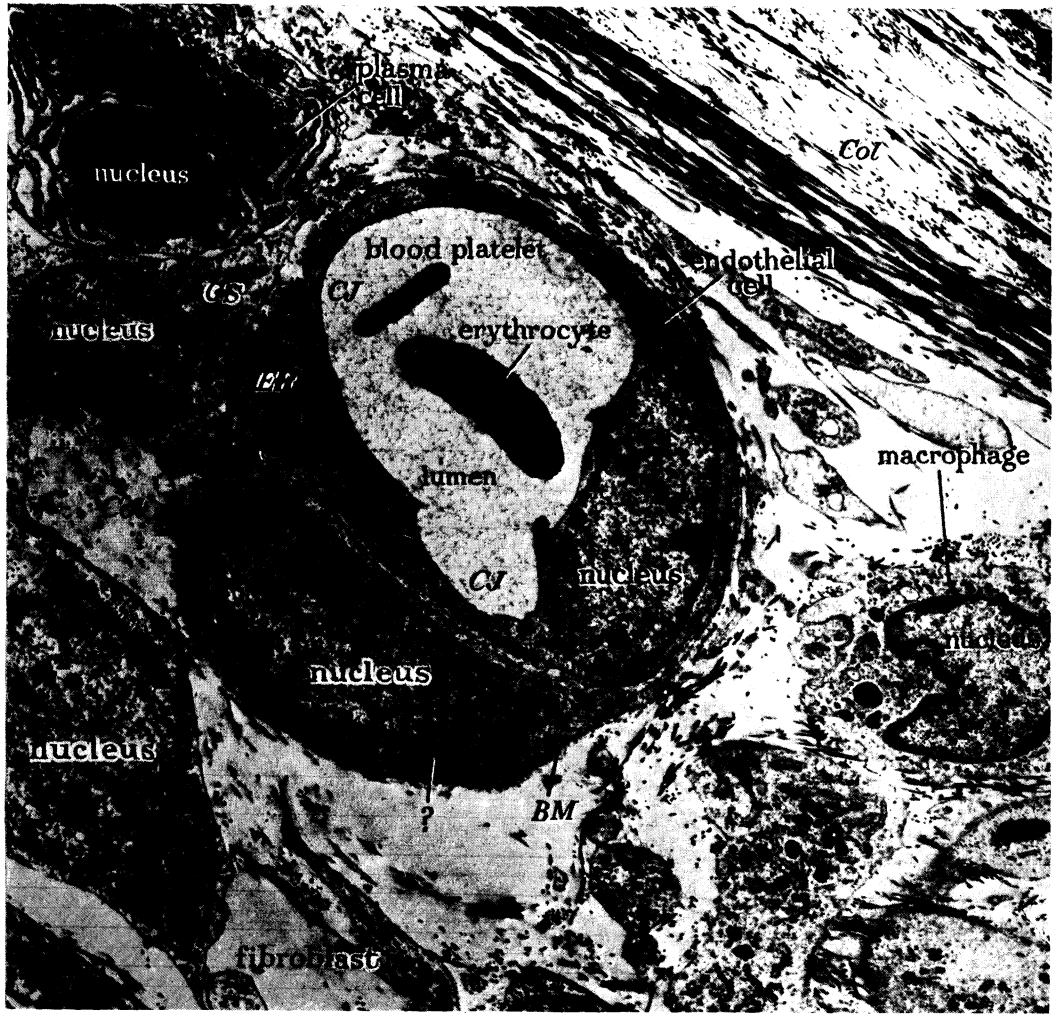

FIGURE 30. Small vessel containing an erythrocyte and platelet within its lumen. A cell marked (?) is disposed in a mainly circular orientation around this vessel (a feature of vascular smooth muscle). This cell is invested by a basement membrane (*BM*) (a feature of both smooth muscle (figure 31, plate 40) and adventitial cells (figure 29)). It possesses much endoplasmic reticulum (*ER*) and numerous mitochondria *M* and has little or no finely fibrous material in its cytoplasm (all features of an adventitial rather than a smooth muscle cell). *Col.* Collagen; *CJ*, cell junction; *GS*, Golgi substance. Phosphotungstic acid; Araldite (× 8250).

FIGURE 31. Wall of an arteriole from a chamber 7 weeks old. The two elements marked (*SM*) are parts of the same smooth muscle cell and are connected at point *X*. Features that identify smooth muscle cells are (1) a highly developed system of fine intracytoplasmic fibrils with evidence of longitudinal orientation (*ff*), (2) numerous pinocytic vesicles (arrows), (3) investment by a system of basement membranes (*BM*). *ER*, Endoplasmic reticulum; *M*, mitochondria; *NM*, nuclear membrane. Epikote 812; uranyl acetate (× 27 000).

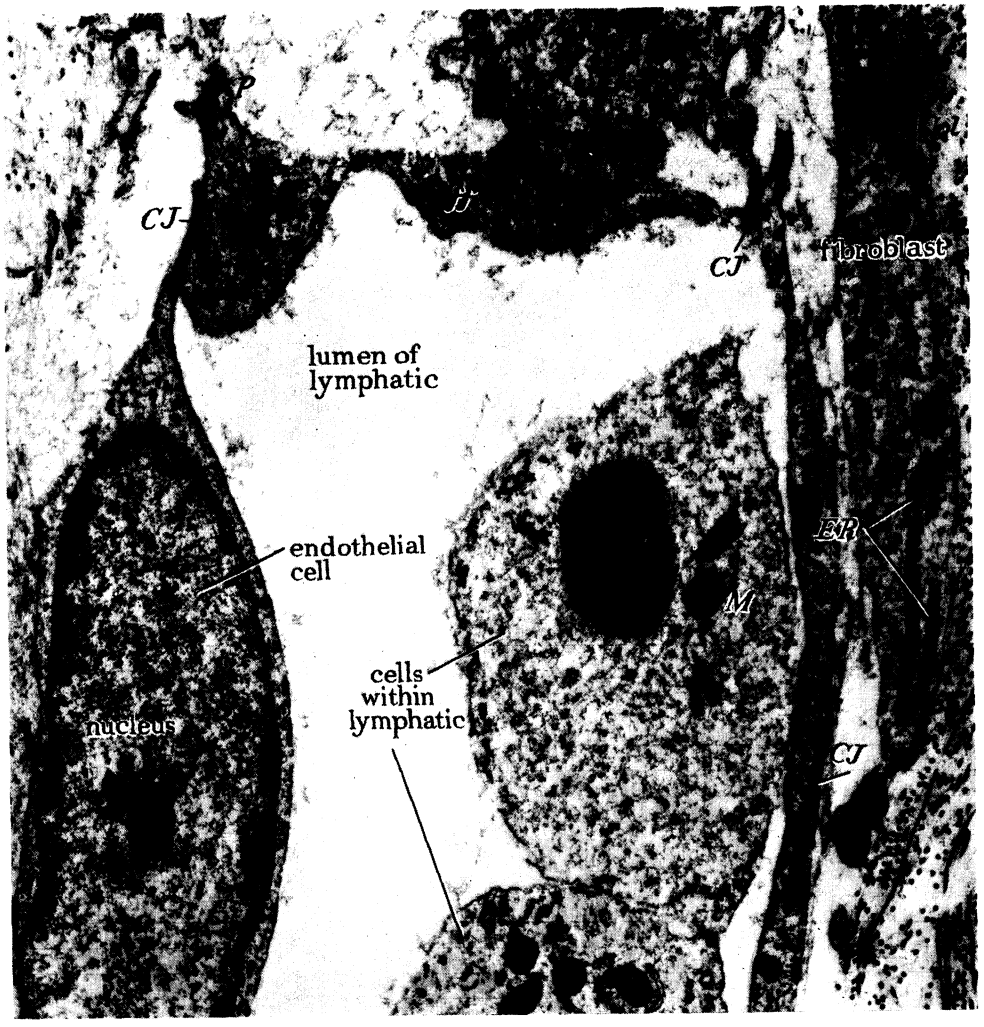

FIGURE 32. Region near the growing tip of a lymphatic vessel with walls lined by endothelium which in places is very thin. The endothelial lining possesses relatively broad based projections (*P*) extending into the extravascular space. *CJ*, Cell junction; *Col*, collagen; *ER*, endoplasmic reticulum; *ff*, fibrillary region of cytoplasm; *M*, mitochondria. Phosphotungstic acid; Araldite (× 15 000).

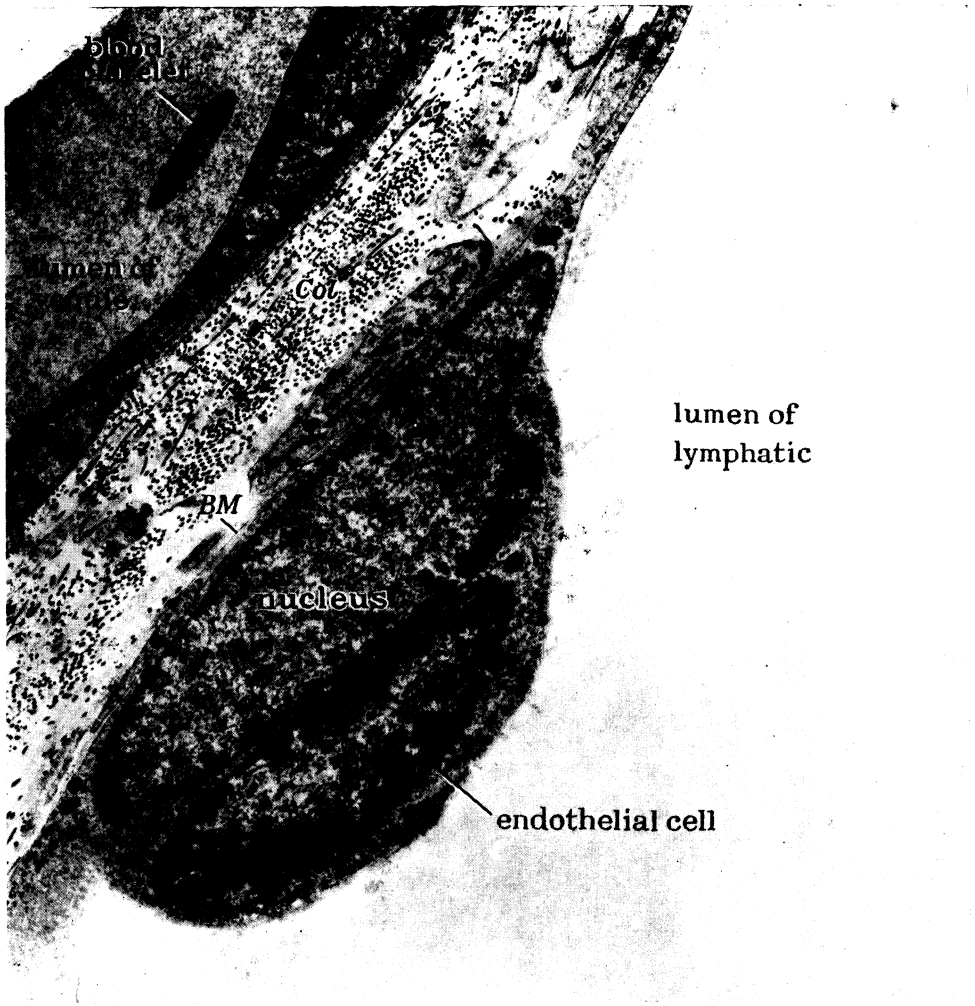

FIGURE 33. Large lymphatic and neighbouring venule from a fully healed chamber (52 days after insertion). This lymphatic had been observed for some time. Compared with that in figure 32, plate 40, the endothelium contains few organelles. The nucleus projects into the lumen. The basement membrane (*BM*) is poorly developed compared to that of a blood vessel of the same calibre. *Col*, Collagen. Phosphotungstic acid; Araldite (× 9750).

FIGURE 34. Wall of a lymphatic vessel from an ear chamber that had been fully healed for 2 months before a series of Thorotrast injections was begun. Oval clumps of Thorotrast granules (*TG*) are numerous in the endothelial cytoplasm. Note absence of basement membrane. *Col*, Collagen; *GS*, Golgi substance; *M*, mitochondria; *NM*, nuclear membrane. Phosphotungstic acid; Araldite (× 25 500).

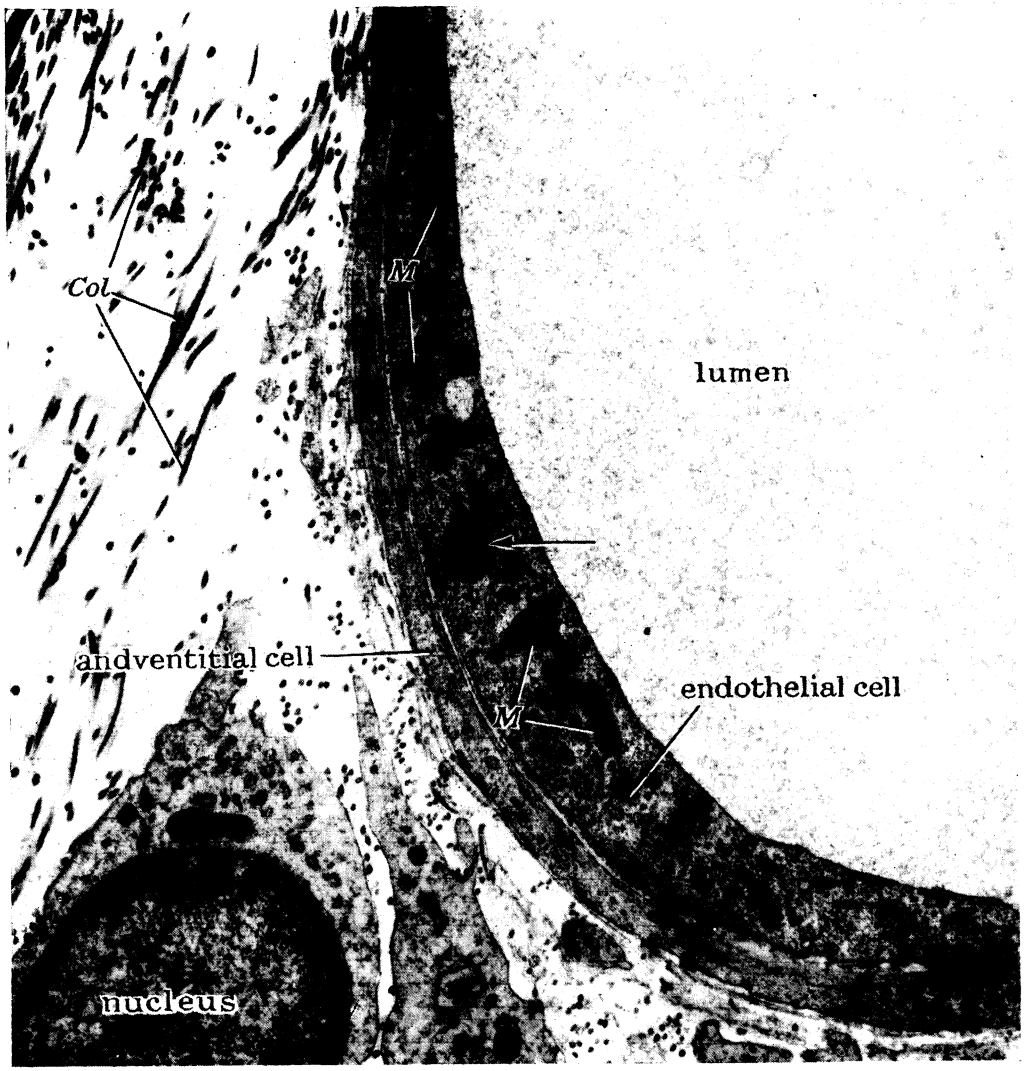

FIGURE 35. Venule from the same chamber as figure 34, plate 41. Within the endothelium is a single clump of Thorotrast granules (arrow). *Col*, Collagen; *M*, mitochondria. Phosphotungstic acid; Araldite (× 16 500).

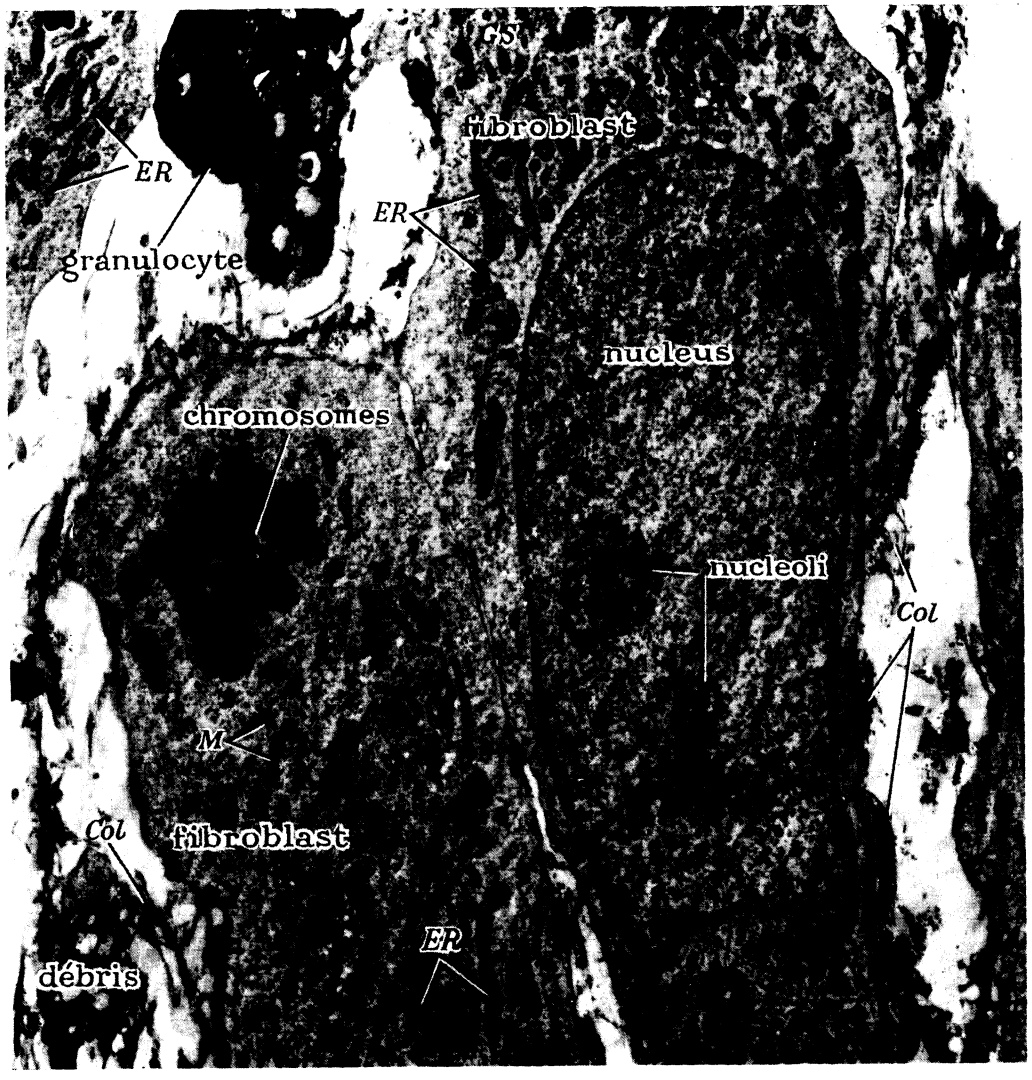

FIGURE 36. Fibroblasts invading fibrin clot and débris. The cell on the left is in mitosis (telophase) and the chromosomes may be recognized. The fibroblast on the right has an elongated nucleus with two well-developed 'skein-like' nucleoli. The granulocyte shows evidence of necrosis (loss of cytoplasmic detail, increased osmiophilia). *Col*, Collagen; *ER*, endoplasmic reticulum; *GS*, Golgi substance; *M*, mitochondria. Phosphotungstic acid; Araldite (× 8250).

FIGURE 37. Several cells invading a region of haemorrhage and debris. A fibroblast is present with nucleus, well-developed endoplasmic reticulum (*ER*) and numbers of mitochondria (*M*) (one of which (*) is trefoil in shape). This cell has a variety of inclusions in its cytoplasm (arrows) and appears to be encircling a large clump of debris. *Col*, Collagen. Phosphotungstic acid; Araldite(× 8000).

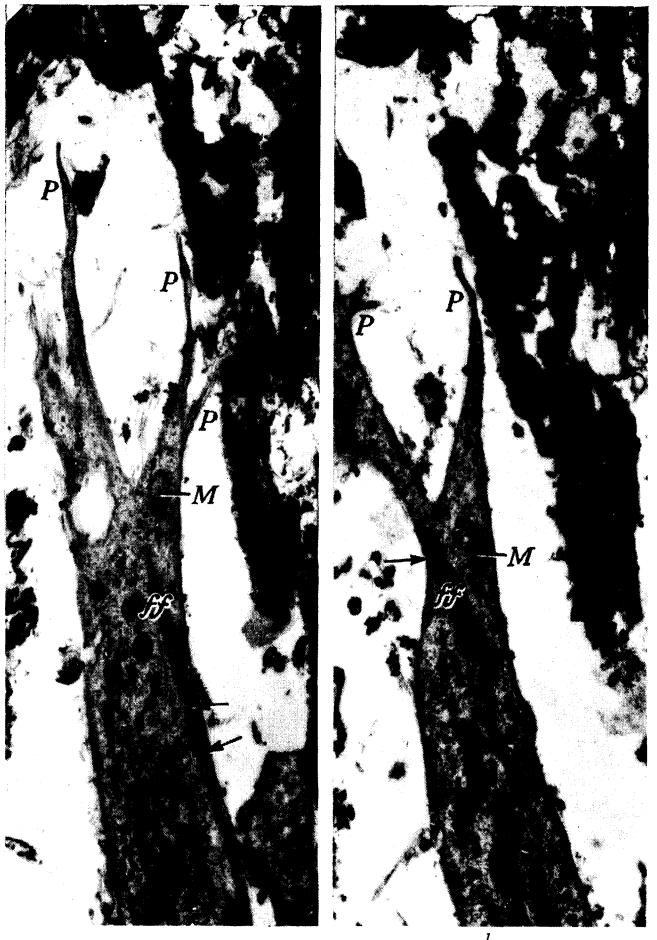

a *b*

FIGURE 38 *a*, *b*. Two sections through the same fibroblast at different levels. It contains a sharply defined fibrillary region (*ff*) 0·4 μm in width which would be an optically visible structure. By comparing the two figures the fibrillary tract may be traced as a bundle running into one of the fine processes of the fibroblast (*P*). This tract is considered to correspond to a 'fibroglial' fibre of Mallory. Arrows indicate regions of coalescence of fibrils. *M*, mitochondrion. Phosphotungstic acid; Araldite (× 6500).

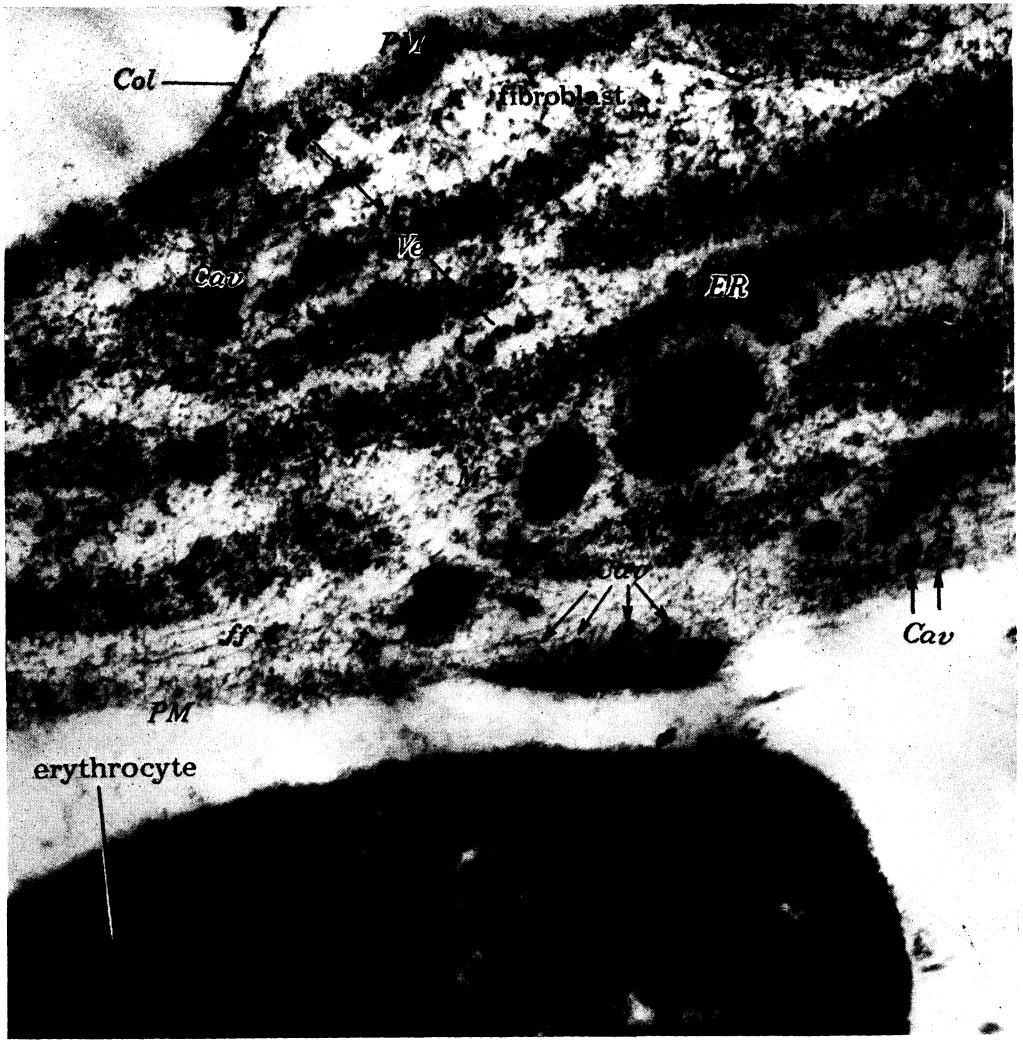

FIGURE 39. Part of a fibroblast and an erythrocyte. Medium-sized vesicles (*Ve*) and caveolae (*Cav*) are indicated by arrows at the plasma membrane (*PM*) of the fibroblast. These structures are very similar in appearance to the vesicles closely related to the endoplasmic reticulum in figure 40. The diameter of the vesicles in this micrograph is 54·5 nm. The vesicles and caveolae are most numerous at regions where fibrillar and collagenous material (*Col*) are related to the plasma membrane (*PM*) of the fibroblast. *ER*, Endoplasmic reticulum; *M*, mitochondrion; *ff*, fibrillary elements of cytoplasm. Phosphotungstic acid; Araldite (×46000).

FIGURE 40. Juxtanuclear region of a fibroblast in healing tissue. Numbers of vesicles are present, some of which (arrows) appear to be budding from the endoplasmic reticulum (*ER*). These vesicles are up to 54·5 nm in diameter and are bounded by dense membranes. Their contents are of moderate electron density. They are dispersed singly, in clusters and in strings through the cytoplasm. *ff*, Fibrillary component of cytoplasm. Phosphotungstic acid; Araldite (×46000).

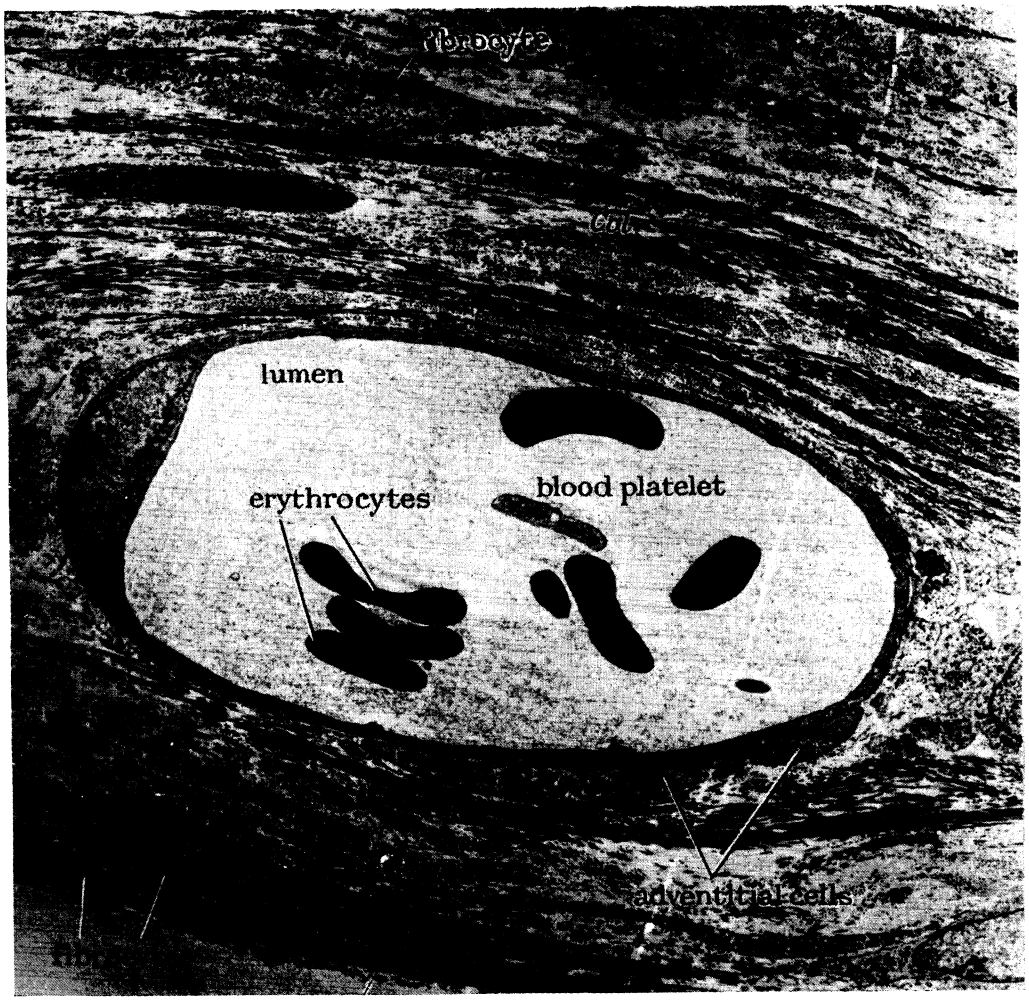

FIGURE 41. Mature venule of scar tissue. Adventitial cells are shown. Dense lamellae of collagen (*Col*) are present in the extravascular regions together with elongated fibrocytes. Phosphotungstic acid; Araldite (× 3500).

FIGURE 42. Dwindled polymorph, the 'small round cell' of Clark *et al.* (1936), in the lumen of a lymphatic vessel. *ER*, Endoplasmic reticulum, which in the dwindled polymorph can be seen as lines of pinched off vesicles (arrows) apparently formed by the fusion of the 'ruffled' plasma membrane. *ff*, Fibrillary region of cytoplasm; *Col*, collagen; *M*, mitochondria. Phosphotungstic acid; Araldite (× 18 000).

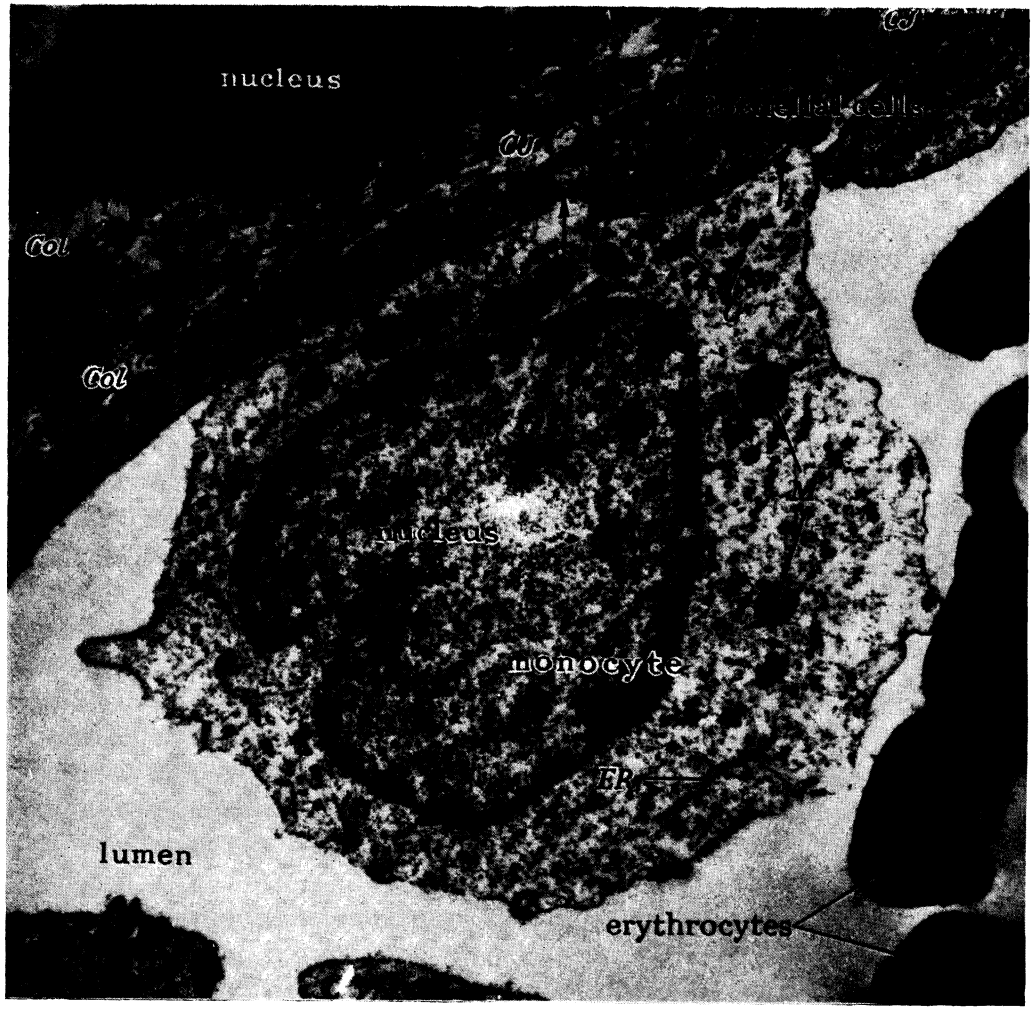

FIGURE 43. A monocyte adhering to the endothelium of a blood vessel. The arrows indicate two small pseudopodia very closely related to cell junctions (*CJ*). *Col*, Collagen; *ER*, endoplasmic reticulum; *G*, dense granules in monocyte cytoplasm; *M*, mitochondria. Phosphotungstic acid; Araldite (× 14 000).

FIGURE 44. Small macrophage with large quantities of Thorotrast (*TG*) segregated within its cytoplasm. Ruffled extensions of the cell give rise, through fusion, to membrane-bounded vesicles (arrows). *Col*, Collagen; *ER*, endoplasmic reticulum; *M*, mitochondria. Phosphotungstic acid; Araldite (× 16 500).

FIGURE 45. Parts of 2 macrophages and 1 fibroblast. The surfaces of the macrophages are thrown into a complex series of folds or 'ruffles' (*R*). Two elements of the ruffled border show fusion of their apposed surfaces at *RF*. At *X* ruffles belonging to the two different macrophages are in extremely close proximity and are almost joined. Highly fibrillary tracts (*ff*) curve through the cytoplasm; they measure up to 0·4 μm in width, and therefore may correspond to optically visible regions of the cells. The endoplasmic reticulum of the macrophages shows signs of orientation (e.g. at *ER*). *GS*, Golgi substance; *M*, mitochondria. Phosphotungstic acid; Araldite ($\times$ 11 000).

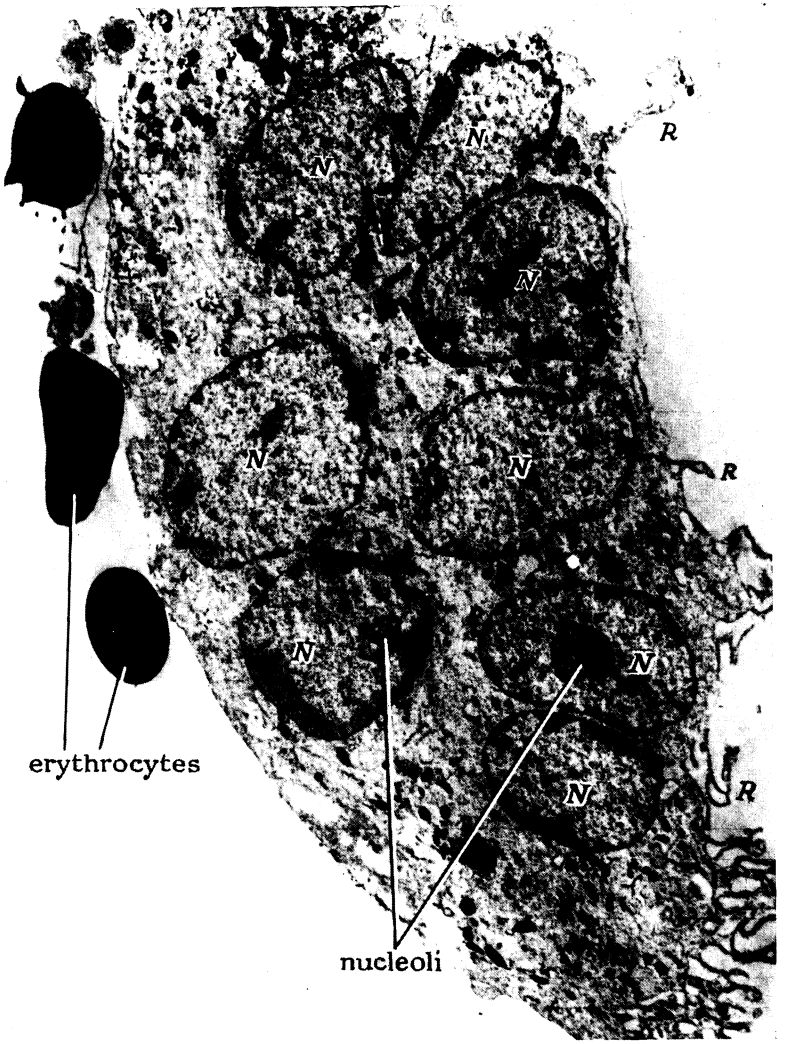

FIGURE 46. A multinucleate giant cell, with adjacent erythrocytes. The giant cell has 8 polygonal nuclei (*N*) in this section. Nucleoli are identified in two of the nuclei and are well-developed mesh-like structures. The diameter of the larger nucleolar profile is 1·5 μm. The surface of the giant cell is thrown into a complex series of ruffles (*R*). Phosphotungstic acid; Araldite ($\times$ 5500).

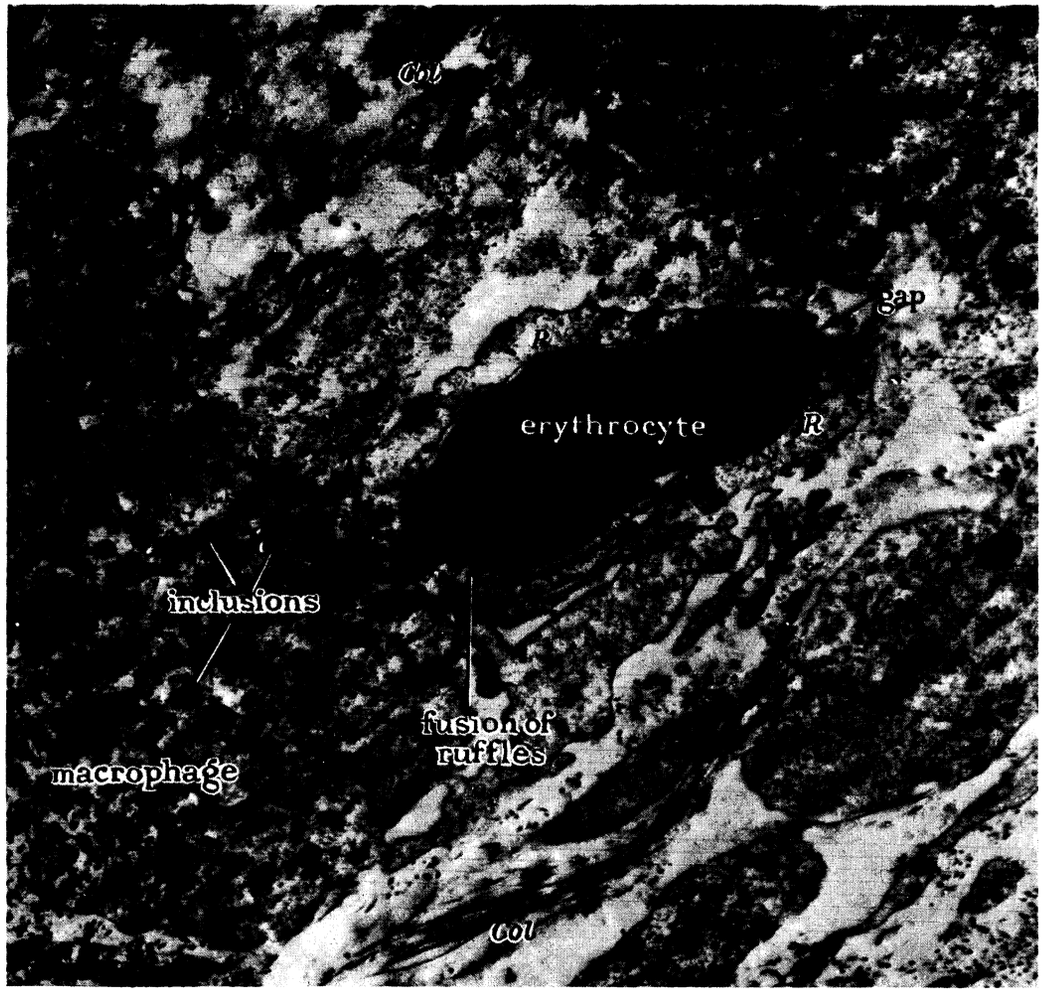

FIGURE 47. A macrophage which contains numerous pleomorphic inclusions and the cytoplasm of which extends into a number of ruffled pseudopodia (*R*). An erythrocyte is enclosed by several of these ruffles except for a small gap. The ruffles enclosing the erythrocyte show evidence of fusion of apposed surfaces. The end of the process would be fusion of the tips of the ruffles across the gap, and the erythrocyte would then be contained in a membrane-bounded cavity within the macrophage. *Col*, Collagen. Phosphotungstic acid; Araldite (× 13 500).

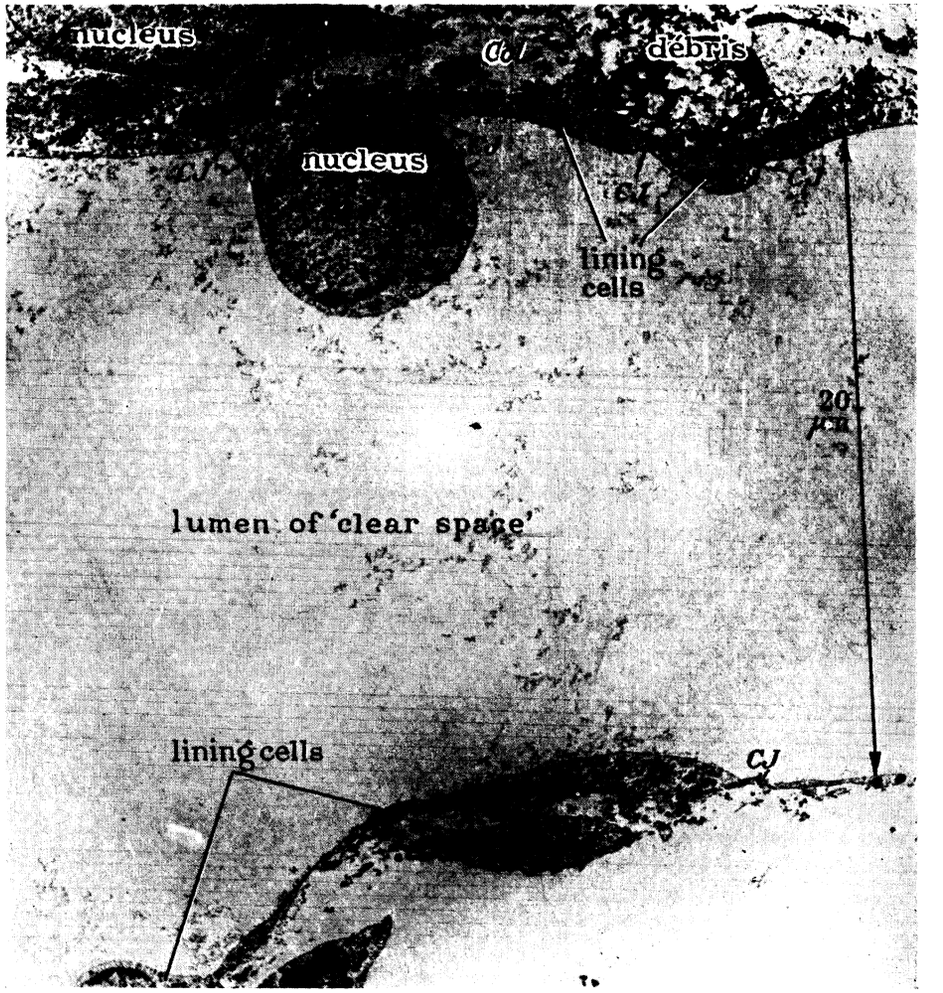

FIGURE 48. Section through part of a 'clear space' in advance of the growing fringe of vessels (see figure 10, plate 29). Collagen fibres (*Col*) and cell débris are present in relation to the wall of the 'clear space', which is lined by a continuous pavement of flattened cells closely abutting edge to edge (*CJ*). There is no related basement membrane. The smallest dimension of this structure (between arrows), measured in the same direction as the depth of the ear chamber is 20 μm. Phosphotungstic acid; Araldite (× 4000).

work, were seen by Ross & Benditt who propounded the hypothesis that these vesicles and caveolae might constitute a possible means of release of collagen precursor from the fibroblast. The present work may be interpreted as affording some confirmation for this hypothesis of 'reverse pinocytosis' during collagen secretion by fibroblasts.

Lining of clear spaces

The cells lining the clear spaces had few features in common with recently formed endothelium but did closely resemble the endothelium-like cells derived from monocytes within ligated arteries that were described by Buck (1961). The lining pavement of cells was produced, it is presumed, in a space in the fibrin clot which was formed by a combination of local enzymatic activity and of scouring by pulsating streams of fluid present in advance of the growing fringe. The boundaries of the space so formed would then present a surface suitable for the production of a mesothelium-like layer (Clarke 1914; Willmer 1945). The transient character of the clear spaces, which rapidly disappeared once the fibrin clot was replaced by repair tissue, made it evident that these structures were dependent upon the particular conditions present in the fibrin meshwork and did not reflect any form of permanent cell differentiation.

I wish to express my gratitude to Professor Sir Howard Florey, P.R.S., for suggesting this research and for his help and interest throughout the course of this work.

I am greatly indebted to Dr A. G. Sanders for his instruction in rabbit ear chamber and allied techniques.

I wish to express my gratitude to Dr M. A. Jennings and Dr J. C. F. Poole for their assistance in preparing this paper for publication.

I am grateful also to Miss P. M. Taylor for valuable technical assistance, to Mr D. W. Jerrome for advice on light and electron microscope techniques, and to Mr S. Buckingham for assistance with photography.

References

Abell, R. G. 1946 The permeability of blood capillary sprouts and newly formed blood capillaries as compared to that of older blood capillaries. *Amer. J. Physiol.* **147**, 237.

Arey, L. B. 1936 Wound healing. *Physiol. Rev.* **16**, 327.

Beard, J. W. & Beard, L. A. 1927 The phagocytic activity of endothelium in the embryo chick. *Amer. J. Anat.* **40**, 295.

Bennett, H. S., Luft, J. H. & Hampton, J. C. 1959 Morphological classifications of vertebrate blood capillaries. *Amer. J. Physiol.* **196**, 381.

Billroth, T. 1856 *Untersuchungen über die Entwicklung der Blutgefässe.* Berlin.

Buck, R. C. 1958 Fine structure of endothelium of large arteries. *J. Biophys. Biochem. Cytol.* **4**, 187.

Buck, R. C. 1961 Intimal thickening after ligature of arteries, an electron microscopic study. *Circ. Res.* **9**, 418.

Caesar, R., Edwards, G. A. & Ruska, H. 1957 Architecture and nerve supply of mammalian smooth muscle tissue. *J. Biophys. Biochem. Cytol.* **3**, 867.

Cameron, D. A. 1961 The fine structure of osteoblasts in the metaphysis of the tibia of the young rat. *J. Biophys. Biochem. Cytol.* **9**, 583.

Cameron, G. R. 1952 *Pathology of the cell.* Edinburgh: Oliver and Boyd.

Caro, L. G. 1961 Electron microscopic radio autography of thin sections: The Golgi zone as a site of protein concentration in pancreatic acinar cells. *J. Biophys. Biochem. Cytol.* **10**, 37.

Carrel, A. & Ebeling, A. H. 1922 Pure cultures of large mononuclear leucocytes. *J. Exp. Med.* **36**, 365.

Caulfield, J. B. 1957 Effects of varying the vehicle for OsO_4 in tissue fixation. *J. Biophys. Biochem. Cytol.* **3**, 827.

Chalkey, H. W., Algire, G. H. & Morris, H. P. 1946 Effects of the level of dietary protein on vascular repair in wounds. *J. Nat. Cancer Inst.* **6**, 363.

Chapman, J. A. 1961 Morphological and chemical studies of collagen formation. I. The fine structure of guinea-pig granulomata. *J. Biophys. Biochem. Cytol.* **9**, 639.

Clark, E. R. 1936 Growth and development of function in blood vessels and lymphatics. *Ann. Intern. Med.* **9**, 1043.

Clark, E. R. & Clark, Eleanor L. 1937 Observations on living mammalian lymphatic capillaries—their relation to the blood vessels. *Amer. J. Anat.* **60**, 253.

Clark, E. R. & Clark, Eleanor L. 1939 Microscopic observations on the growth of blood capillaries in the living mammal. *Amer. J. Anat.* **64**, 251.

Clark, E. R. & Clark, Eleanor L. 1940 Microscopic observations on the extra-endothelial cells of living mammalian blood vessels. *Amer. J. Anat.* **66**, 1.

Clark, E. R. & Clark, Eleanor L. 1943 Caliber changes in minute blood vessels observed in the living mammal. *Amer. J. Anat.* **73**, 215.

Clark, E. R., Clark, Eleanor L. & Abell, R. G. 1933 Cytological studies on the new growth of blood capillaries in the living mammal. (Abstract.) *Anat. Rec.* **55** (suppl.), 50.

Clark, E. R., Clark, Eleanor L. & Rex, R. O. 1936 Observations on polymorphonuclear leukocytes in the living animal. *Amer. J. Anat.* **59**, 123.

Clark, E. R., Clark, Eleanor L. & Williams, R. G. 1934 Microscopic observations in the living rabbit of the new growth of nerves and the establishment of nerve-controlled contractions of newly formed arterioles. *Amer. J. Anat.* **55**, 47.

Clark, E. R., Kirby-Smith, H. T., Rex, R. O. & Williams, R. G. 1930 Recent modifications in the method of studying living cells and tissues in transparent chambers inserted in the rabbit's ear. *Anat. Rec.* **47**, 187.

Clarke, W. C. 1914 Experimental mesothelium. *Anat. Rec.* **8**, 95.

Corner, G. W. 1920 On the widespread occurrence of reticular fibrils produced by capillary endothelium. *Contr. Embryol. Carneg. Instn*, **9**, 87.

Dalton, A. J. & Felix, Marie D. 1954 Cytologic and cytochemical characteristics of the Golgi substance of epithelial cells of the epididymis—*in situ*, in homogenates and after isolation. *Amer. J. Anat.* **94**, 171.

Ebert, R. H. & Florey, H. W. 1939 The extravascular development of the monocyte observed *in vivo*. *Brit. J. Exp. Path.* **20**, 342.

Ebert, R. H., Florey, H. W. & Pullinger, B. D. 1939 A modification of a Sandison–Clark chamber for observation of transparent tissue in the rabbit's ear. *J. Path. Bact.* **48**, 79.

Epstein, M. A. 1957 The fine structural organization of Rous tumour cells. *J. Biophys. Biochem. Cytol.* **3**, 851.

Fawcett, D. W. 1959 The fine structure of capillaries, arterioles and small arteries. In *The Microcirculation* (Symposium on factors influencing exchange of substances across capillary wall), p. 1. Ed. Reynolds and Zweifach. University of Illinois Press.

Foot, N. C. 1921 Studies on endothelial reactions. V. The endothelium in the healing of aseptic wounds in the omentum of rabbits. *J. Exp. Med.* **34**, 635.

Foot, N. C. 1925 The endothelial phagocyte—a critical review. *Anat. Rec.* **30**, 15.

Frey-Wyssling, A. 1953 Submicroscopic morphology of protoplasm. Amsterdam, Houston, London, New York: Elsevier Publishing Co.

Glauert, Audrey M. & Glauert, R. H. 1958 Araldite as an embedding medium for electron microscopy. *J. Biophys. Biochem. Cytol.* **4**, 191.

Godman, G. C. & Porter, K. R. 1960 Chondrogenesis, studied with the electron microscope. *J. Biophys. Biochem. Cytol.* **8**, 719.

Gonzales, F. & Karnovsky, M. J. 1961 Electron microscopy of osteoclasts in healing fractures of rat bone. *J. Biophys. Biochem. Cytol.* **9**, 299.

Hadfield, G. 1951 Granulation tissue. *Ann. Roy. Coll. Surg. Eng.* **9**, 397.

Hay, Elizabeth D. 1958 The fine structure of blastema cells and differentiating cartilage cells in regenerating limbs of Amblystoma larvae. *J. Biophys. Biochem. Cytol.* **4**, 583.

Hodge, A. J. 1956 Effects of the physical environment on some lipoprotein layer systems and observations on their morphogenesis. *J. Biophys. Biochem. Cytol.* **2** (suppl.), 221.

Holfreter, J. 1947 Changes of structure and the kinetics of differentiating embryonic cells. *J. Morph.* **80**, 57.

Jackson, D. S. 1957 Connective tissue growth stimulated by Carageenin. I. The formation and removal of collagen. *Biochem. J.* **65**, 277.

Jackson, D. S., Flickinger, D. B. & Dunphy, J. E. 1960 Biochemical studies of connective tissue repair. *Ann. N.Y. Acad. Sci.* **86**, 943.

Jackson, Sylvia Fitton 1953 Fibrogenesis *in vivo* and *in vitro*. In *Nature and structure of collagen*, p. 140. Ed. Randall. London: Butterworths Scientific Publications.

Karrer, H. E. 1960 Electron microscope study of developing chick embryo aorta. *J. Ultrastructure Res.* **4**, 420.

Kisch, B. 1957 Electron microscopy of the capillary wall. II. Filiform processes of the endothelium. *Exp. Med. Surg.* **15**, 89.

Lewis, Margaret R. 1926 The formation of macrophages, epithelioid cells and giant cells from leucocytes in incubated blood. *Amer. J. Path.* **1**, 91.

Lewis, W. H. 1925–26 The transformation of mononuclear blood cells into macrophages, epithelioid cells and giant cells. *Harvey Lect.* **21**, 77. Baltimore: Williams and Wilkins.

Luft, J. H. 1961 Improvements in Epoxy resin embedding methods. *J. Biophys. Biochem. Cytol.* **9**, 409.

Lutz, B. R. & Fulton, G. P. 1958 Smooth muscle and blood flow in small blood vessels. In *Factors regulating blood flow*, p. 13. Ed. Fulton and Zweifach. American Physiological Society, Inc.

Mallory, F. B. 1903 A hitherto undescribed fibrillar substance produced by connective tissue cells. *J. Med. Res.* **10**, 334.

Marchesi, V. T. 1961 The site of leucocyte emigration during inflammation. *Quart. J. Exp. Physiol.* **46**, 115.

Marchesi, V. T. & Florey, H. W. 1960 Electron micrographic observations on the emigration of leucocytes. *Quart. J. Exp. Physiol.* **45**, 343.

Maximov, A. 1916 The cultivation of connective tissue of adult mammals *in vitro*. *Arch. Russ. Anat. Hist. Embryol.* **1**, 105.

Maximoff, A. 1917*a* De l'action stimulante de l'extrait de moelle osseuse sur la croissance et l'evolution des cellules dans les cultures de tissue lymphoide. *C.R. Soc. Biol., Paris*, **80**, 225.

Maximoff, A. 1917*b* Sur la culture *in vitro* du tissu lymphoïde des mammifères. *C.R. Soc. Biol., Paris*, **80**, 222.

Medawar, P. B. 1945 Size, shape and age. In Le Gros Clark, Sir W. E. & Medawar, P. B., Ed., *Essays on growth and form*, p. 157. Oxford: Clarendon Press.

Moore, D. H. & Ruska, Helmut 1957 The fine structure of capillaries and arteries. *J. Biophys. Biochem. Cytol.* **3**, 457.

Palade, G. E. 1952 A study of fixation for electron microscopy. *J. Exp. Med.* **95**, 285.

Palade, G. E. 1953*a* An electron microscope study of the mitochondrial structure. *J. Histochem. Cytochem.* **1**, 188.

Palade, G. E. 1953*b* Fine structure of blood capillaries. (Abstract.) *J. Appl. Phys.* **24**, 1424.

Palade, G. E. 1955*a* A small particulate component of the cytoplasm. *J. Biophys. Biochem. Cytol.* **1**, 59.

Palade, G. E. 1955*b* Relations beween the endoplasmic reticulum and the plasma membrane in macrophages. (Abstract.) *Anat. Rec.* **121**, 445.

Palade, G. E. 1955*c* Studies on the endoplasmic reticulum. II. Simple dispositions in cells *in situ*. *J. Biophys. Biochem. Cytol.* **1**, 567.

Palade, G. E. 1956 The endoplasmic reticulum. *J. Biophys. Biochem. Cytol.* **2** (suppl.), 85.

Palade, G. E. & Porter, K. R. 1954 Studies on the endoplasmic reticulum. I. Its identification in cells *in situ*. *J. Exp. Med.* **100**, 641.

Peach, R., Williams, G. & Chapman, J. A. 1961 A light- and electron-optical study of regenerating tendon. *Amer. J. Path.* **38**, 495.

Pease, D. C. & Molinari, Sandra 1960 Electron microscopy of muscular arteries; pial vessels of the cat and monkey. *J. Ultrastructure Res.* **3**, 447.

Policard, A. & Collet, A. 1958 Les données nouvelles apportées par la microscopie électronique à la connaissance du fonctionnement des capillaires sanguins. *Rev. franc. Etud. clin. Biol.* **3**, 205.

Policard, A., Collet, A. & Giltaire-Ralyte, Lucette 1955 Observations au microscope électronique sur la structure inframicroscopique des artérioles des mammifères. *Bull. Micr. Appl.* **5**, 3.

Policard, A., Collet, A. & Pregermain, S. 1957 Etude au microscope électronique des capillaires pulmonaires. *Acta Anat.* **30**, 624.

Porter, K. R. 1951 Repair processes in connective tissues. In *Transactions of 2nd conference on Connective tissues sponsored by Josiah Macy Jnr. Foundation, New York*, p. 126.

Porter, K. R. 1953 Observations on a submicroscopic basophilic component of cytoplasm. *J. Exp. Med.* **97**, 727.

Porter, K. R. 1955 Changes in cell fine structure accompanying mitosis. In *Fine Structure of Cells* (Symposium), p. 236. Groningen, Holland: Noordhoff Ltd.

Porter, K. R. & Pappas, G. D. 1959 Collagen formation by fibroblasts of the chick embryo dermis. *J. Biophys. Biochem. Cytol.* **5**, 153.

Porter, K. R. & Thompson, Helen, P. 1947 Some morphological features of cultured rat sarcoma cells as revealed by the electron microscope. *Cancer Res.* **7**, 431.

Ross, R. & Benditt, E. P. 1961 Wound healing and collagen formation. I. Sequential changes in components of guinea-pig skin wounds observed in the electron microscope. *J. Biophys. Biochem. Cytol.* **11**, 677.

Sabin, Florence R. 1921 Studies on blood. The vitally stainable granules as a specific criterion for erythroblasts and the differentiation of the three strains of the white blood-cells as seen in the living chick's yolk-sac. *Bull. Johns Hopk. Hosp.* **32**, 314.

Sanders, A. G., Dodson, L. F. & Florey, H. W. 1954 An improved method for the production of tubercles in a chamber in the rabbit's ear. *Brit. J. Exp. Path.* **35**, 331.

Sandison, J. C. 1924 A new method for the microscopic study of living growing tissues by the introduction of a transparent chamber in the rabbit's ear. *Anat. Rec.* **28**, 281.

Sandison, J. C. 1932 Contraction of blood vessels and observations on the circulation in the transparent chamber in the rabbit's ear. *Anat. Rec.* **54**, 105.

Schmidt, F. O. & Gross, J. 1948 Further progress in the electron microscopy of collagen. *J. Amer. Leath. Chem. Ass.* **43**, 659.

Schneider, W. C. 1959 Mitochondrial metabolism. *Advanc. Enzymol.* **21**, 1.

Sjöstrand, F. S. 1955 The ultrastructure of mitochondria. In *Fine Structure of Cells* (Symposium), p. 16. Groningen, Holland: Noordhoff Ltd.

Stearns, Mary L. 1939 Growth and differentiation of connective tissue as observed microscopically in the living rabbit. (Abstract.) *Anat. Rec.* **73** (suppl.), 49.

Thoma, R. 1893 *Untersuchungen über die Histogenese und Histomechanik des Gefäss systems.* Stuttgart.

Van den Brenk, H. A. S. 1956 Studies in restorative growth processes in mammalian wound healing. *Brit. J. Surg.* **43**, 525.

Weiss, J. M. 1953 The ergastoplasm—its fine structure and relation to protein synthesis as studied with the electron microscope in the pancreas of the Swiss albino mouse. *J. Exp. Med.* **98**, 607.

Weiss, P. 1959 Cellular dynamics. *Rev. Mod. Phys.* **31**, 11.

Weiss, P. & Garber, Beatrice 1952 Shape and movement of mesenchyme cells as functions of the physical structure of the medium. Contributions to a quantitative morphology. *Proc. Nat. Acad. Sci., Wash.*, **38**, 264.

Williams, R. G. 1959 Experiments on the growth of blood vessels in thin tissue and in small autographs. *Anat. Rec.* **133**, 465.

Willmer, E. N. 1945 Growth and form in tissue cultures. In Le Gros Clark, Sir W. E. & Medawar, P. B., Ed., *Essays on growth and form*, p. 264. Oxford: Clarendon Press.

Wright, G. P. 1958 *An introduction to pathology.* 3rd ed. London: Longmans Green and Co.

Yamada, E. 1955 The fine structure of the gall bladder epithelium of the mouse. *J. Biophys. Biochem. Cytol.* **1**, 445.

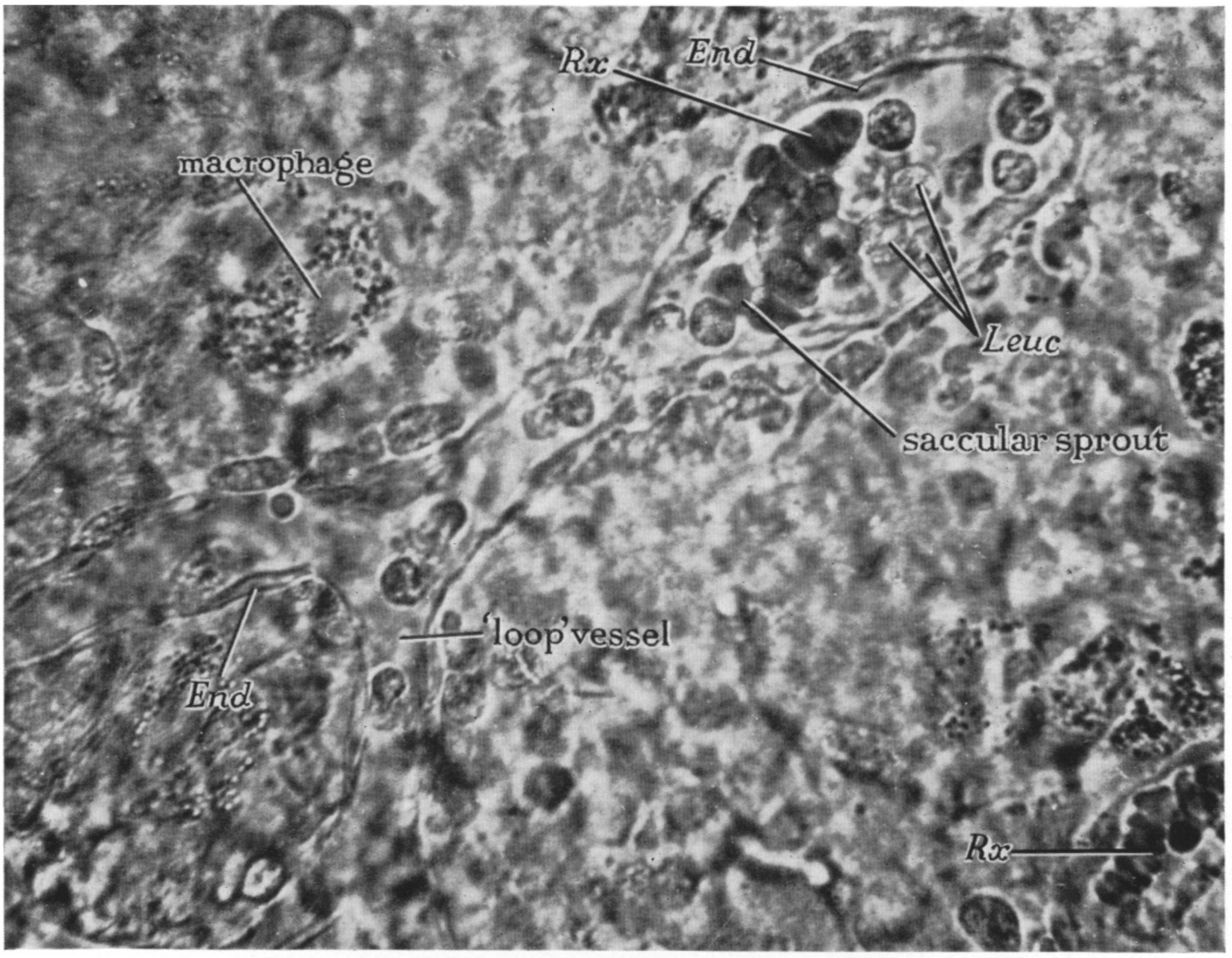

3

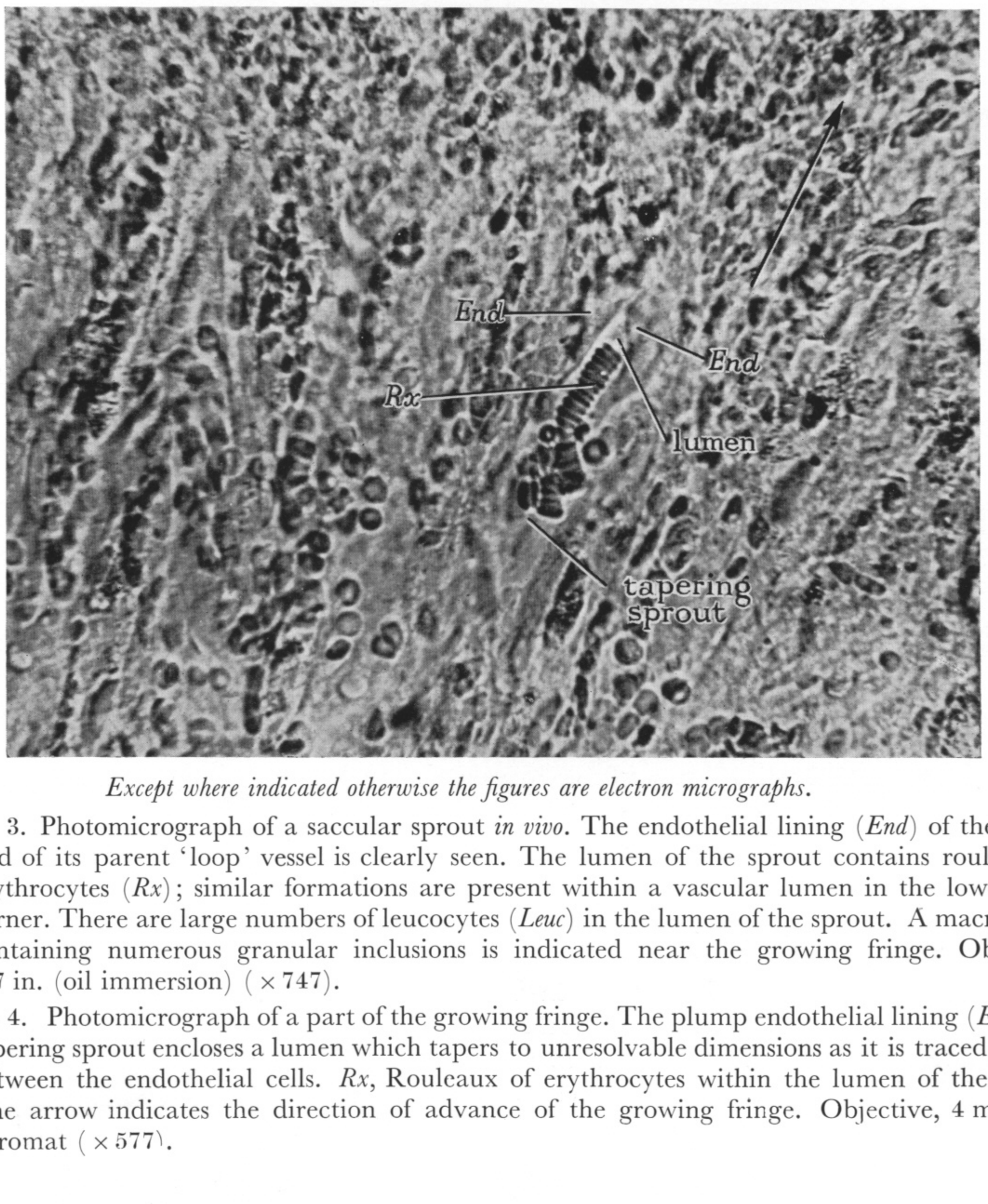

4

Except where indicated otherwise the figures are electron micrographs.

FIGURE 3. Photomicrograph of a saccular sprout *in vivo*. The endothelial lining (*End*) of the sprout and of its parent 'loop' vessel is clearly seen. The lumen of the sprout contains rouleaux of erythrocytes (*Rx*); similar formations are present within a vascular lumen in the lower right corner. There are large numbers of leucocytes (*Leuc*) in the lumen of the sprout. A macrophage containing numerous granular inclusions is indicated near the growing fringe. Objective, 1/7 in. (oil immersion) (× 747).

FIGURE 4. Photomicrograph of a part of the growing fringe. The plump endothelial lining (*End*) of a tapering sprout encloses a lumen which tapers to unresolvable dimensions as it is traced distally between the endothelial cells. *Rx*, Roulcaux of erythrocytes within the lumen of the sprout. The arrow indicates the direction of advance of the growing fringe. Objective, 4 mm apochromat (× 577).

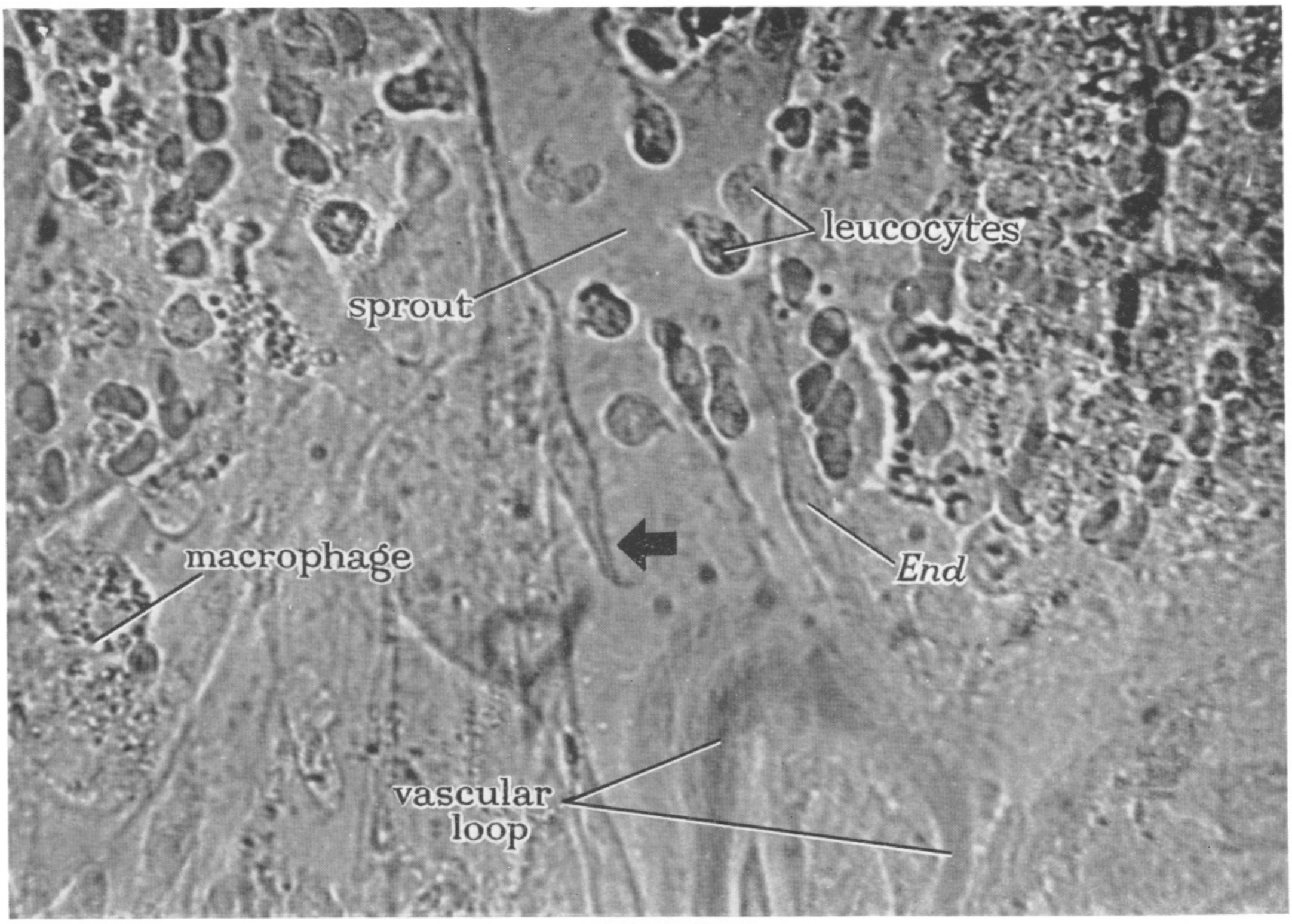

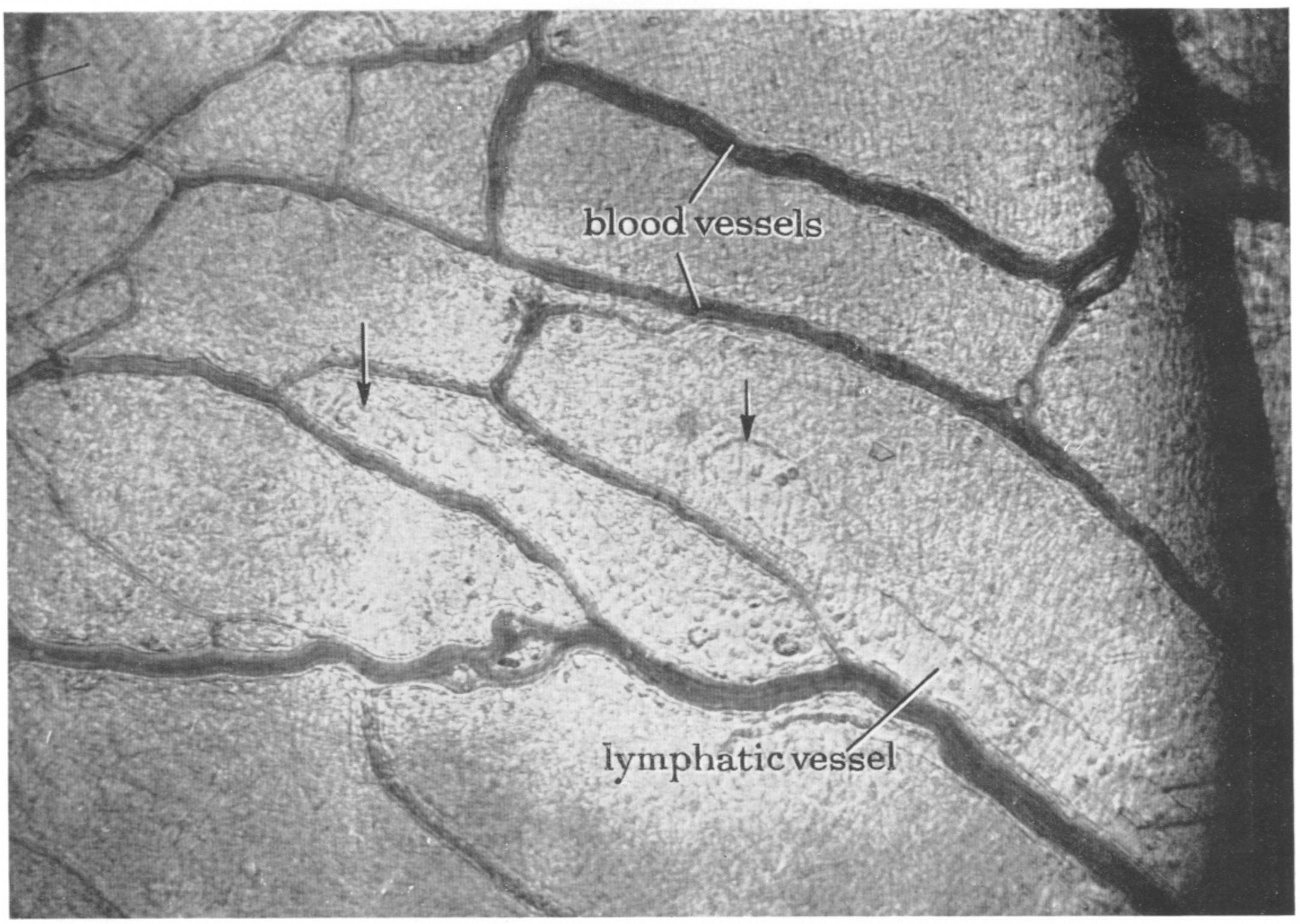

FIGURE 5. Photomicrograph of the growing fringe. A vascular loop with active circulation is giving rise to a sprout. The endothelial wall of the sprout is clearly seen (*End*) and one endothelial cell has a long pointed process extending into the lumen of the sprout (arrow). Objective, 1/7 in. (oil immersion) (× 747).

FIGURE 6. Photomicrograph of scar tissue in a rabbit ear chamber. The black shadow curving across the right side of the micrograph is the edge of the table of the chamber. A rich network of blood vessels is present and a lymphatic vessel is invading the ear chamber tissue along the lines of existing blood vessels. The saccular ends of the two branches of this lymphatic are indicated by arrows (× 146).

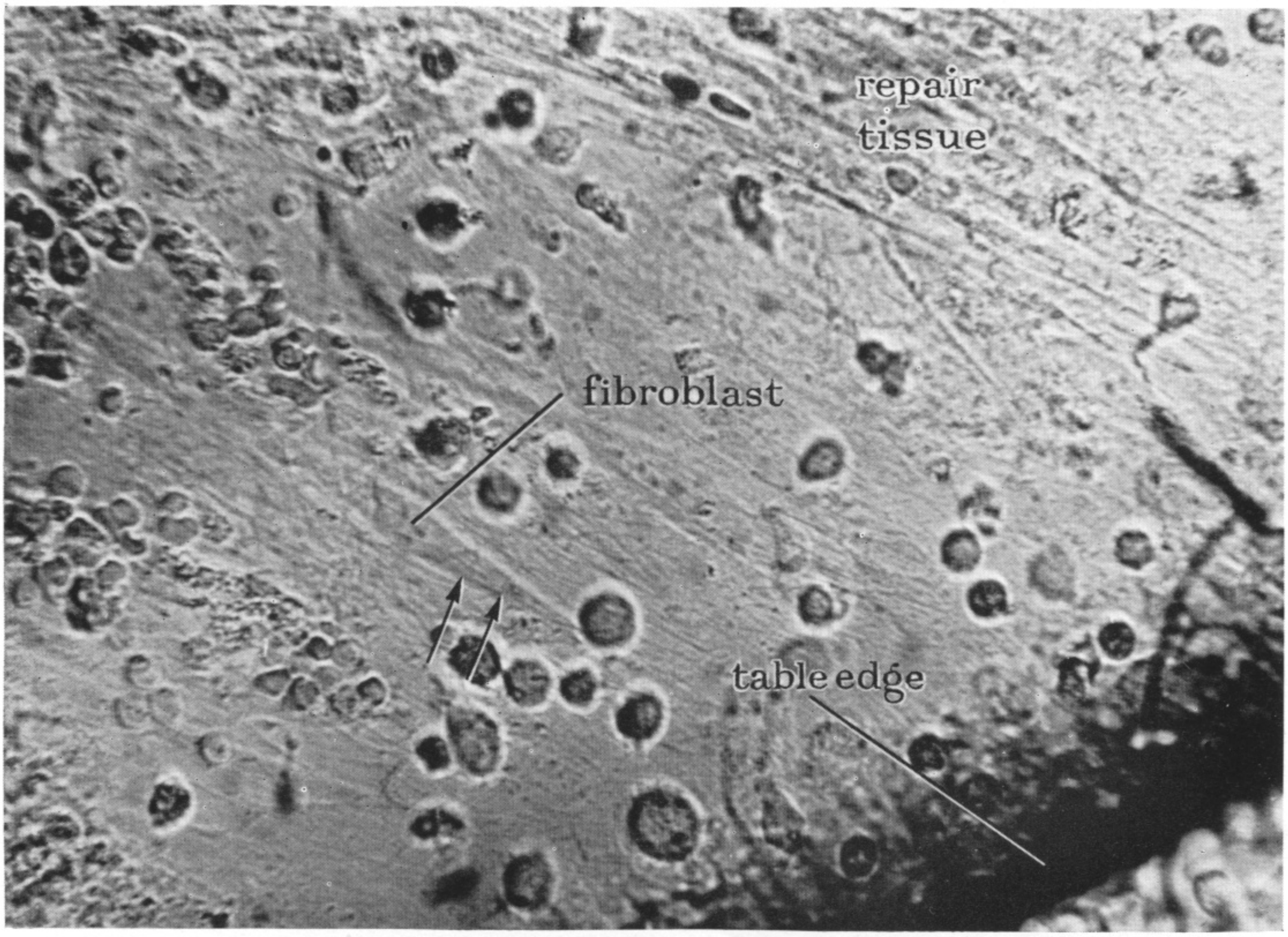

7

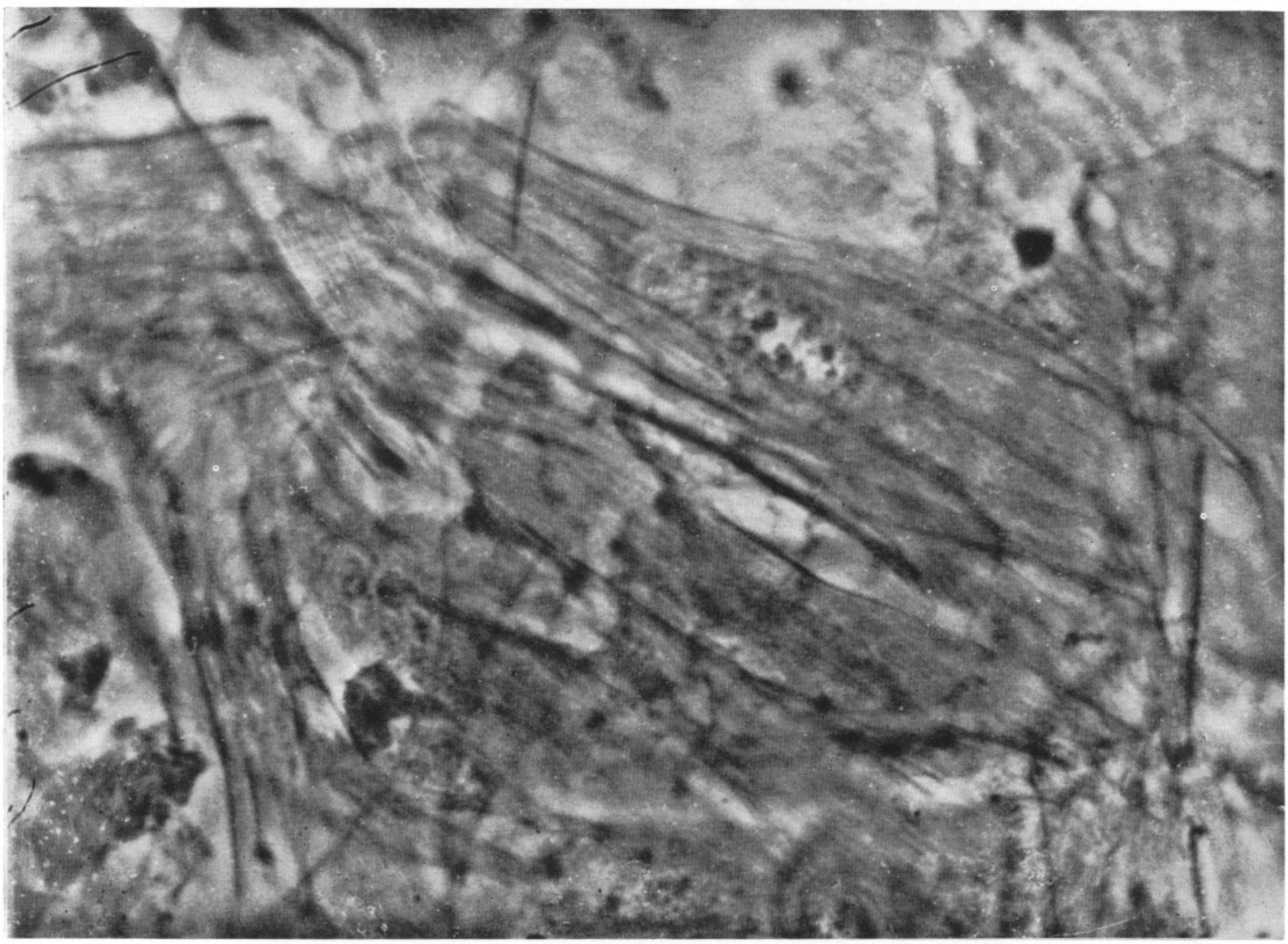

8

FIGURE 7. Photomicrograph of early repair tissue near the edge of the table. An isolated fibroblast is indicated with very fine fibrils apparently in or over its cytoplasm (arrows). Objective, 4 mm apochromat (× 577).

FIGURE 8. Photomicrograph of a section from a healing ear chamber to illustrate fibroglial fibres within fibroblasts. Fixation, mercuric-formol; stain, acid fuchsin (Mallory). Objective, 1/12 in. (oil immersion); filter, Wratten B 2 (green) (× 1333).

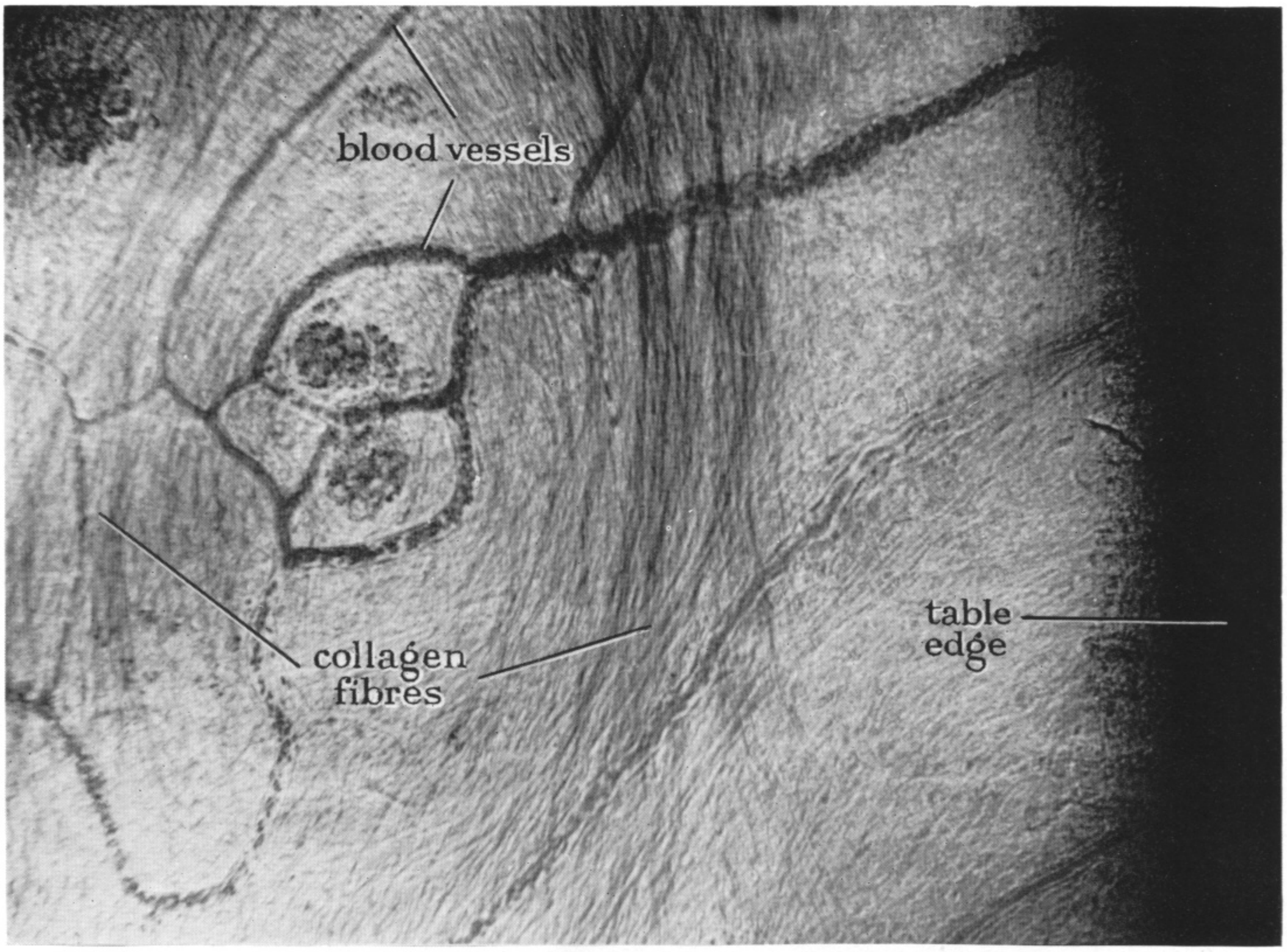

9

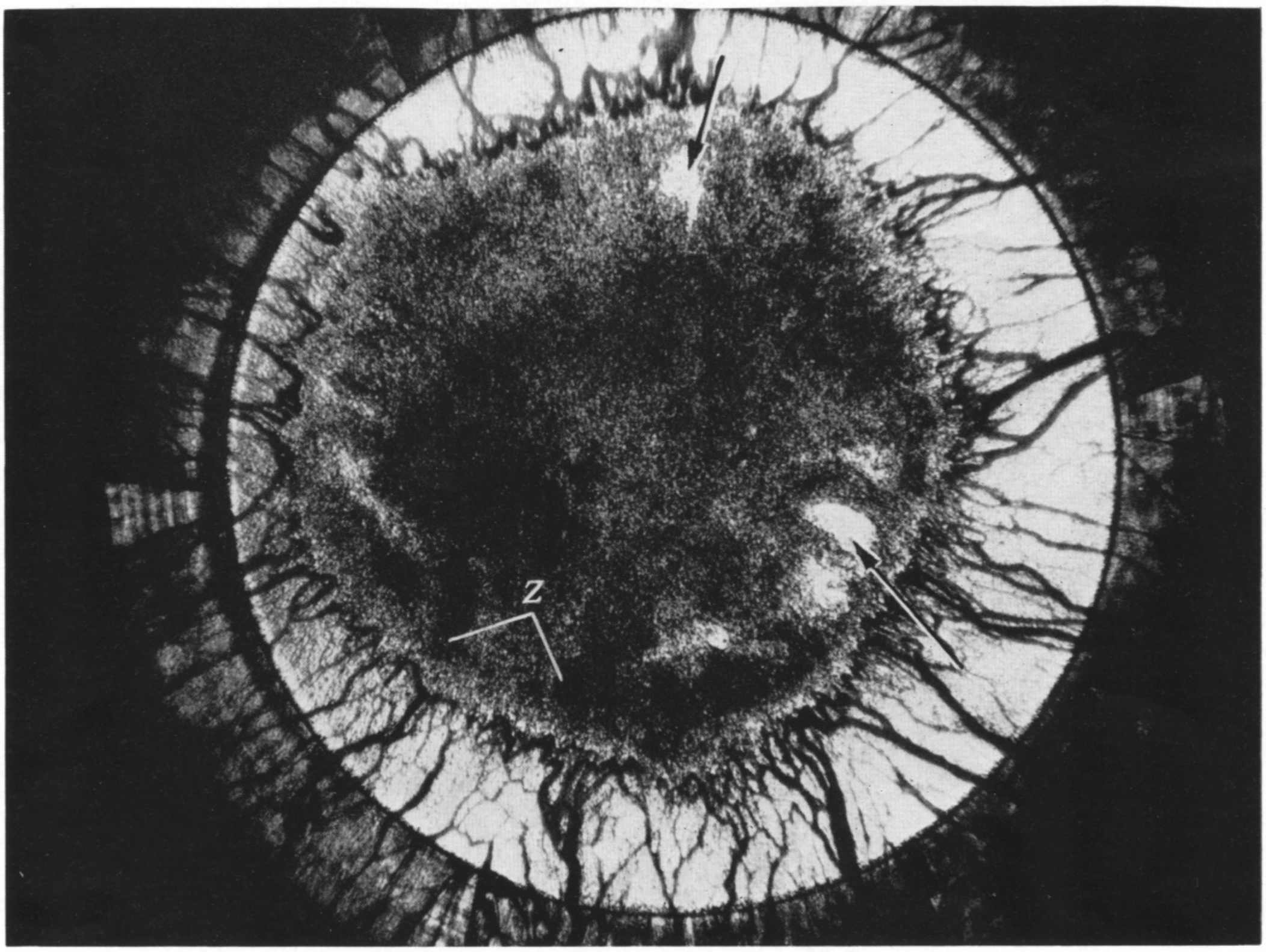

10

FIGURE 9. Photomicrograph of part of an ear chamber that had been fully healed for 3 weeks. Abundant collagen fibres with circular orientation are shown by examination with polarized light. Objective, × 10; filters, crossed polaroid (× 146).

FIGURE 10. Photomicrograph of a rabbit ear chamber showing fairly even invasion by the highly vascular growing fringe. This corresponds well to the illustrations prepared by Billroth (1856) of the vascular pattern of granulation tissue. Several clear spaces are visible distal to the growing fringe, two of which are indicated by arrows. These clear spaces are largely within the zone of haemorrhage (Z). Objective, Zeiss A; filter, Wratten B 2 (green) (× 27).

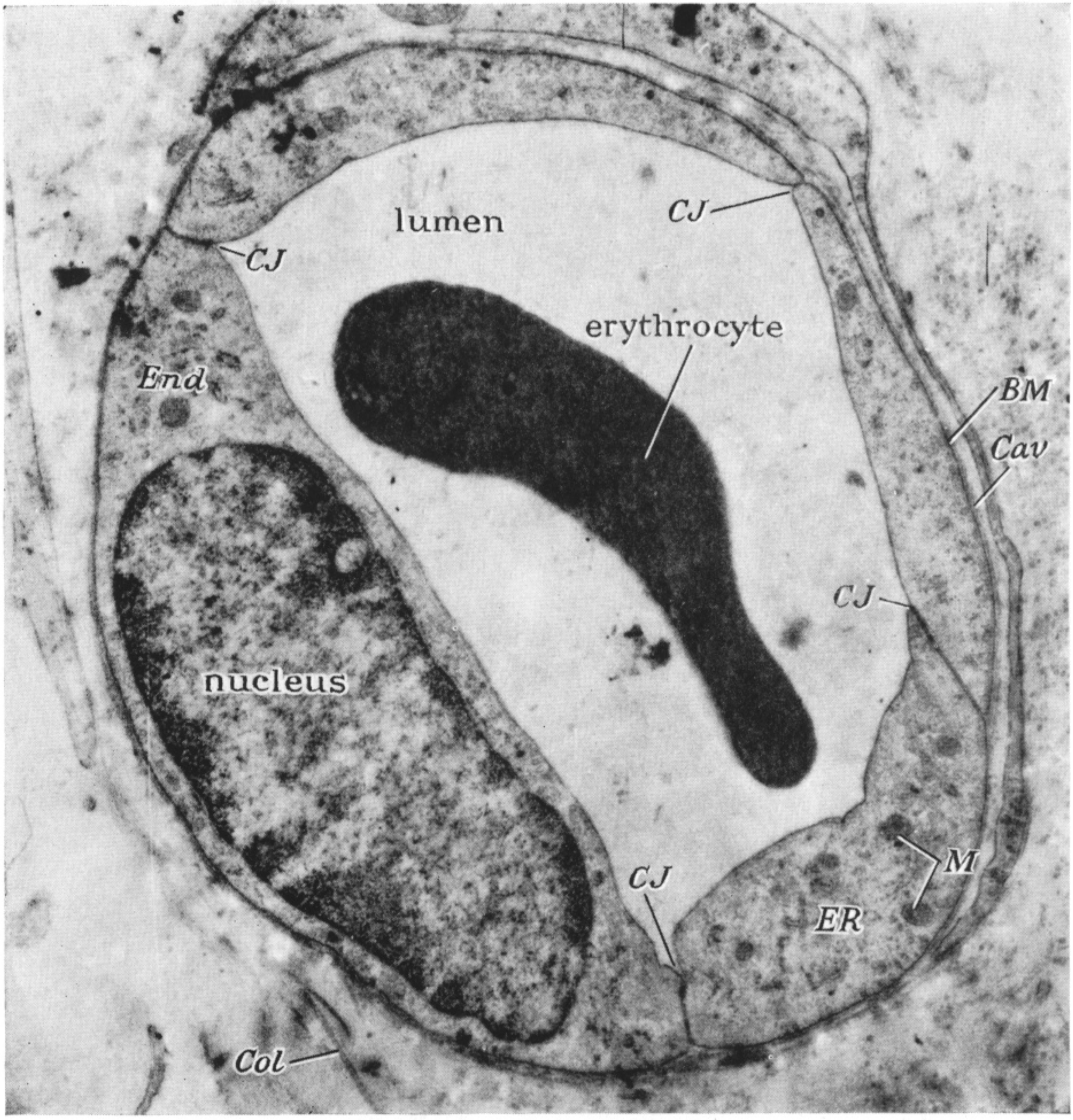

FIGURE 11. Mature blood capillary. The endothelial lining (*End*) is formed by 4 cells with 4 cell junctions (*CJ*). There are numerous caveolae intracellulares (*Cav*), an inconspicuous endoplasmic reticulum (*ER*), and mitochondria (*M*). *BM*, Basement membrane; *Col*, collagen. Epikote 812, uranyl acetate (× 13 500).

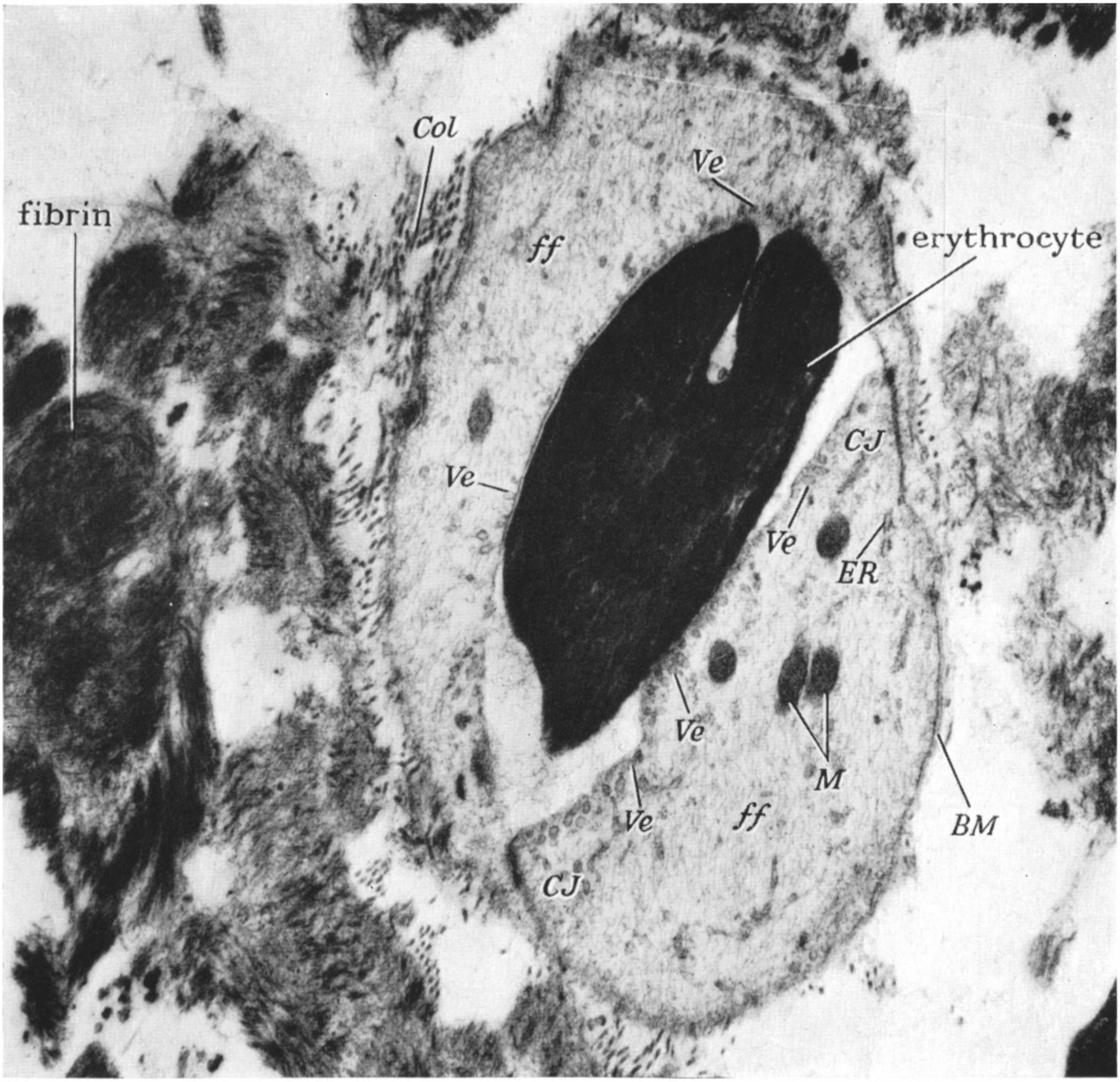

FIGURE 12. Recently formed vessel with narrow lumen, the greatest diameter being 4·5 μm. The endothelium is plump in relation to the lumen (as in figure 4). This vessel is penetrating the fibrin clot. *BM*, Basement membrane; *Col*, collagen; *CJ*, cell junction; *ER*, endoplsamic reticulum; *ff*, fibrillary region of cytoplasm; *M*, mitochondria; *Ve*, vesicles. Phosphotungstic acid; Araldite ($\times$ 17 000).

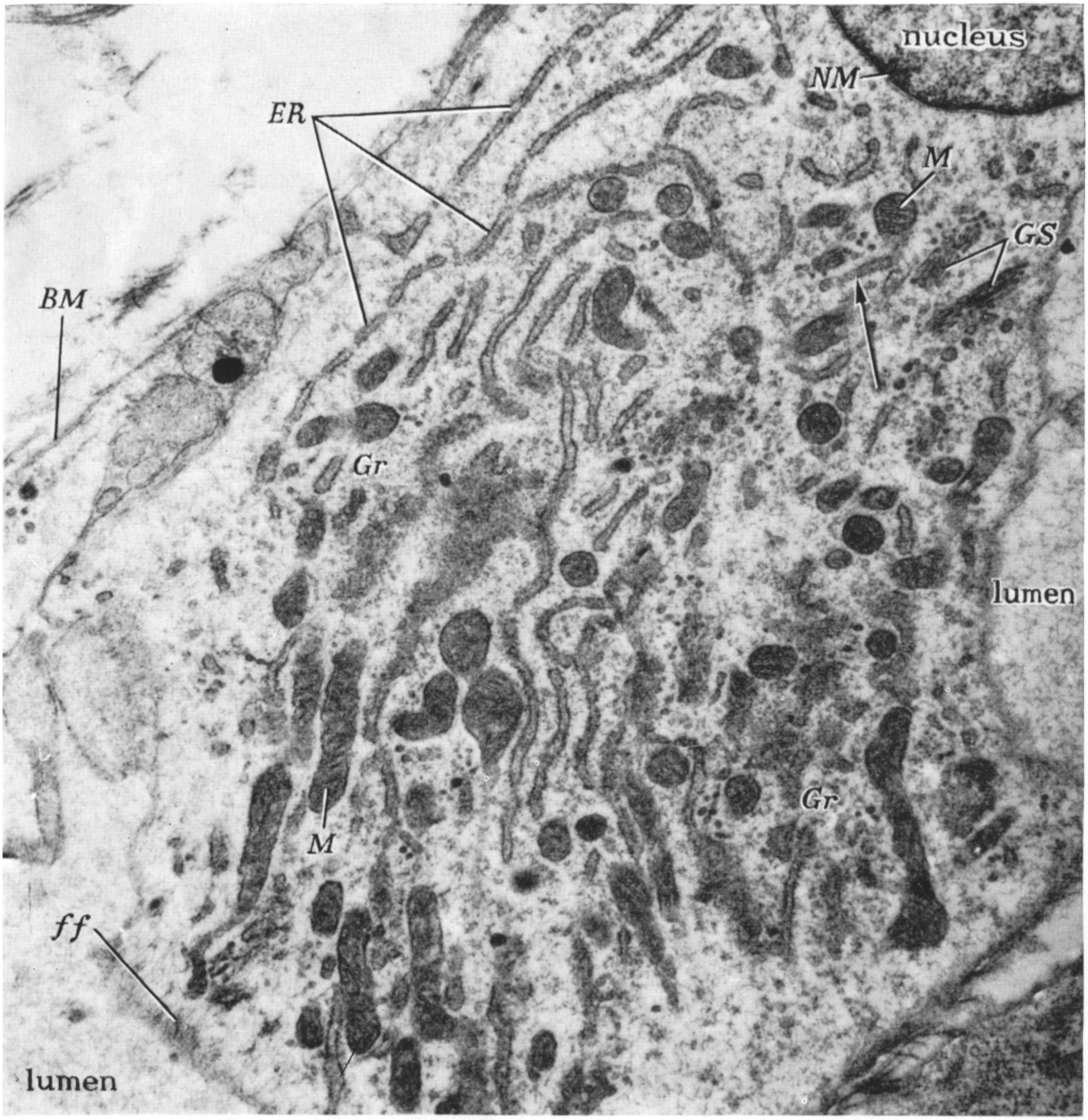

FIGURE 13. Endothelium from the distal part of a vessel that was invading fibrin clot. It contains numerous elements of endoplasmic reticulum (*ER*) between the paired membranes of which is moderately electron-dense material. The lacunes of the endoplasmic reticulum are about 680 Å wide and are studded with numerous dense ribosomes (*RNP* granules) which in one region (arrow) show a linear disposition. Closely apposed smooth surfaced pairs of membranes together with groups of small vesicles are part of the Golgi substance (*GS*). Numerous elongated mitochondria (*M*) with plentiful transverse cristae are present. The hyaloplasm contains much finely fibrous (*ff*) and granular material (*Gr*). *BM*, Basement membrane; *NM*, nuclear membrane. Phosphotungstic acid; Araldite (× 18000).

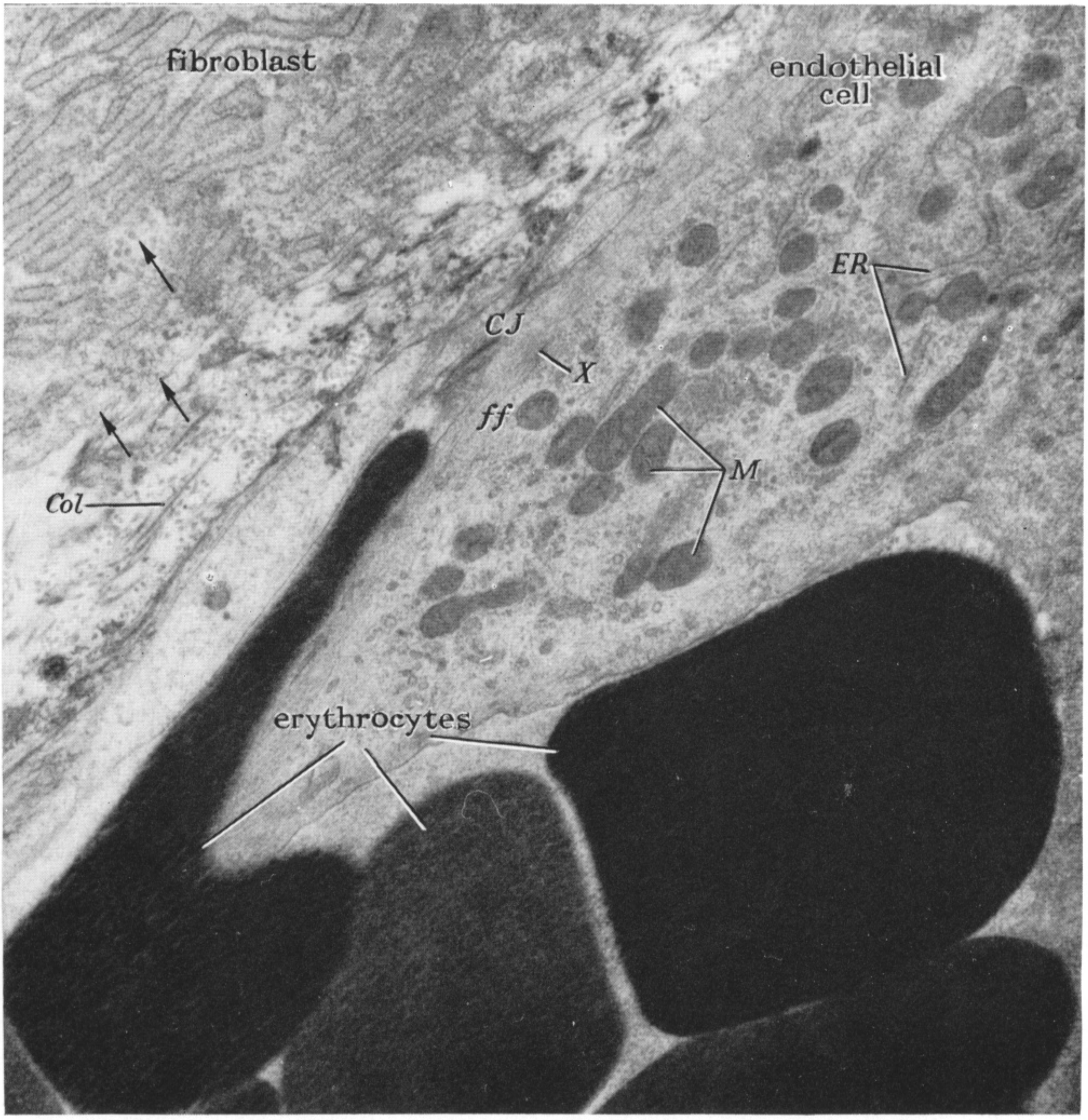

FIGURE 14. Endothelium of a recently formed vessel. A radicle of a greatly distorted erythrocyte is insinuated at a cell junction (*CJ*). This endothelium possesses much endoplasmic reticulum (*ER*) and numerous mitochondria (*M*). A region of highly fibrillary cytoplasm about $0{\cdot}2\,\mu$ wide (*ff*) forms a distinct peripheral zone in one endothelial cell; in certain parts (e.g. at *X*) the fine fibrils are condensed to form small dark bodies. Note numerous small vesicles (indicated by arrows) within the fibroblast. *Col*, collagen. Phosphotungstic acid; Araldite ($\times 18\,000$).

FIGURE 15. Immature venule and branch. Three granulocytes (*Grc* 1, 2 and 3) are related to the vessel wall. *Grc* 1 is passing through the endothelial lining (*End*) of the venule. This granulocyte has not penetrated the basement membrane which may be identified in relation to it (*BM*). *Grc* 2 has penetrated the endothelium (perhaps at arrow) and lies between it and the perivascular sheath. *Col*, Collagen; *CJ*, cell junction; *N*, nucleus. Phosphotungstic acid; Araldite (× 4 000).

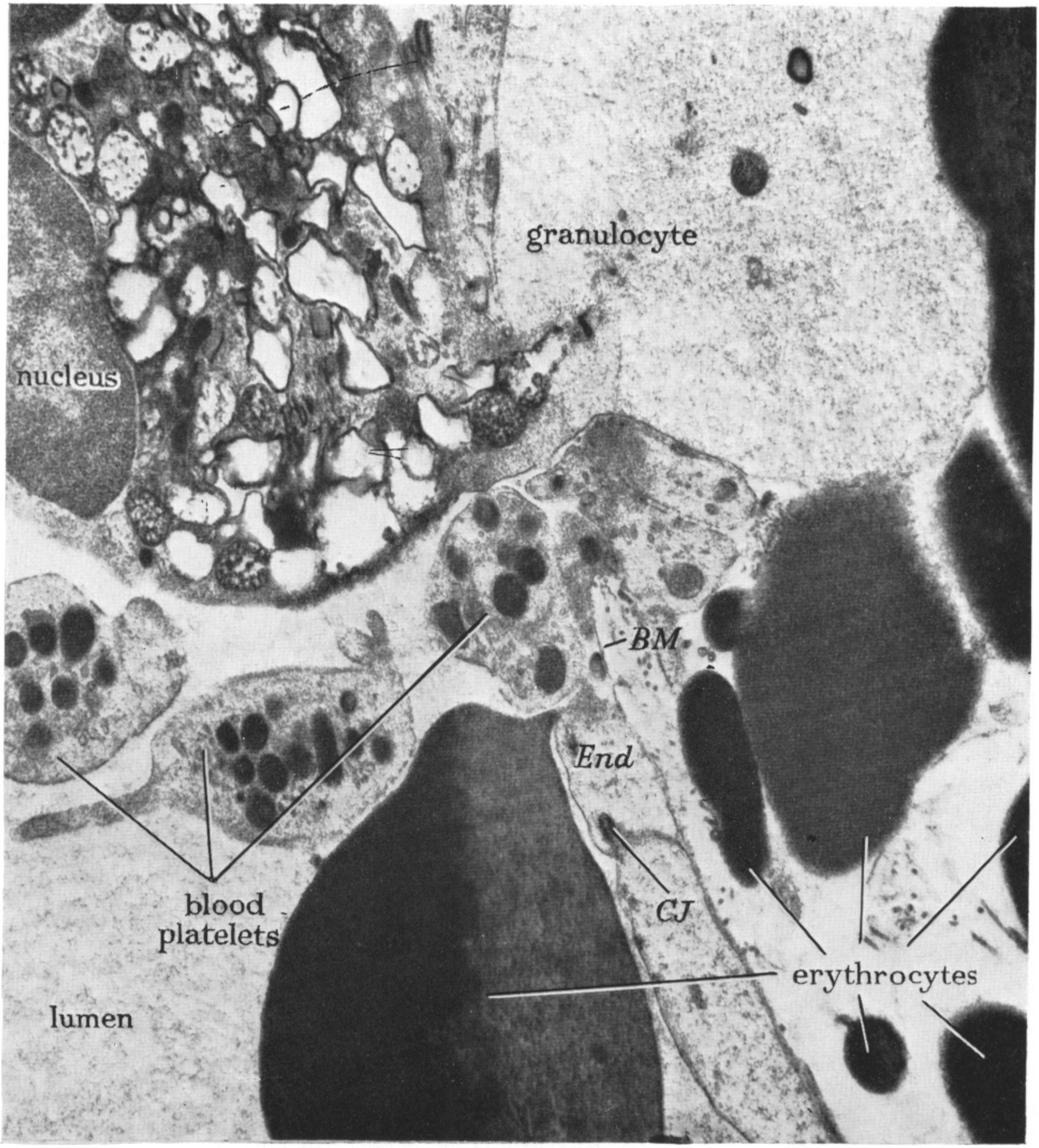

FIGURE 16. Wall of an immature vessel with a granulocyte, an erythrocyte and blood platelets passing through the endothelium (*End*) near a cell junction (*CJ*) into the extravascular space. The basement membrane (*BM*) is being traversed by the granulocyte and platelets, but it is still present across the lower part of the gap (as seen in the figure) and appears to be partly obstructing the passage of the various formed elements of the blood. Phosphotungstic acid; Araldite ($\times$ 16 500).

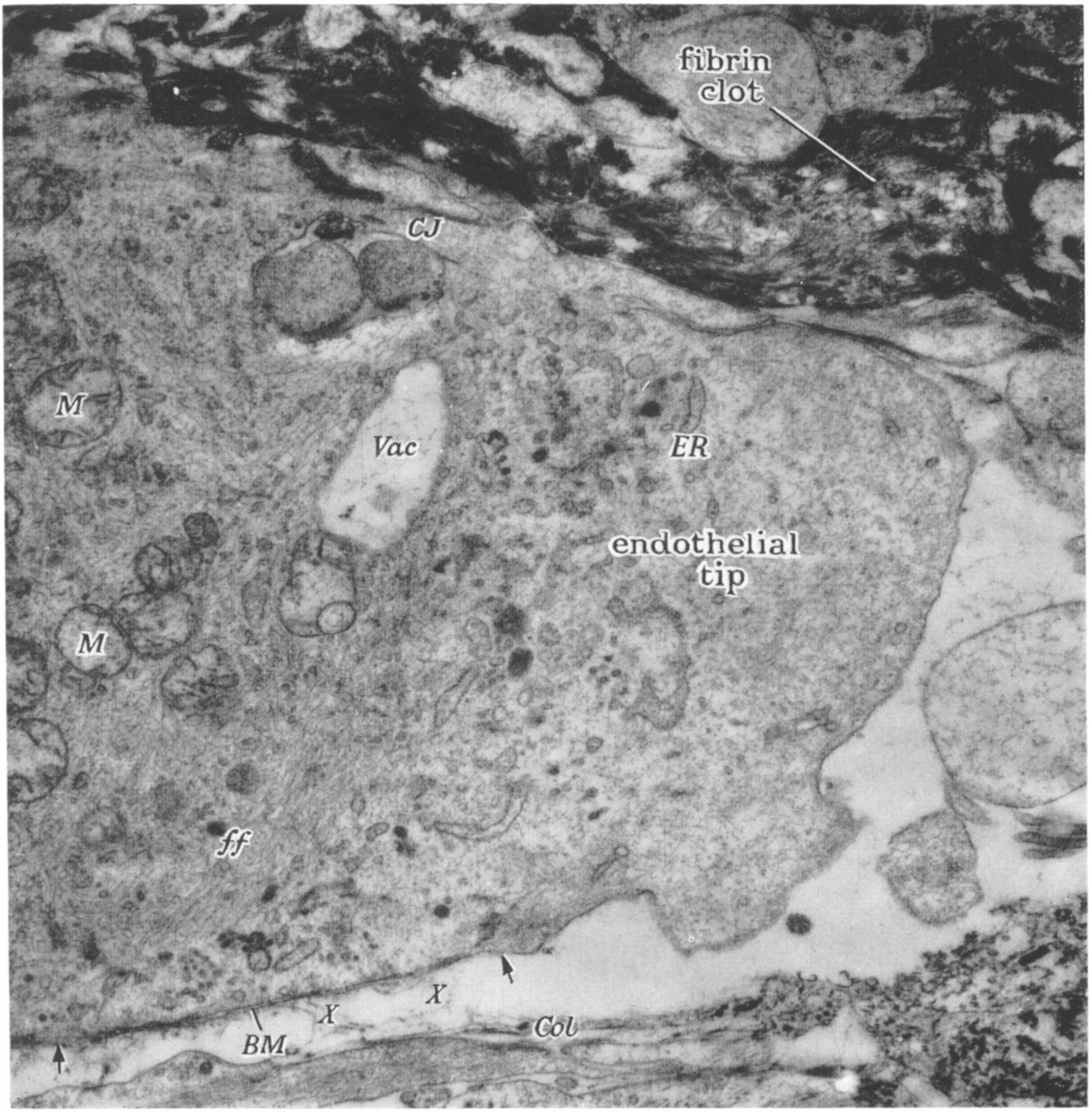

FIGURE 17. Endothelial tip of a vessel invading the fibrin clot. The extent of the basement membrane (*BM*) is indicated by arrows. This incomplete basement membrane has a frayed appearance, and at *XX* the frayed portion can be traced towards a region where very early collagen fibrils (*Col*) are present. *CJ*, Endothelial cell junction; *ER*, endoplasmic reticulum; *ff*, finely fibrillar region of cytoplasm; *M*, mitochondria; *Vac*, vacuole. Phosphotungstic acid; Araldite ($\times 18\,000$).

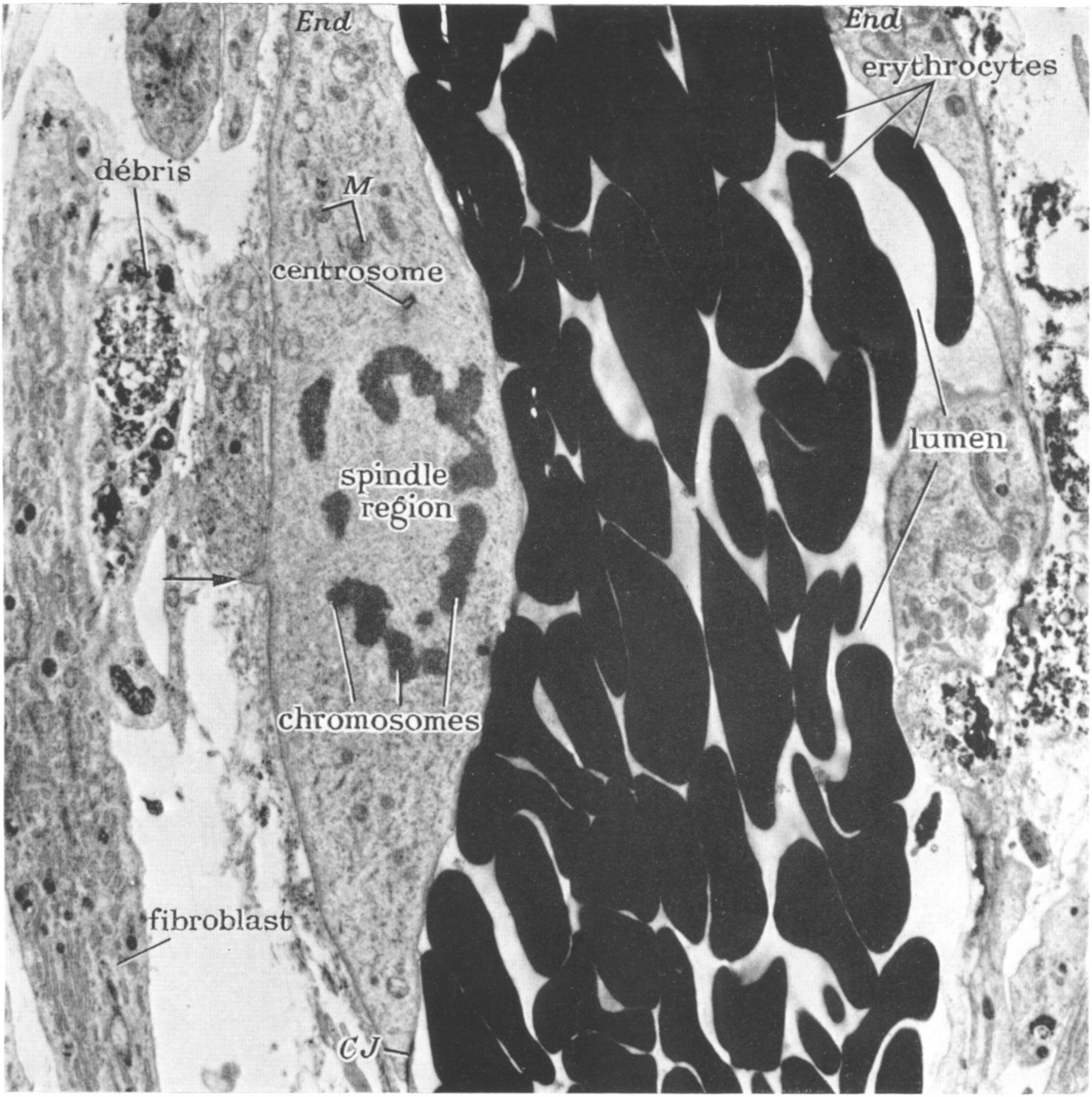

FIGURE 18. Mitosis of an endothelial cell situated just proximal to tip of a young vessel. Arrow indicates projection from the basal surface of the cell; *CJ*, cell junction; *End*, endothelium; *M*, mitochondria. Phosphotungstic acid; Araldite (× 5 500).

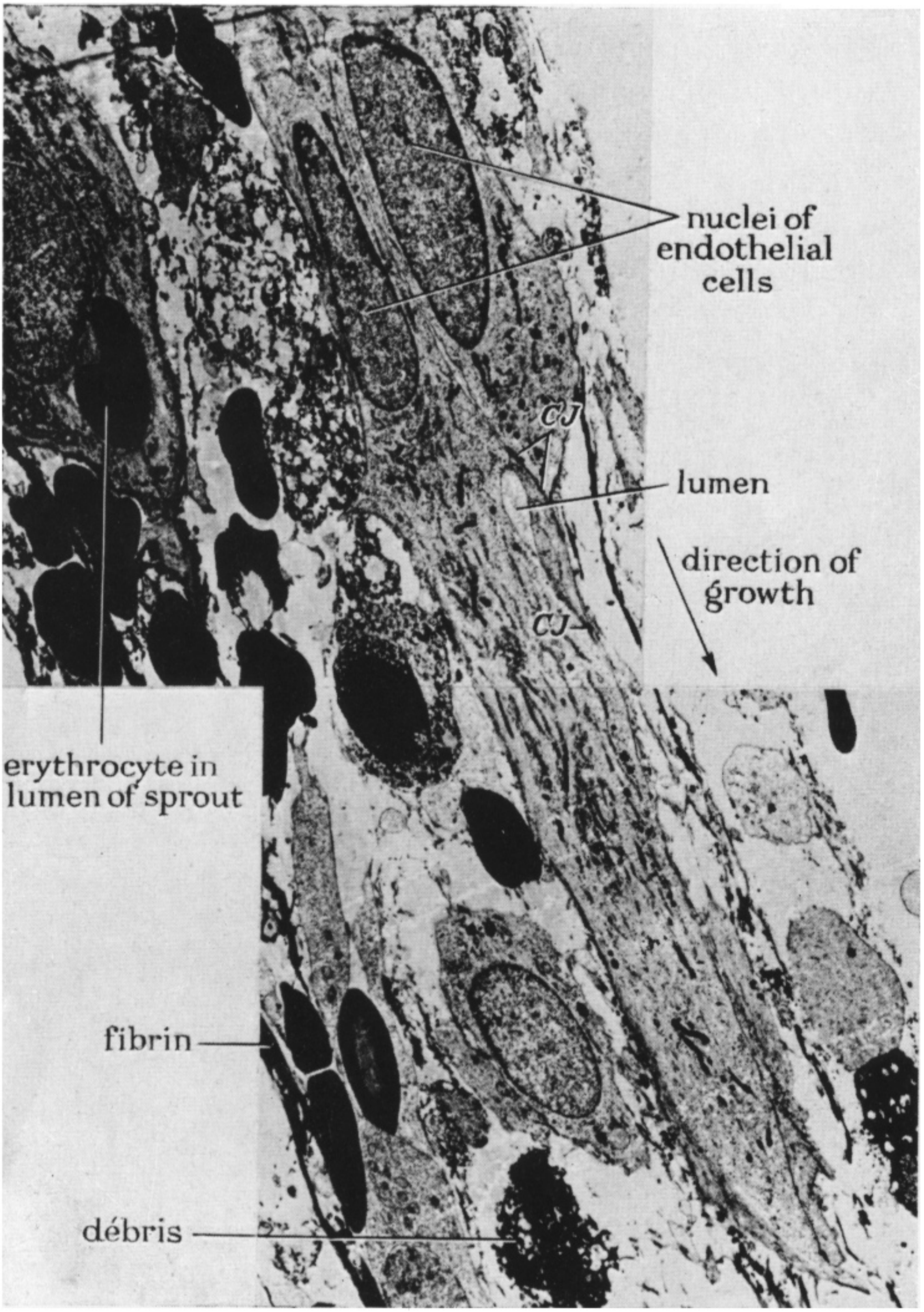

FIGURE 19. A cord of apposed endothelial cells is invading region of fibrin clot and débris in the direction indicated by the arrow. A slit-like lumen is present between two cells of the cord. Typical endothelial cell junctions are present (*CJ*). On the left is another sprout with a single red cell in its lumen. Phosphotungstic acid; Araldite ($\times 4000$).

FIGURE 20. Endothelial sprout penetrating fibrin clot, with four small spaces (*L*) present between two endothelial cells. At arrow a narrow septum between two of the spaces is perforated. *Col*, Collagen; *CJ*, endothelial cell junctions (5); *ER*, endoplasmic reticulum; *GS*, Golgi substance; *M*, mitochondria. Phosphotungstic acid; Araldite ($\times$ 8500).

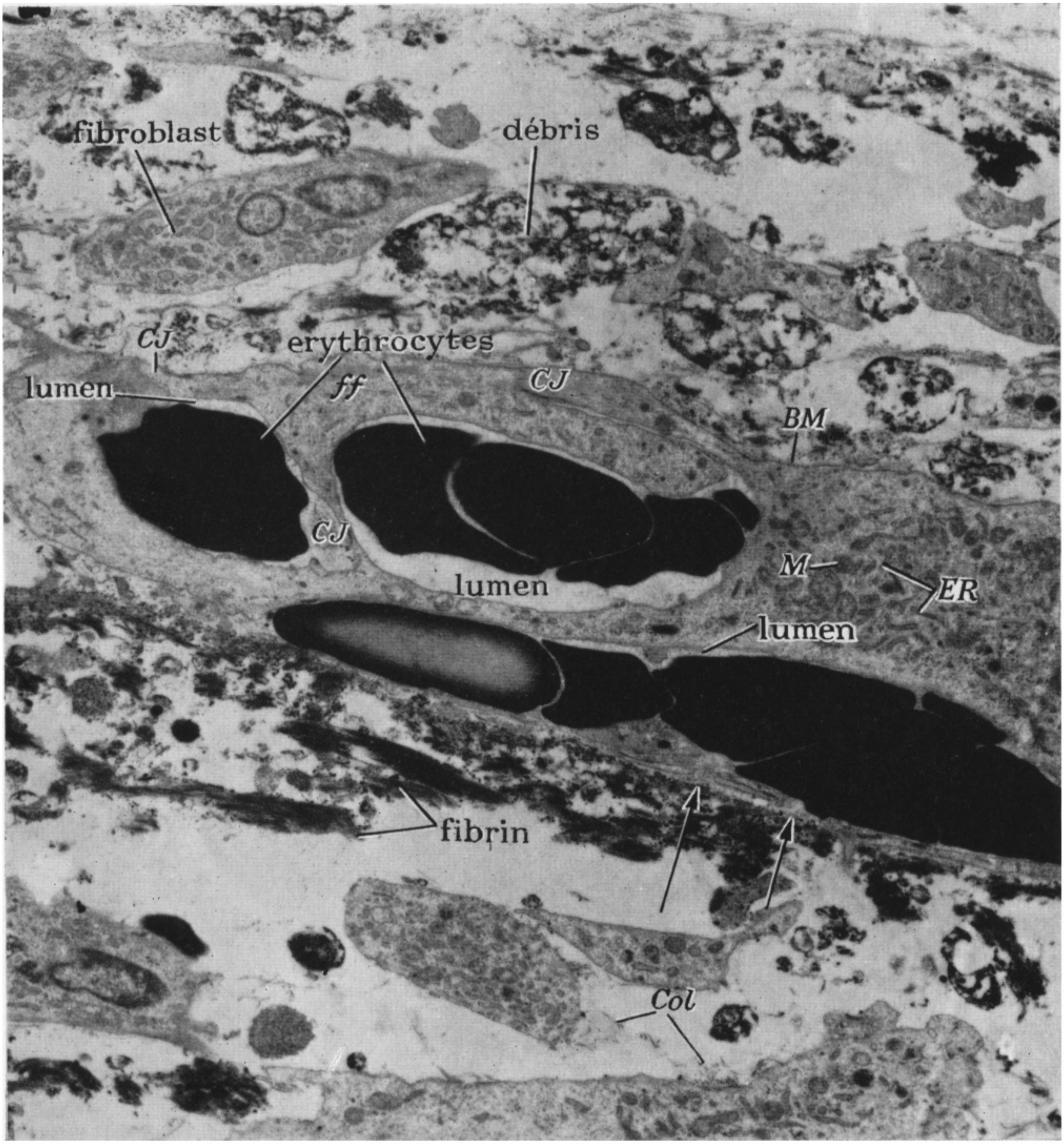

FIGURE 21. Endothelial sprout invading fibrin clot. In three places a lumen containing erythrocytes can be seen. Apparent defects in the wall of the lowest lumen are indicated by arrows. The two upper lumina are contained by the same two endothelial cells, which share 3 cell junctions (*CJ*). *BM*, Basement membrane; *Col*, collagen; *ER*, endoplasmic reticulum; *ff*, fibrillar region of cytoplasm; *M*, mitochondria. Phosphotungstic acid; Araldite (× 6000).

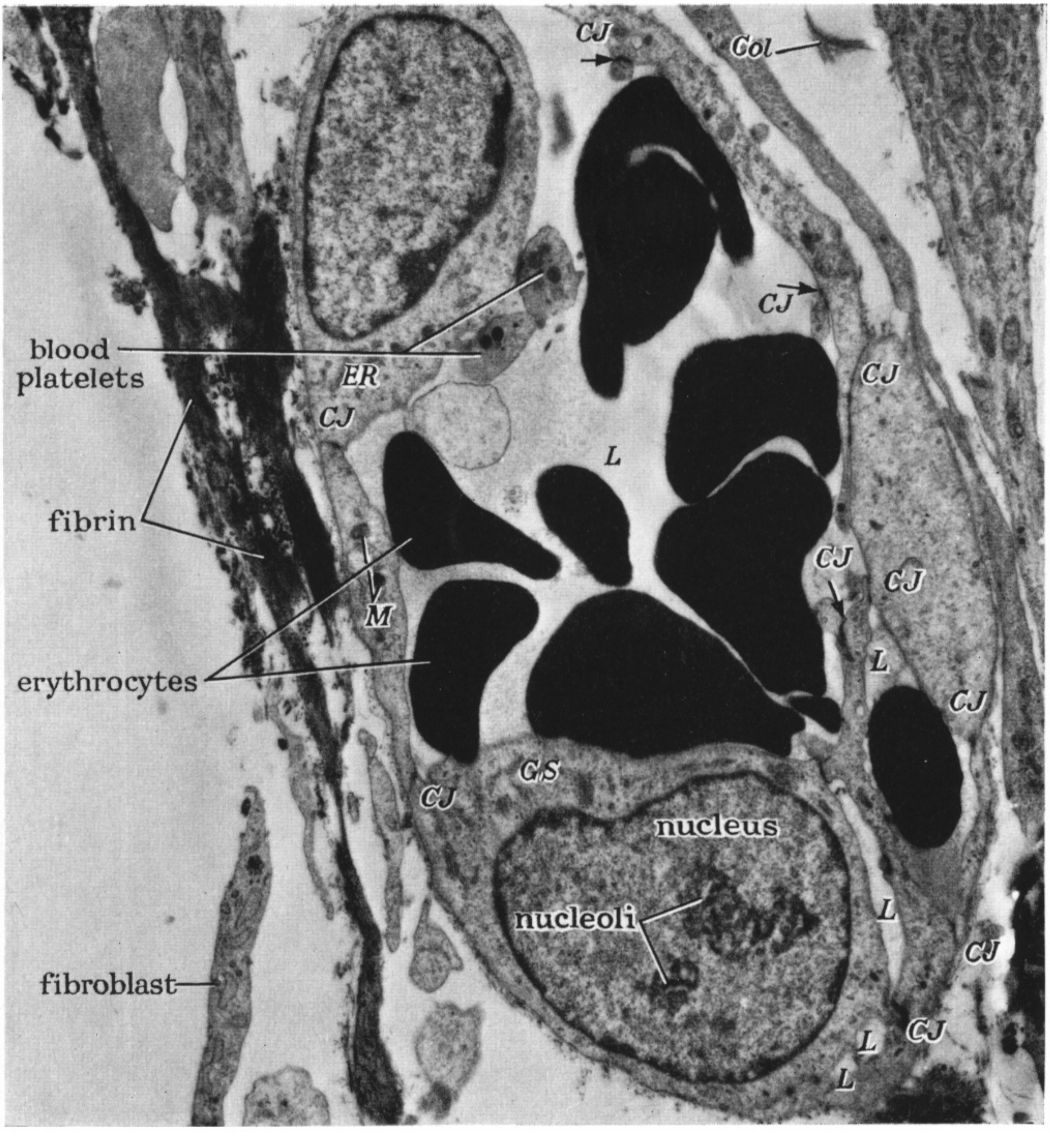

FIGURE 22. Endothelial sprout invading fibrin clot. Lumina (*L*) can be seen in five places one being much larger than the others. Cell junctions (*CJ*) are numerous and the three indicated by arrows are probably at sites where there were previously septa across the largest lumen. The four smaller lumina were probably destined to enlarge and coalesce, by loss of septa and separation of junctions, until one continuous lumen remained, bounded by the endothelial cells shown here. *Col*, collagen; *ER*, endoplasmic reticulum; *GS*, Golgi substance; *M*, mitochondria. Phosphotungstic acid; Araldite (× 8000).

FIGURE 23. A saccular sprout. A similar vessel *in vivo* is shown in figure 3, plate 26. *Col*, Collagen; *CJ*, endothelial cell junction; *GS*, Golgi substance; *IS*, projection of endothelial cell spanning lumen of sprout; arrow indicates small luminal slit; *M*, mitochondria. Phosphotungstic acid; Araldite (× 8500).

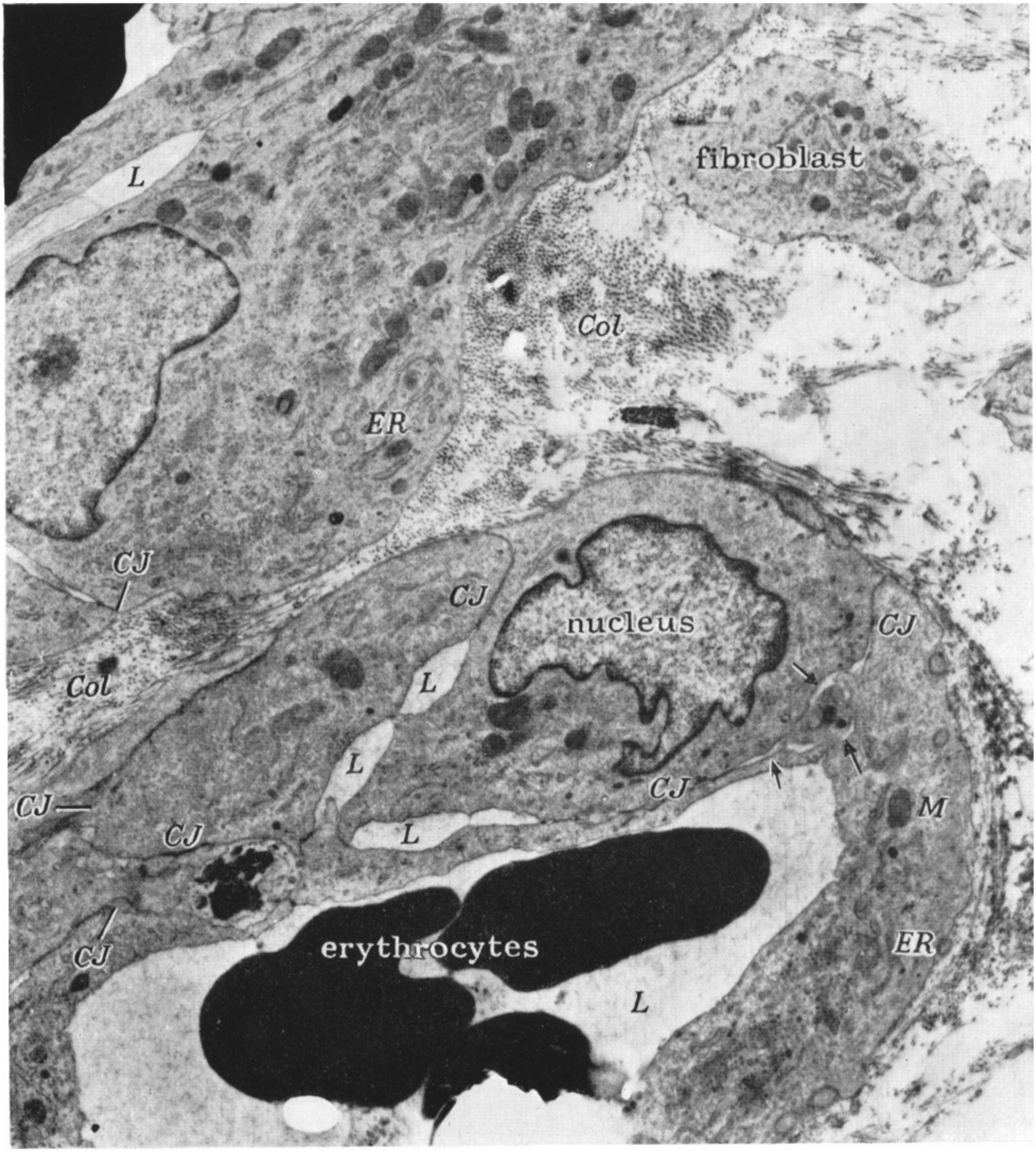

FIGURE 24. Early stage in the intercalation of a cell (with labelled nucleus) into the endothelial wall of a vessel with lumen (*L*) containing erythrocytes. Three smaller lumina are marked (*L*) and there are several small slits (indicated by arrows) developing in relation to the nucleated endothelial cell. By enlargement of these spaces, with the accompanying disappearance of septa and cell junction (*CJ*), a stage such as that illustrated in figure 21, plate 35 would be reached. *Col*, Collagen; *ER*, endoplasmic reticulum; *M*, mitochondrion. Phosphotungstic acid; Araldite (× 9000).

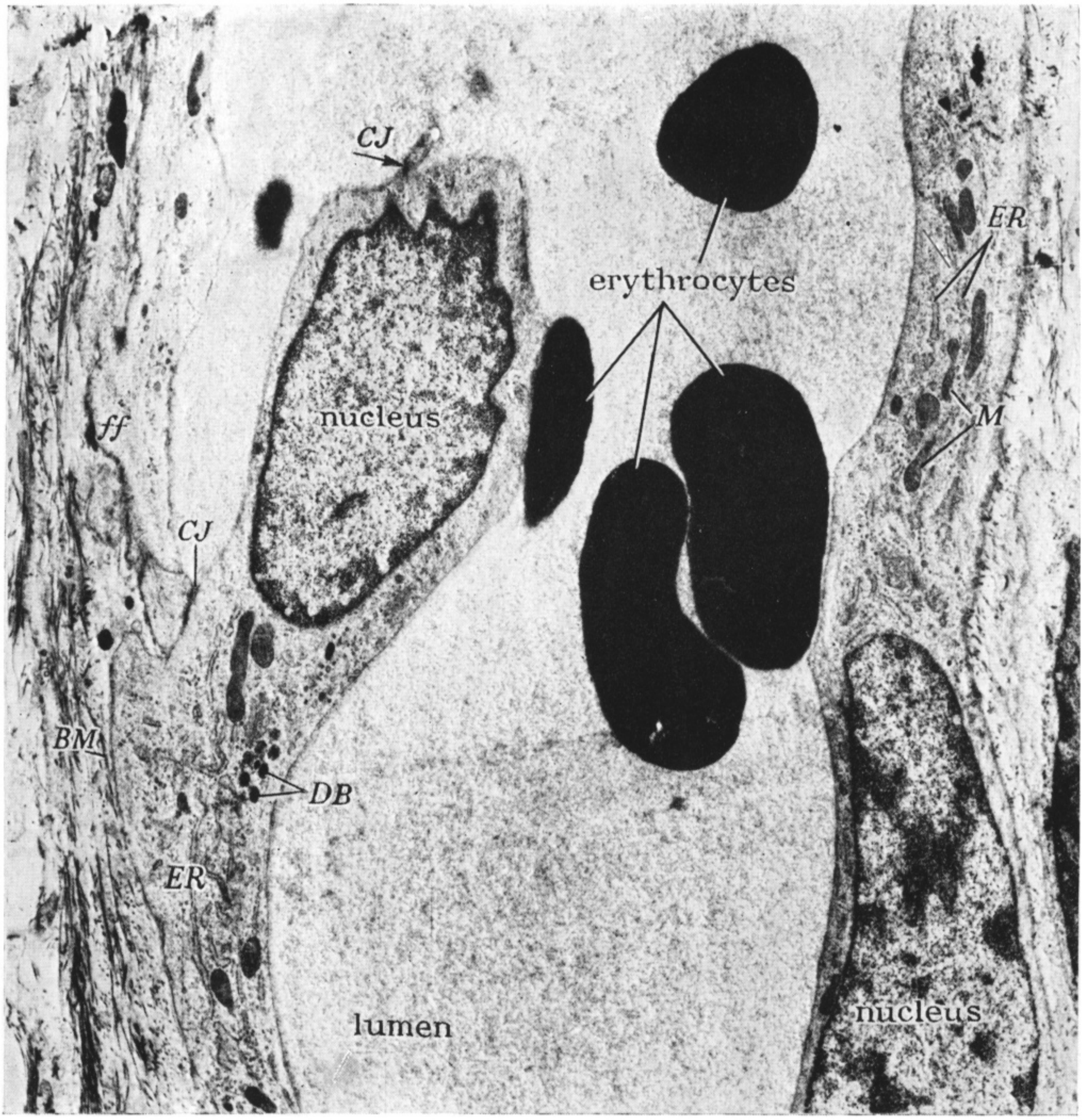

FIGURE 25. Late stage of the process of intercalation of an endothelial cell into the wall of a vessel with patent lumen (cf. figure 5, plate 27). Arrow indicates a cell junction (*CJ*) recently deprived of connexions, associated with an endothelial projection that had previously acted as septum dividing the lumen. *BM*, Basement membrane; *Col*, collagen; *DB*, dense cytoplasmic inclusion bodies; *ER*, endoplasmic reticulum; *ff*, fibrillary region of cytoplasm; *M*, mitochondria. Phosphotungstic acid; Araldite (× 8000).

FIGURE 26. A region where two endothelial sprouts (*Sp* I, *Sp* II) within the fibrin clot have united by cell junctions (*CJ*). The lumen of sprout II is filled with tightly packed erythrocytes, whilst the lumen of sprout I is a mere slit (*L*) within the cord of closely apposed cells. *ER*, Endoplasmic reticulum; *ff*, fibrillary region of cytoplasm; *GS*, Golgi substance; *M*, mitochondria. Phosphotungstic acid; Araldite (× 8000).

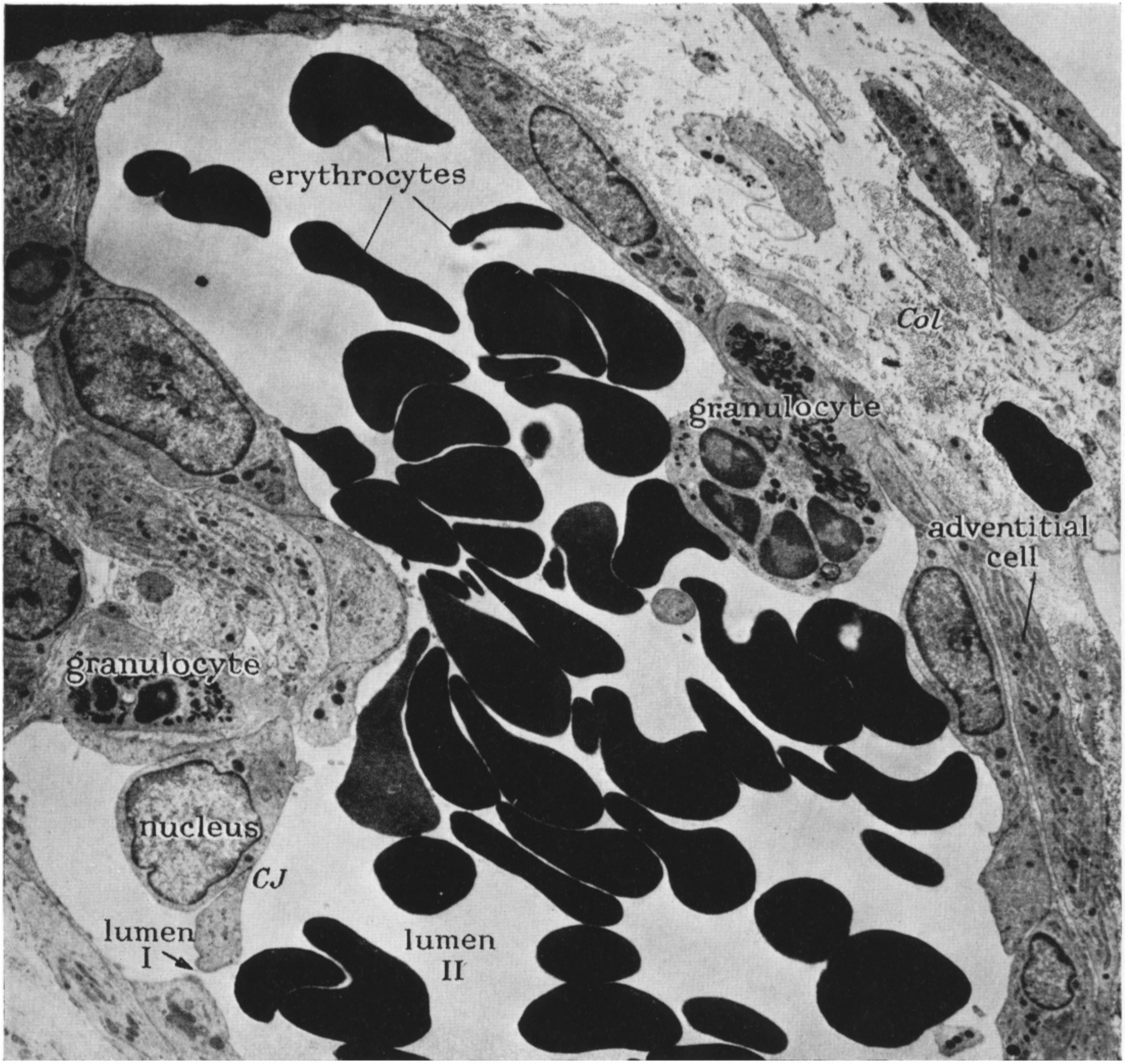

FIGURE 27. Immature vessels. The two lumina present (I and II) are connected by a small channel (arrow) produced by the separation of the cells forming the dividing septum. *Col*, Collagen. Phosphotungstic acid; Araldite (× 4000).

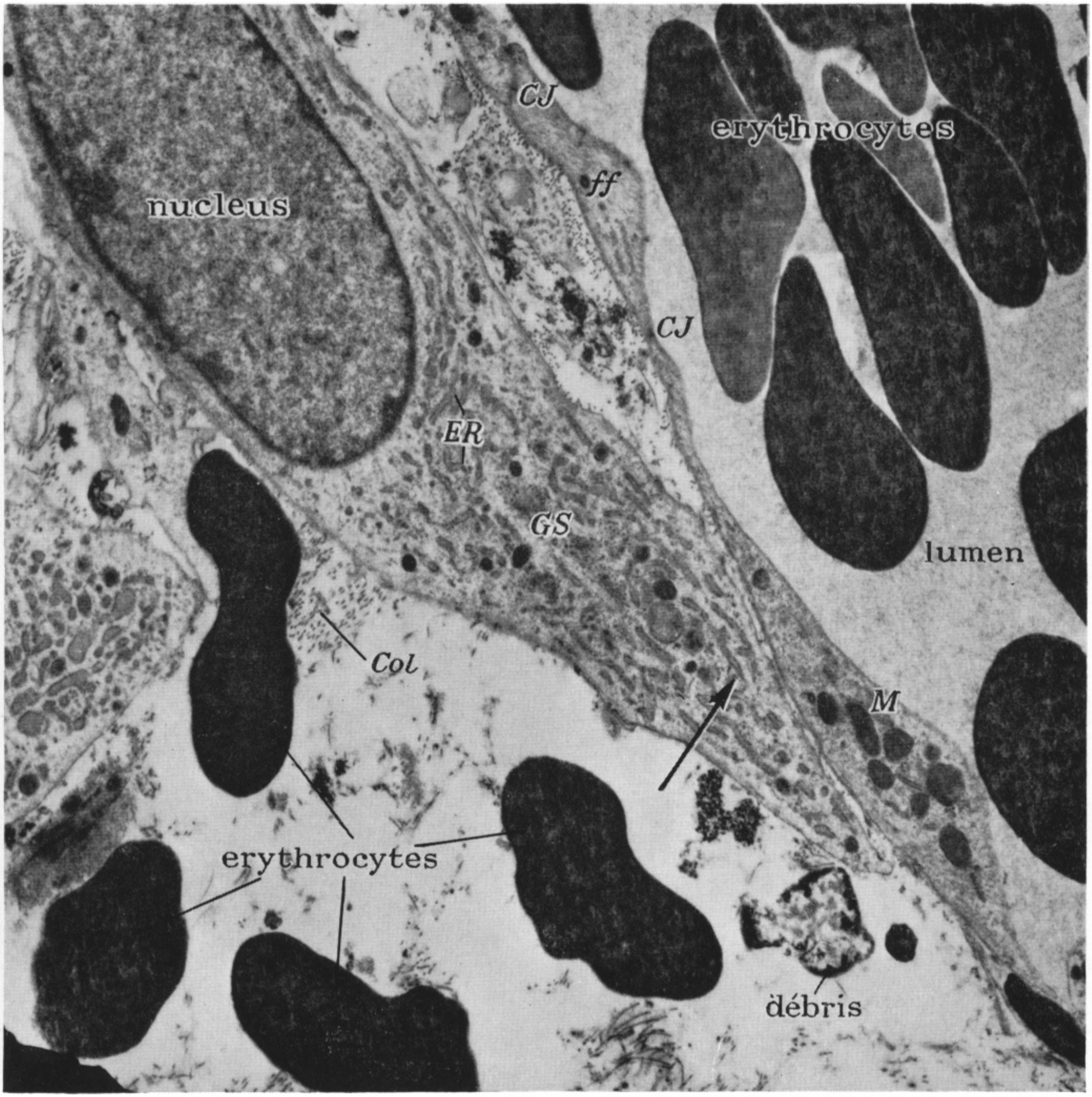

FIGURE 28. Large fibroblast-like cell (with nucleus) lying in close relation through one tapered extremity (arrow) to the thin endothelial lining of a vessel with a wide lumen. *Col*, Collagen; *CJ*, cell junction; *ER*, endoplasmic reticulum; *ff*, fibrillary region of cytoplasm; *GS*, Golgi substance; *M*, mitochondria. Phosphotungstic acid; Araldite ($\times$ 8750).

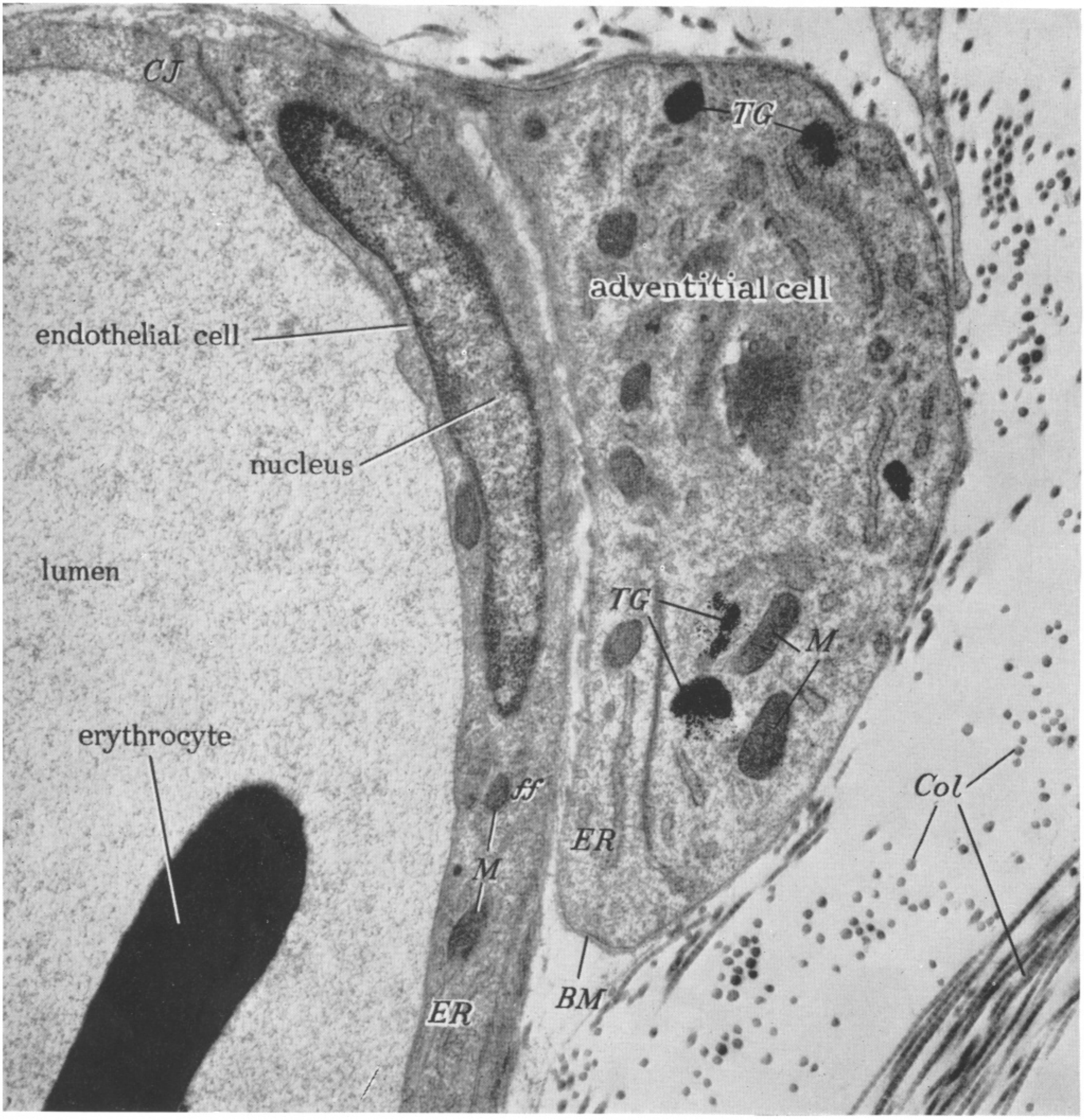

FIGURE 29. Adventitial cell lying in close relation to the endothelium of a vessel. The adventitial cell possesses a basement membrane (*BM*) and contains stored granules of Thorotrast (*TG*) in several sharply localized masses. *Col*, Collagen; *CJ*, cell junction; *ER*, endoplasmic reticulum; *ff*, fibrillary region of cytoplasm; *M*, mitochondria. Phosphotungstic acid; Araldite (×17500).

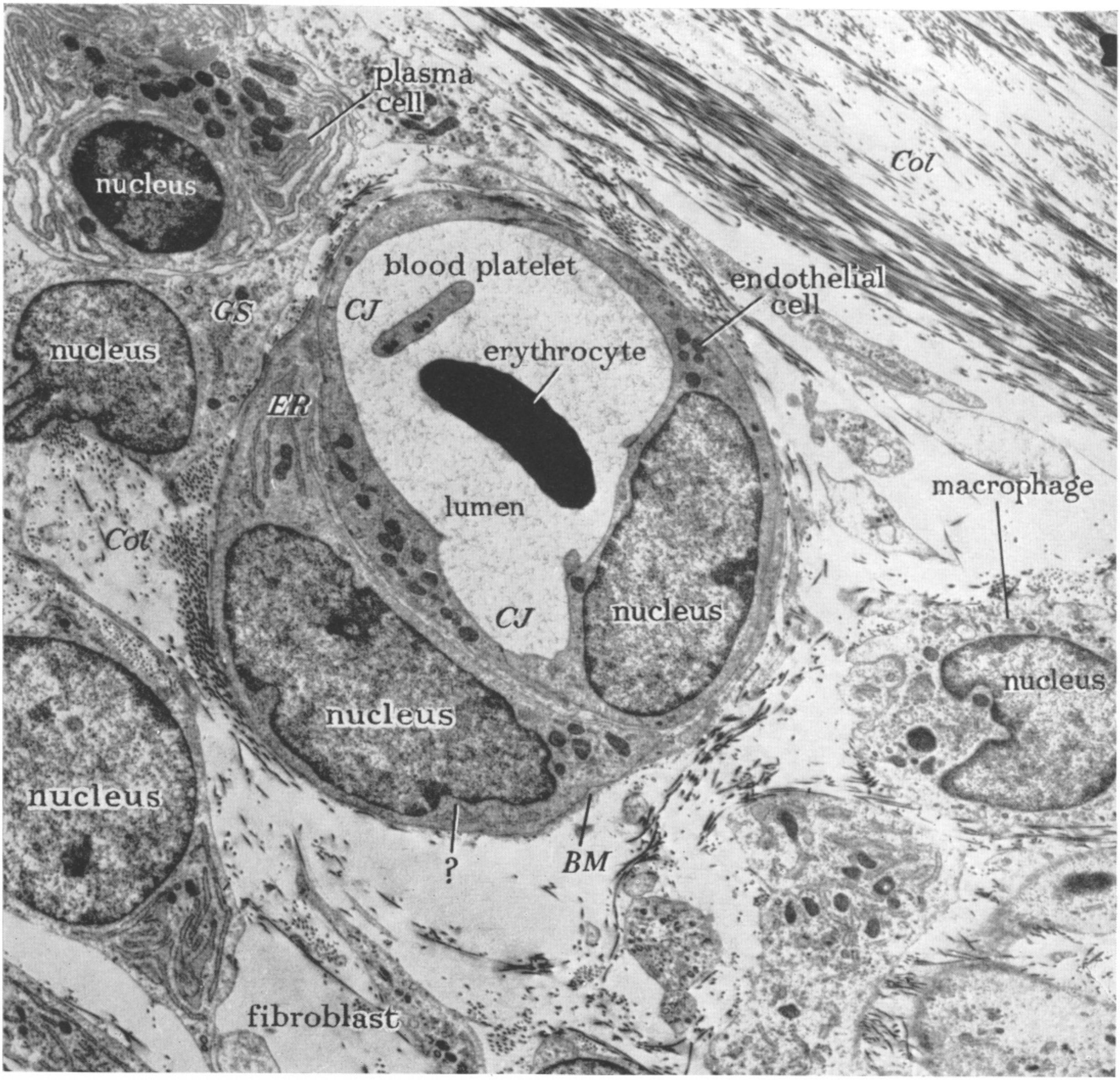

FIGURE 30. Small vessel containing an erythrocyte and platelet within its lumen. A cell marked (?) is disposed in a mainly circular orientation around this vessel (a feature of vascular smooth muscle). This cell is invested by a basement membrane (*BM*) (a feature of both smooth muscle (figure 31, plate 40) and adventitial cells (figure 29)). It possesses much endoplasmic reticulum (*ER*) and numerous mitochondria *M* and has little or no finely fibrous material in its cytoplasm (all features of an adventitial rather than a smooth muscle cell). *Col*. Collagen; *CJ*, cell junction; *GS*, Golgi substance. Phosphotungstic acid; Araldite (× 8250).

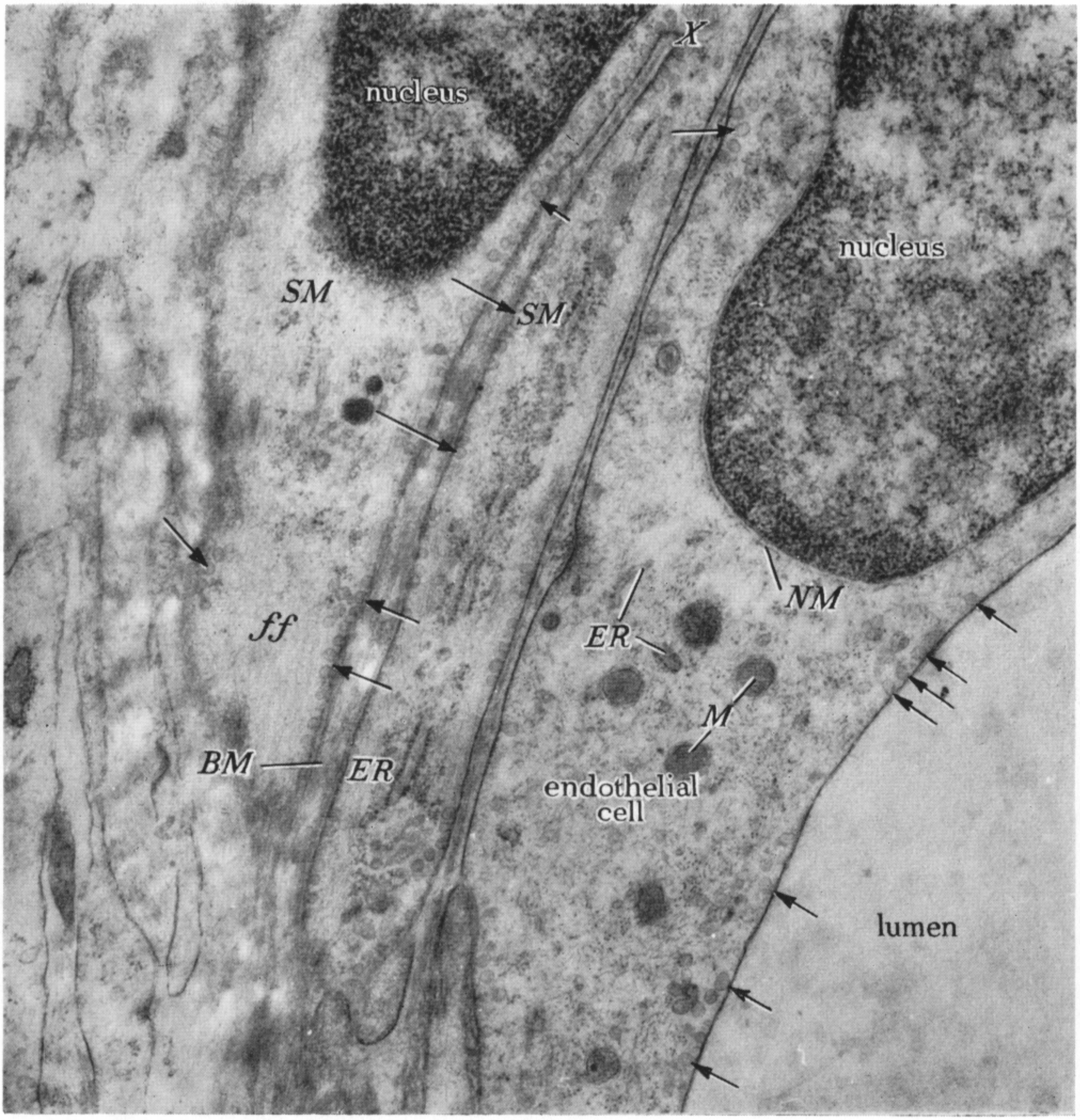

FIGURE 31. Wall of an arteriole from a chamber 7 weeks old. The two elements marked (*SM*) are parts of the same smooth muscle cell and are connected at point *X*. Features that identify smooth muscle cells are (1) a highly developed system of fine intracytoplasmic fibrils with evidence of longitudinal orientation (*ff*), (2) numerous pinocytic vesicles (arrows), (3) investment by a system of basement membranes (*BM*). *ER*, Endoplasmic reticulum; *M*, mitochondria; *NM*, nuclear membrane. Epikote 812; uranyl acetate (× 27 000).

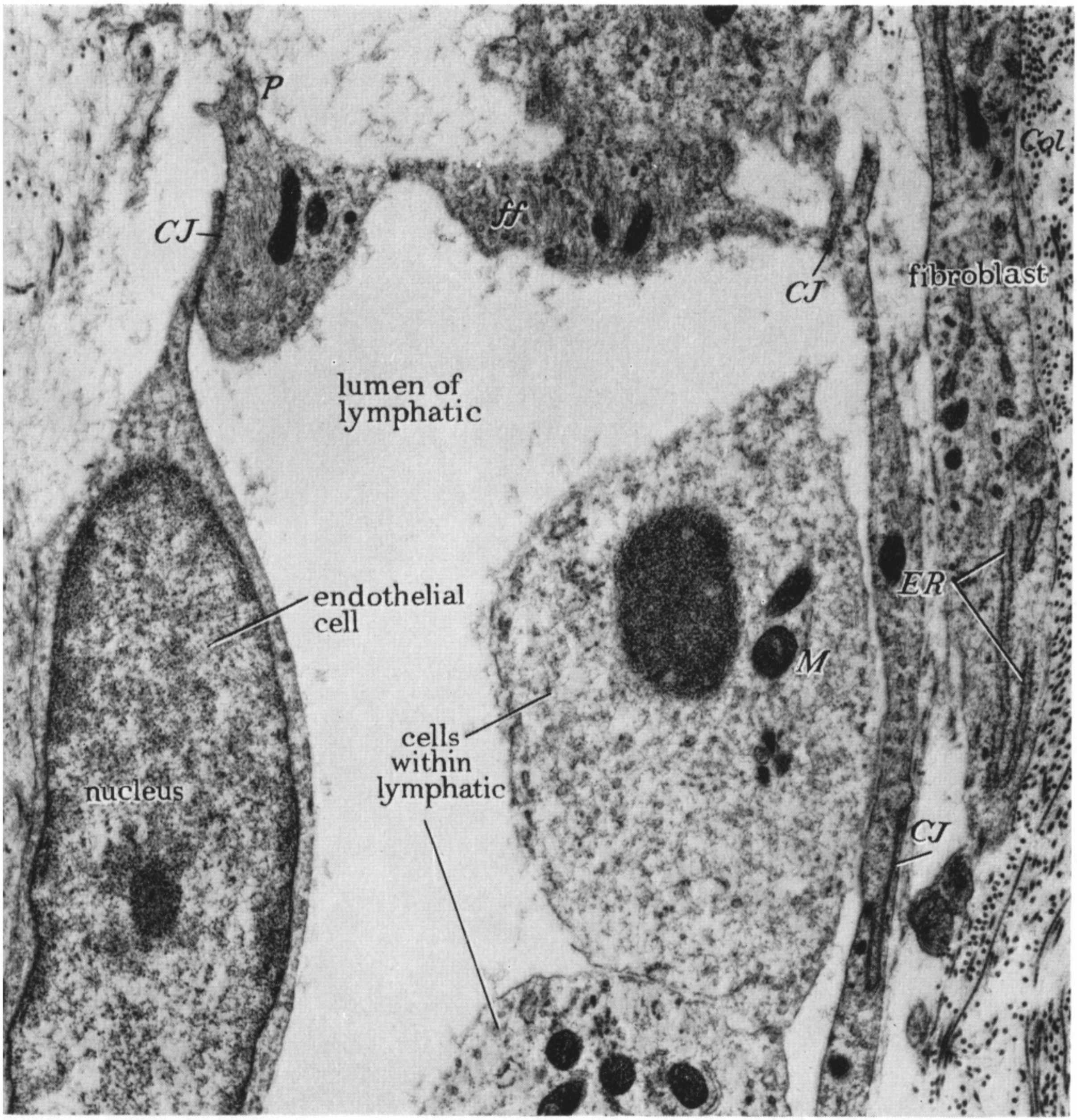

FIGURE 32. Region near the growing tip of a lymphatic vessel with walls lined by endothelium which in places is very thin. The endothelial lining possesses relatively broad based projections (*P*) extending into the extravascular space. *CJ*, Cell junction; *Col*, collagen; *ER*, endoplasmic reticulum; *ff*, fibrillary region of cytoplasm; *M*, mitochondria. Phosphotungstic acid; Araldite (× 15 000).

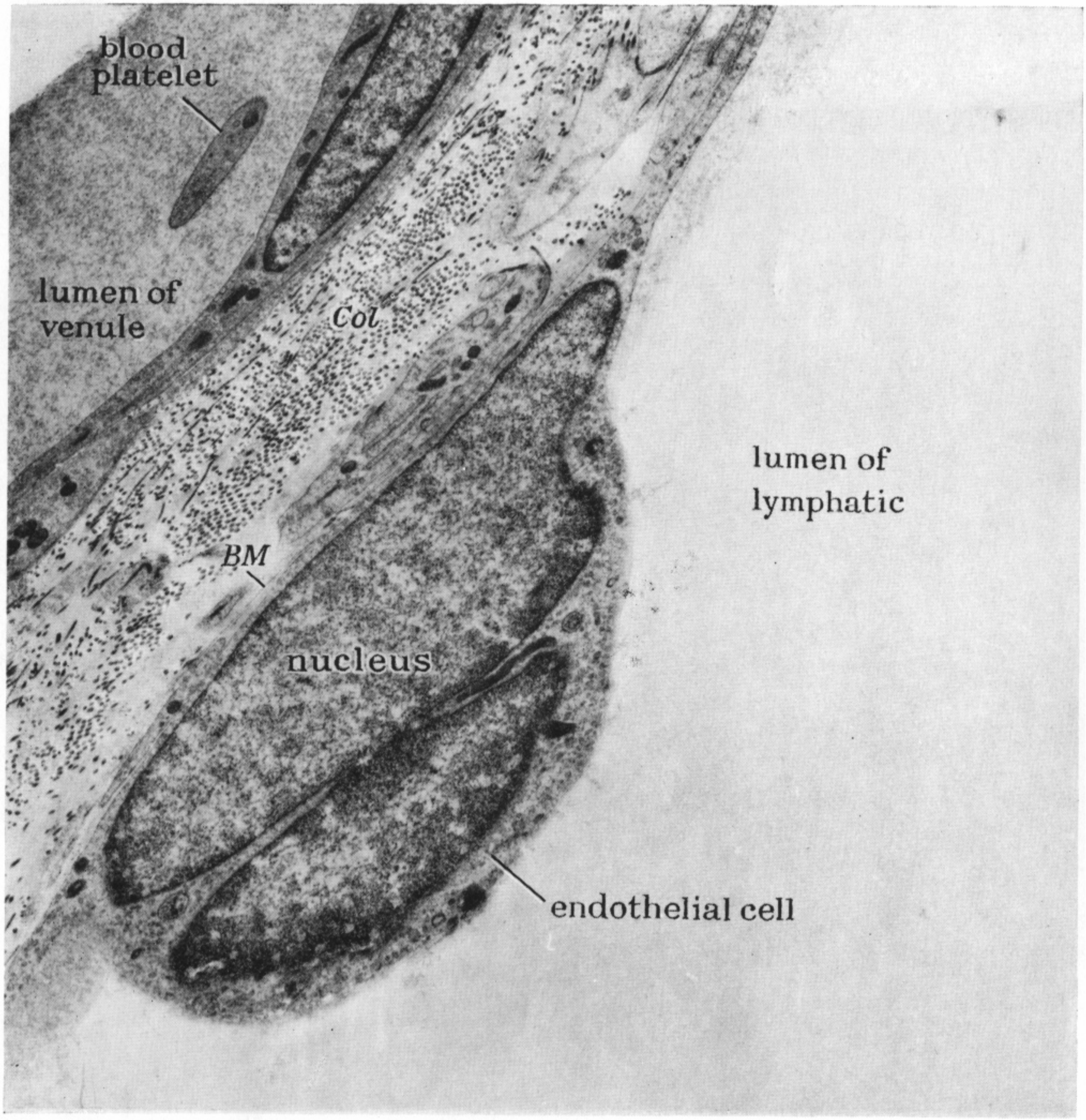

FIGURE 33. Large lymphatic and neighbouring venule from a fully healed chamber (52 days after insertion). This lymphatic had been observed for some time. Compared with that in figure 32, plate 40, the endothelium contains few organelles. The nucleus projects into the lumen. The basement membrane (*BM*) is poorly developed compared to that of a blood vessel of the same calibre. *Col*, Collagen. Phosphotungstic acid; Araldite (× 9750).

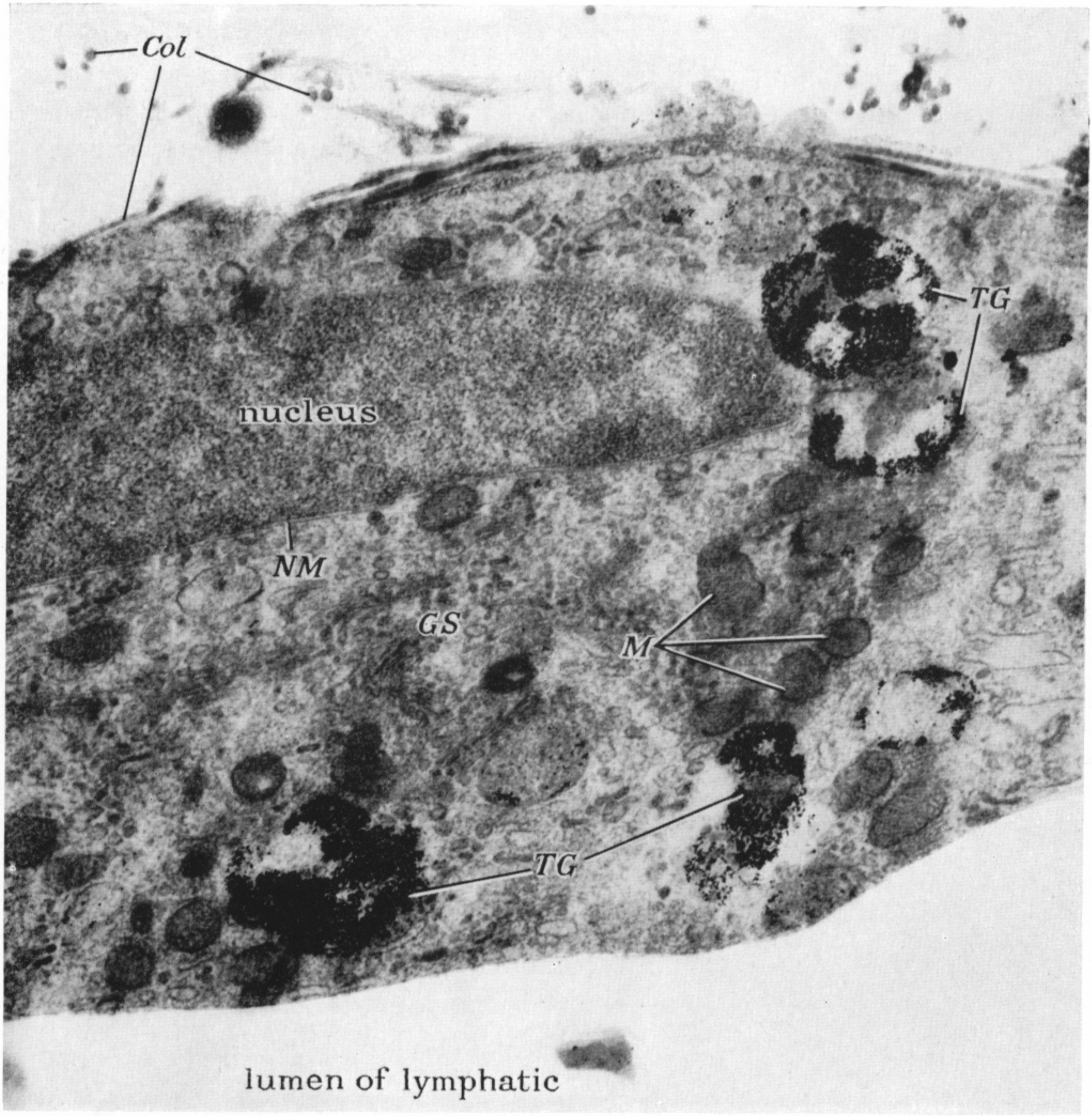

FIGURE 34. Wall of a lymphatic vessel from an ear chamber that had been fully healed for 2 months before a series of Thorotrast injections was begun. Oval clumps of Thorotrast granules (*TG*) are numerous in the endothelial cytoplasm. Note absence of basement membrane. *Col*, Collagen; *GS*, Golgi substance; *M*, mitochondria; *NM*, nuclear membrane. Phosphotungstic acid; Araldite (× 25 500).

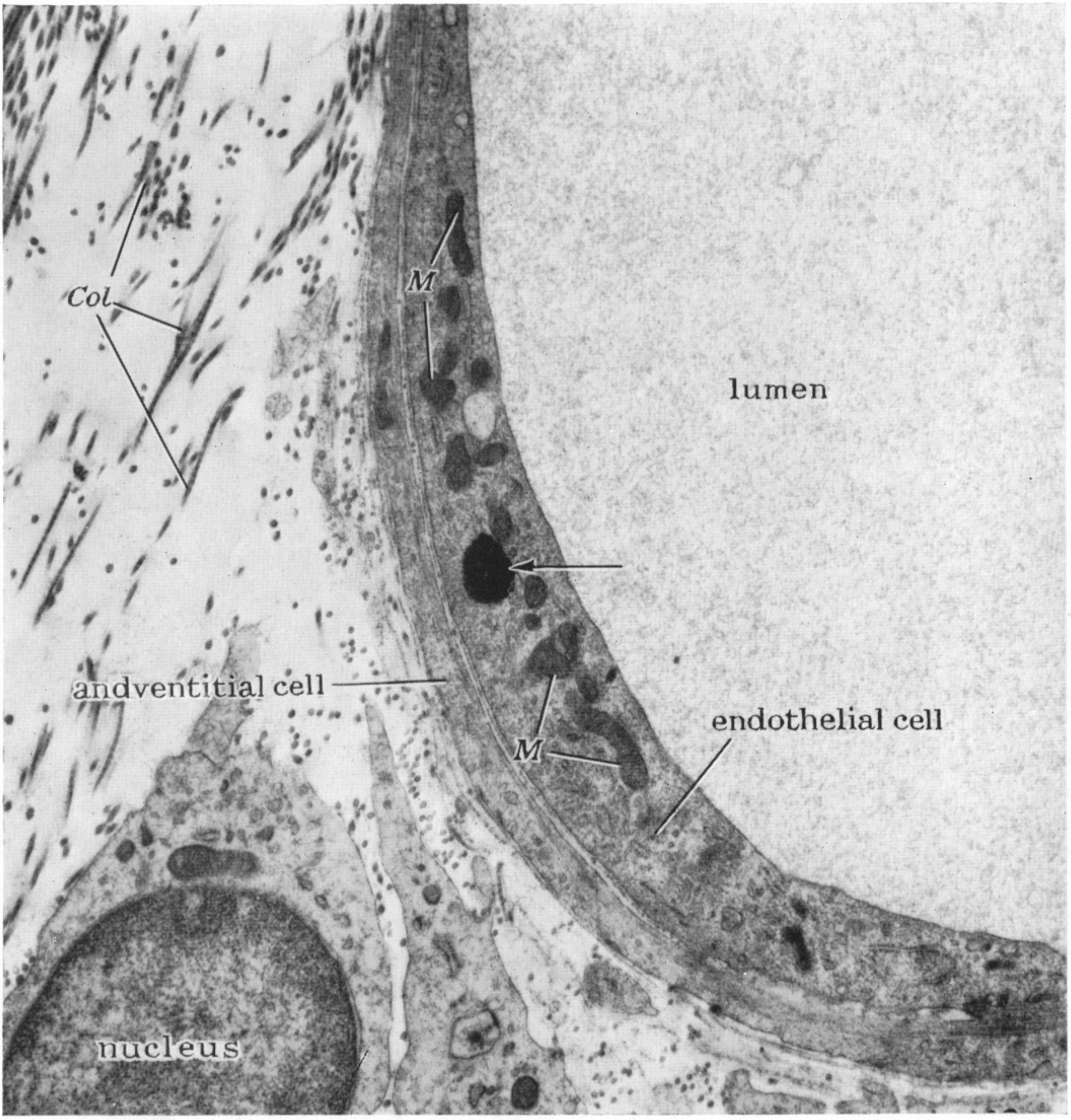

FIGURE 35. Venule from the same chamber as figure 34, plate 41. Within the endothelium is a single clump of Thorotrast granules (arrow). *Col*, Collagen; *M*, mitochondria. Phosphotungstic acid; Araldite (× 16 500).

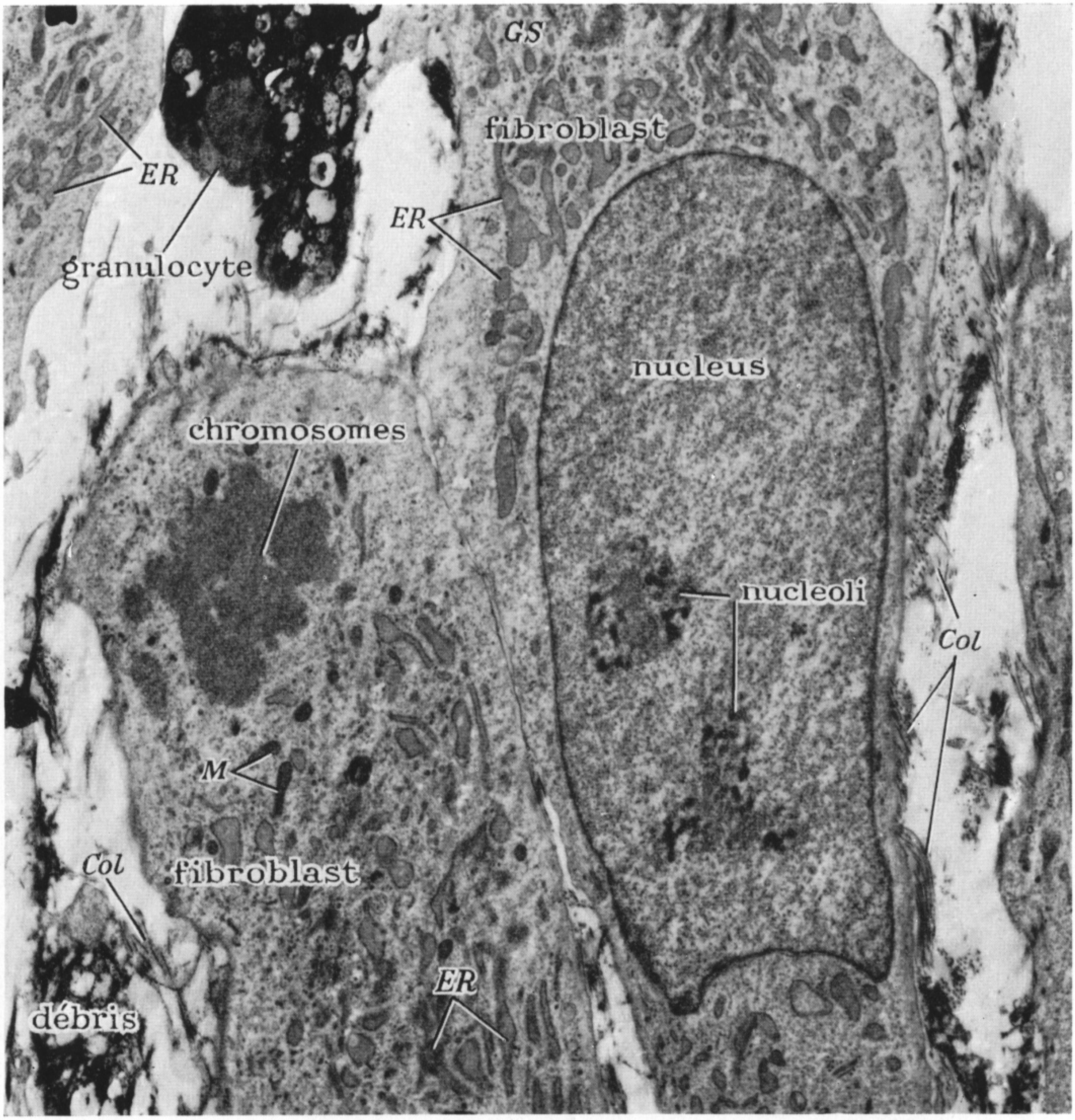

FIGURE 36. Fibroblasts invading fibrin clot and débris. The cell on the left is in mitosis (telophase) and the chromosomes may be recognized. The fibroblast on the right has an elongated nucleus with two well-developed 'skein-like' nucleoli. The granulocyte shows evidence of necrosis (loss of cytoplasmic detail, increased osmiophilia). *Col*, Collagen; *ER*, endoplasmic reticulum; *GS*, Golgi substance; *M*, mitochondria. Phosphotungstic acid; Araldite ($\times 8250$).

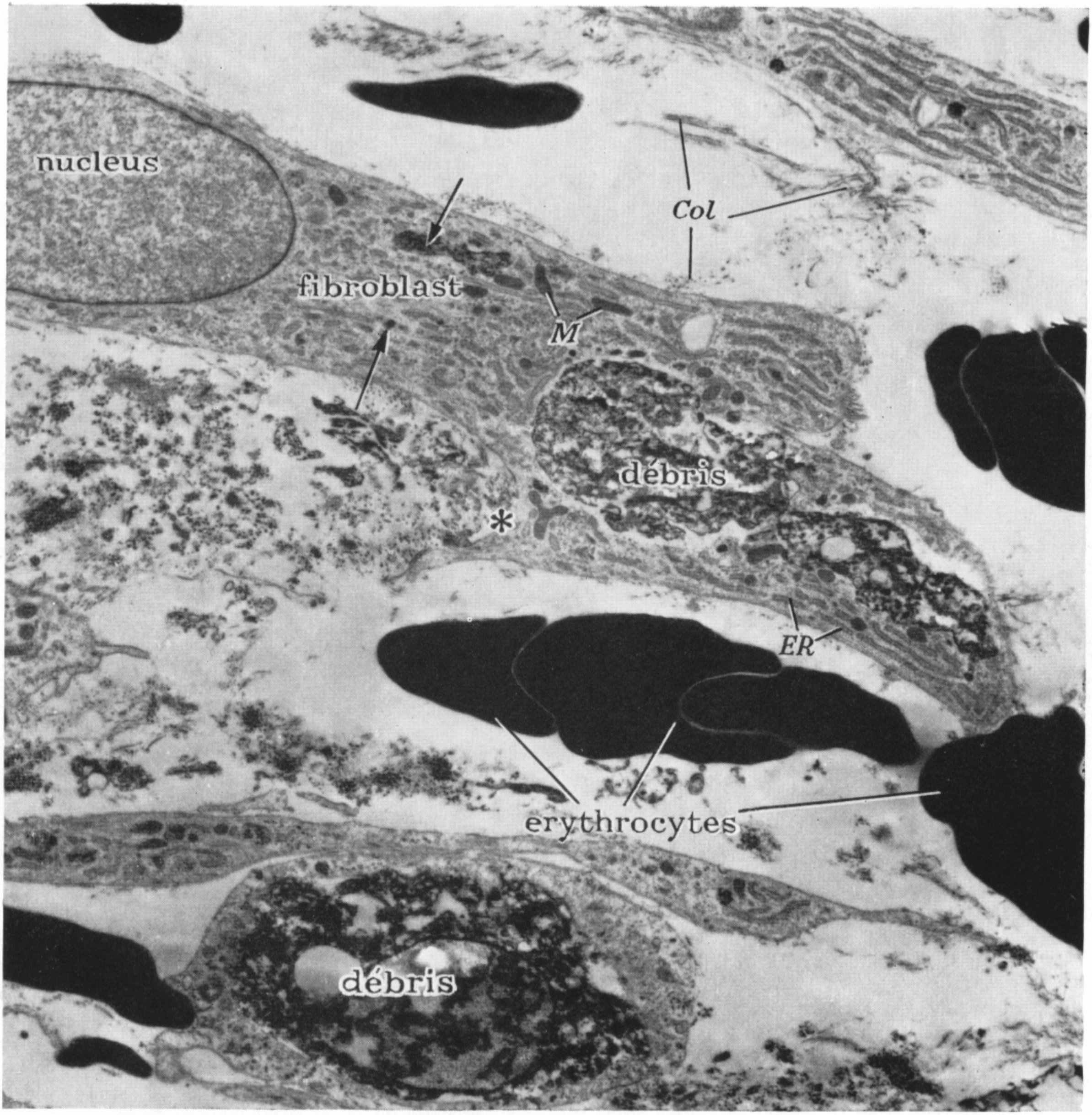

FIGURE 37. Several cells invading a region of haemorrhage and debris. A fibroblast is present with nucleus, well-developed endoplasmic reticulum (*ER*) and numbers of mitochondria (*M*) (one of which (*) is trefoil in shape). This cell has a variety of inclusions in its cytoplasm (arrows) and appears to be encircling a large clump of debris. *Col*, Collagen. Phosphotungstic acid; Araldite(× 8000).

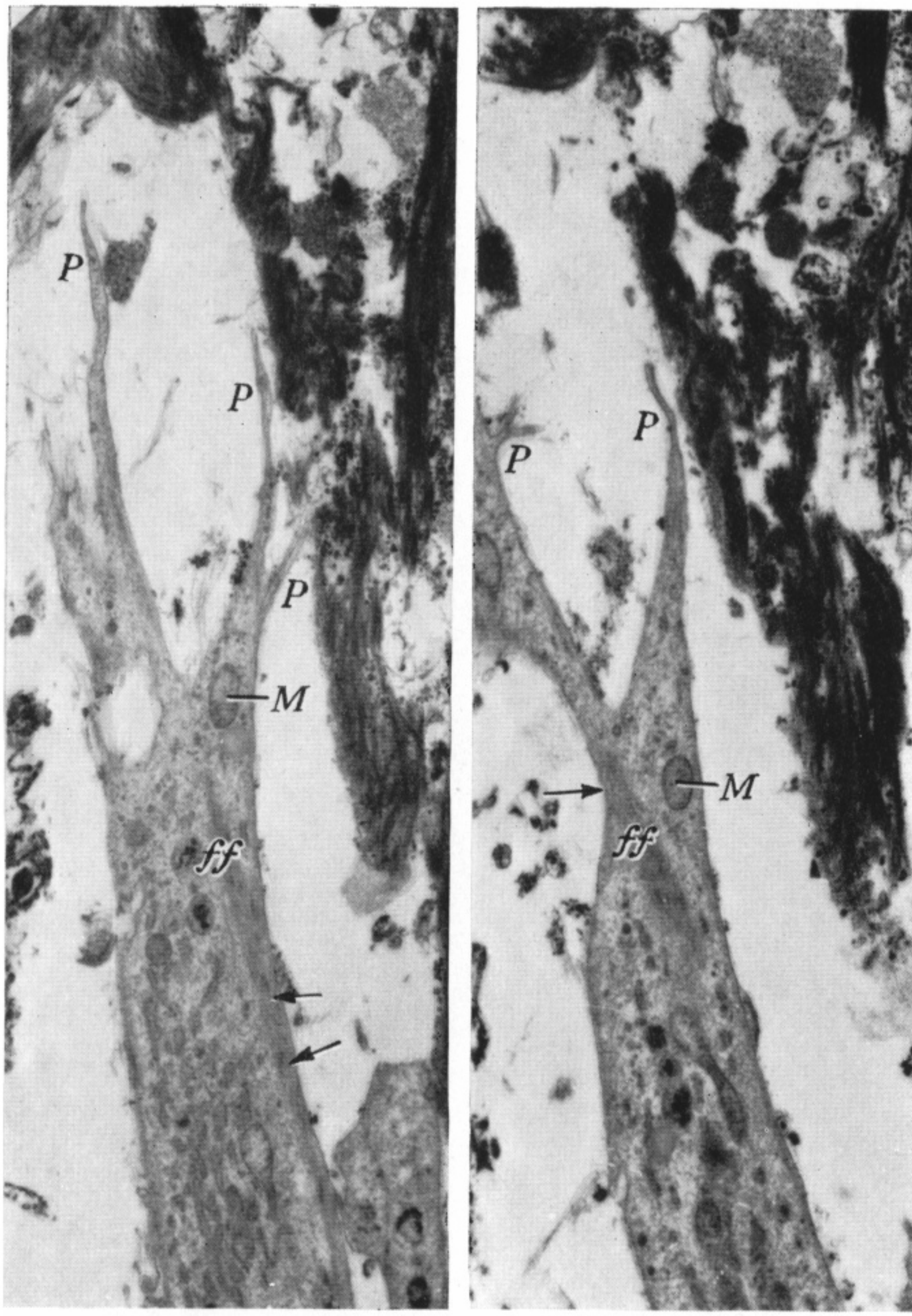

a *b*

FIGURE 38 *a*, *b*. Two sections through the same fibroblast at different levels. It contains a sharply defined fibrillary region (*ff*) 0·4 μm in width which would be an optically visible structure. By comparing the two figures the fibrillary tract may be traced as a bundle running into one of the fine processes of the fibroblast (*P*). This tract is considered to correspond to a 'fibroglial' fibre of Mallory. Arrows indicate regions of coalescence of fibrils. *M*, mitochondrion. Phosphotungstic acid; Araldite ($\times$ 6500).

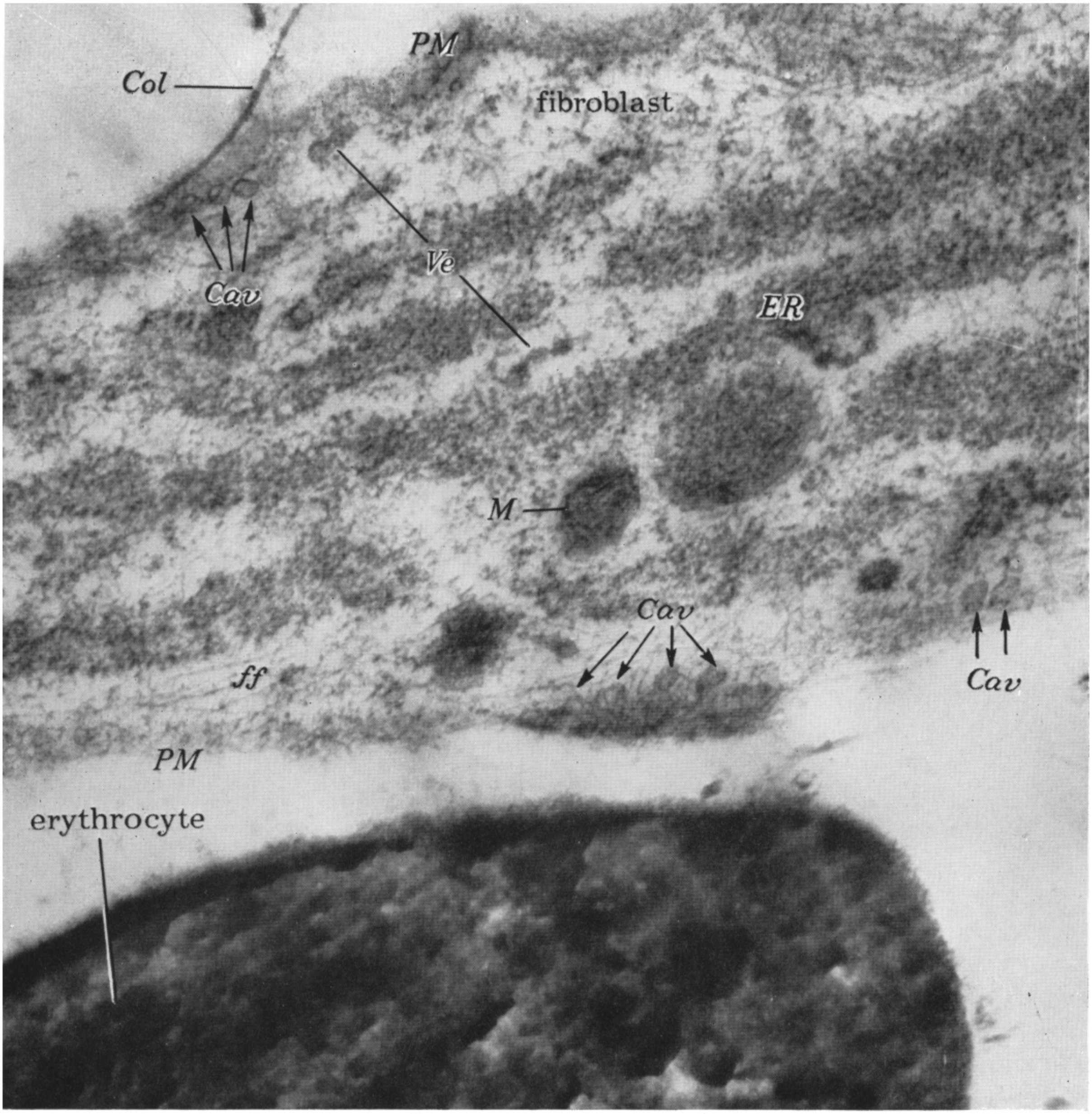

FIGURE 39. Part of a fibroblast and an erythrocyte. Medium-sized vesicles (*Ve*) and caveolae (*Cav*) are indicated by arrows at the plasma membrane (*PM*) of the fibroblast. These structures are very similar in appearance to the vesicles closely related to the endoplasmic reticulum in figure 40. The diameter of the vesicles in this micrograph is 54·5 nm. The vesicles and caveolae are most numerous at regions where fibrillar and collagenous material (*Col*) are related to the plasma membrane (*PM*) of the fibroblast. *ER*, Endoplasmic reticulum; *M*, mitochondrion; *ff*, fibrillary elements of cytoplasm. Phosphotungstic acid; Araldite (× 46 000).

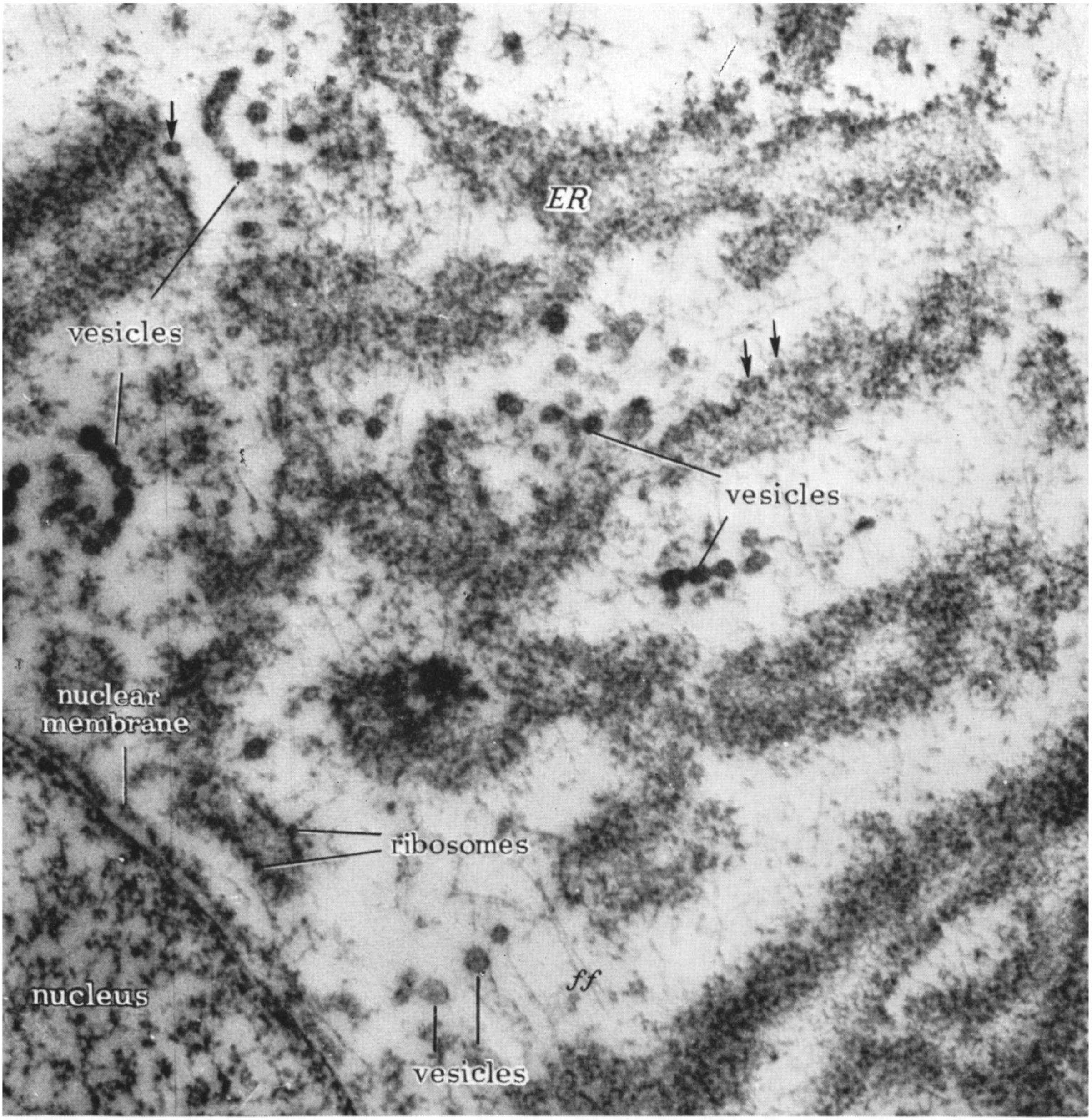

FIGURE 40. Juxtanuclear region of a fibroblast in healing tissue. Numbers of vesicles are present, some of which (arrows) appear to be budding from the endoplasmic reticulum (*ER*). These vesicles are up to 54·5 nm in diameter and are bounded by dense membranes. Their contents are of moderate electron density. They are dispersed singly, in clusters and in strings through the cytoplasm. *ff*, Fibrillary component of cytoplasm. Phosphotungstic acid; Araldite (× 46 000).

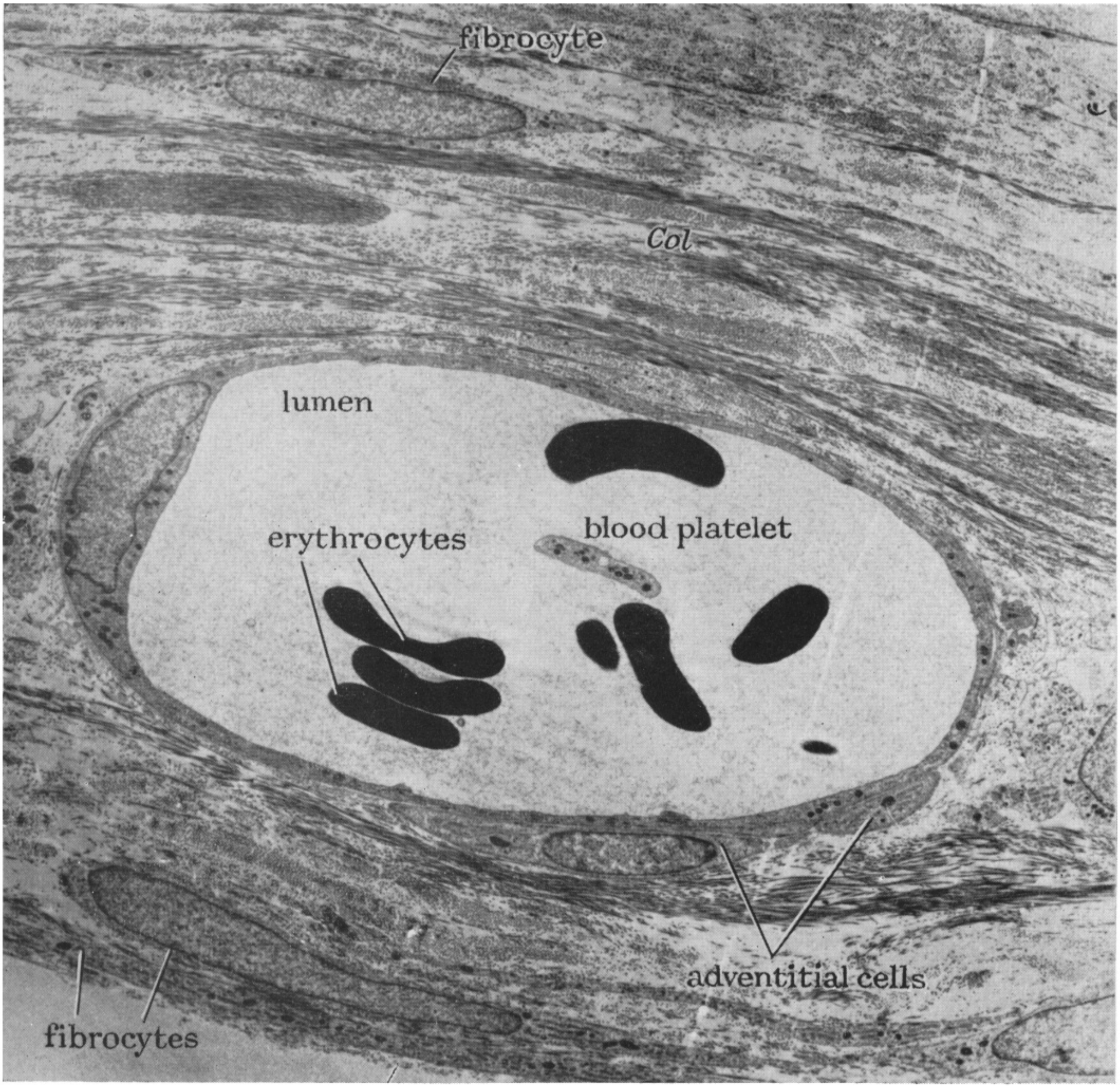

FIGURE 41. Mature venule of scar tissue. Adventitial cells are shown. Dense lamellae of collagen (*Col*) are present in the extravascular regions together with elongated fibrocytes. Phosphotungstic acid; Araldite ($\times 3500$).

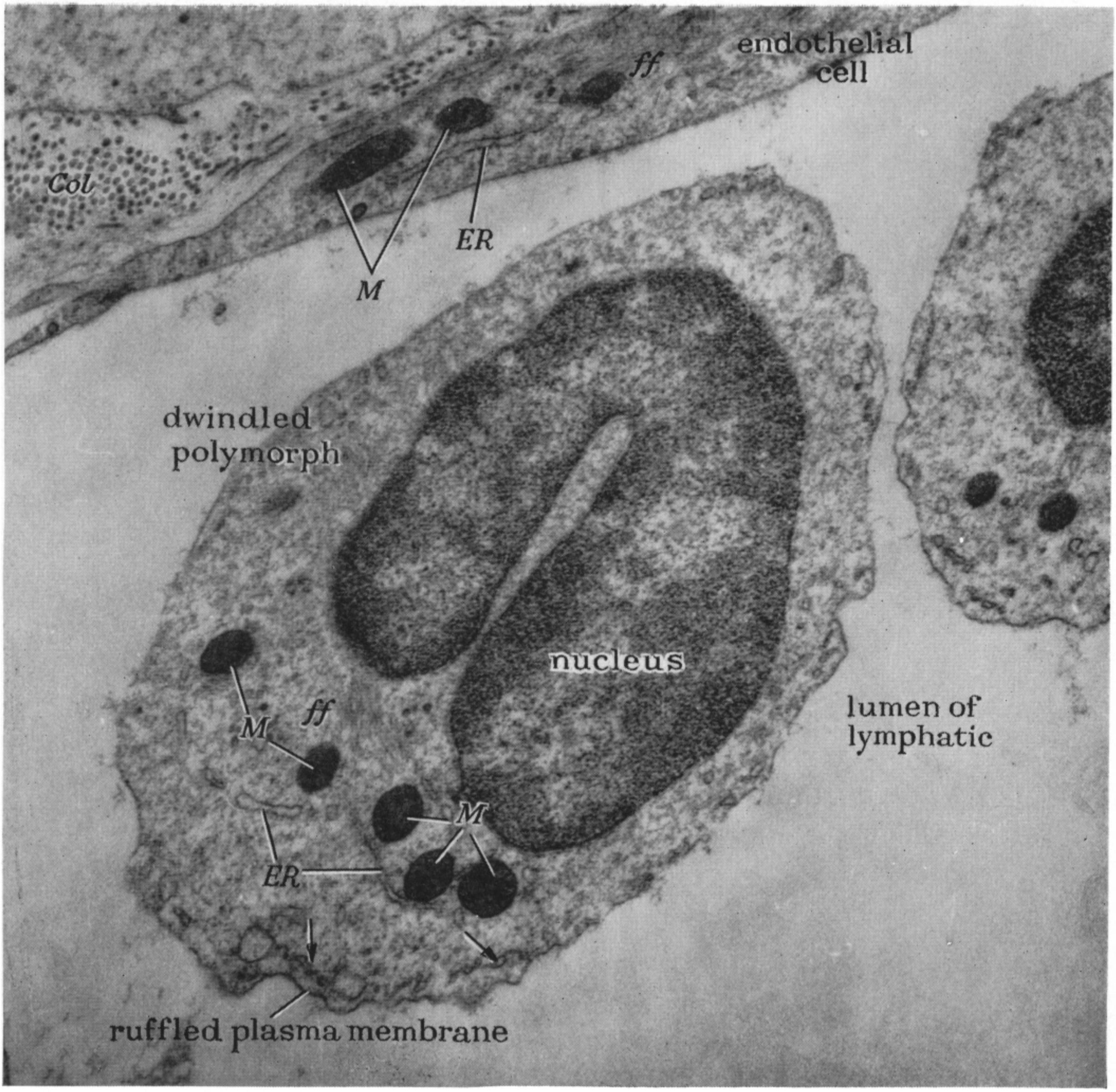

FIGURE 42. Dwindled polymorph, the 'small round cell' of Clark *et al.* (1936), in the lumen of a lymphatic vessel. *ER*, Endoplasmic reticulum, which in the dwindled polymorph can be seen as lines of pinched off vesicles (arrows) apparently formed by the fusion of the 'ruffled' plasma membrane. *ff*, Fibrillary region of cytoplasm; *Col*, collagen; *M*, mitochondria. Phosphotungstic acid; Araldite (× 18 000).

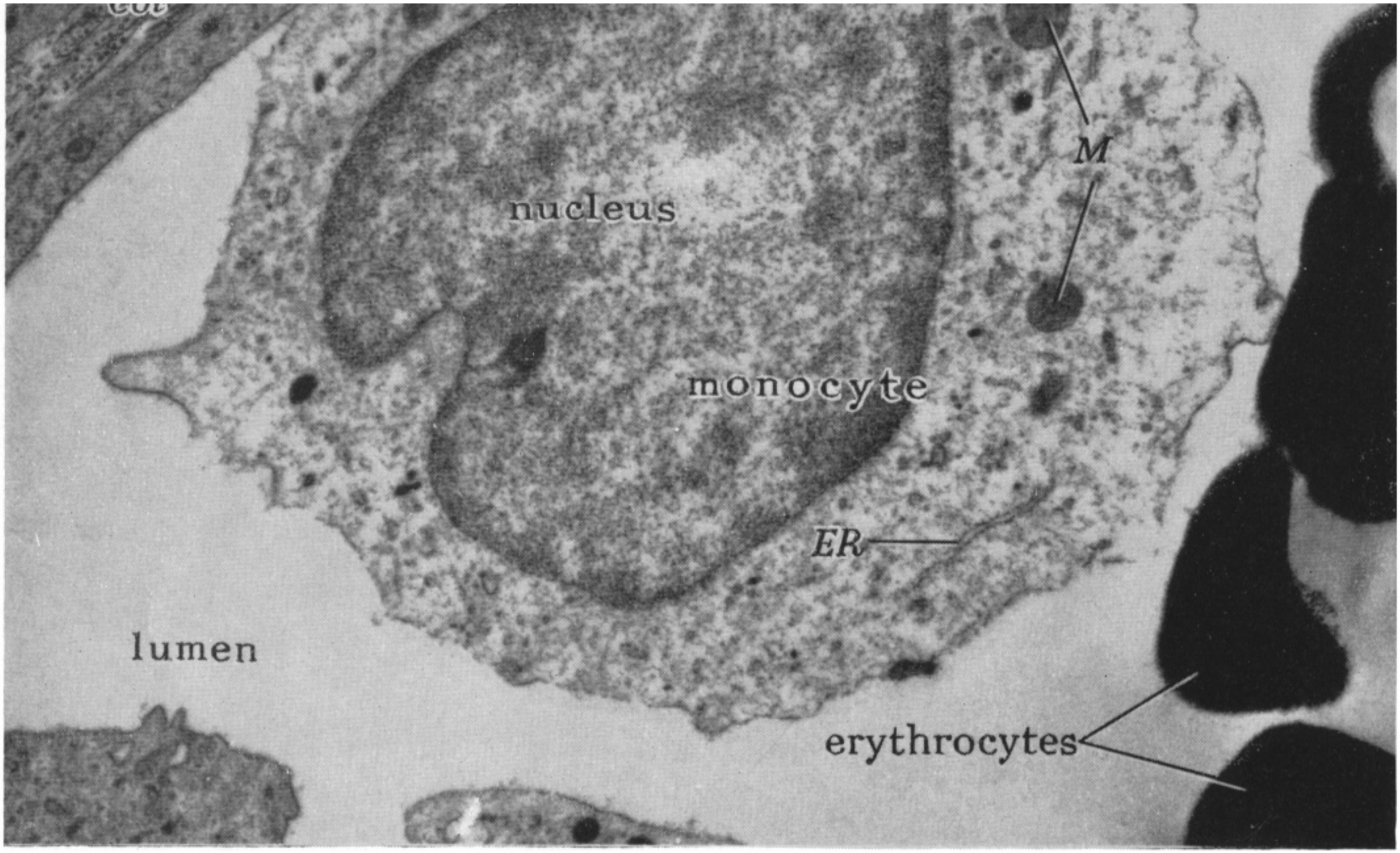

FIGURE 43. A monocyte adhering to the endothelium of a blood vessel. The arrows indicate two small pseudopodia very closely related to cell junctions (*CJ*). *Col*, Collagen; *ER*, endoplasmic reticulum; *G*, dense granules in monocyte cytoplasm; *M*, mitochondria. Phosphotungstic acid; Araldite (× 14 000).

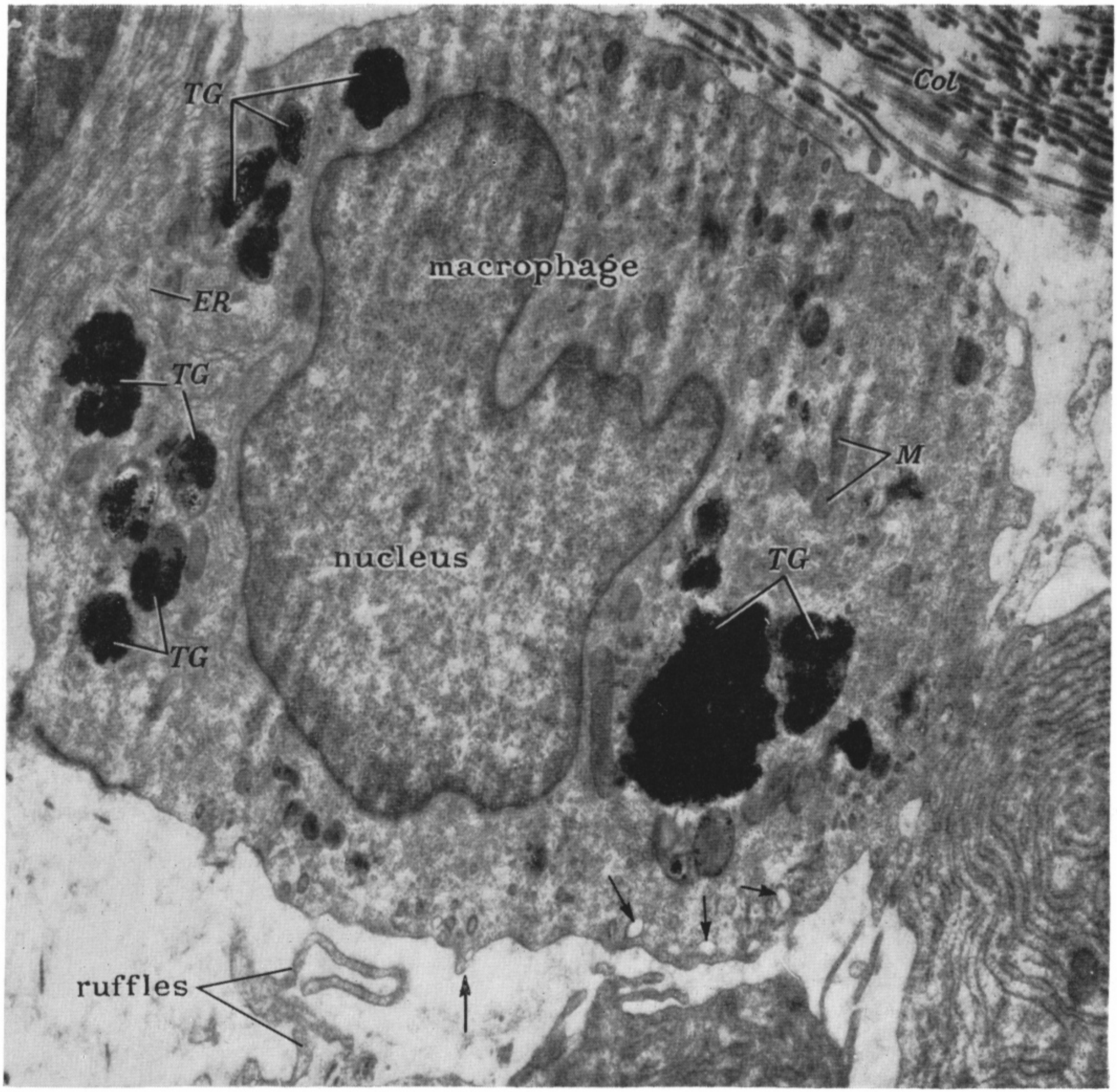

FIGURE 44. Small macrophage with large quantities of Thorotrast (*TG*) segregated within its cytoplasm. Ruffled extensions of the cell give rise, through fusion, to membrane-bounded vesicles (arrows). *Col*, Collagen; *ER*, endoplasmic reticulum; *M*, mitochondria. Phosphotungstic acid; Araldite (× 16 500).

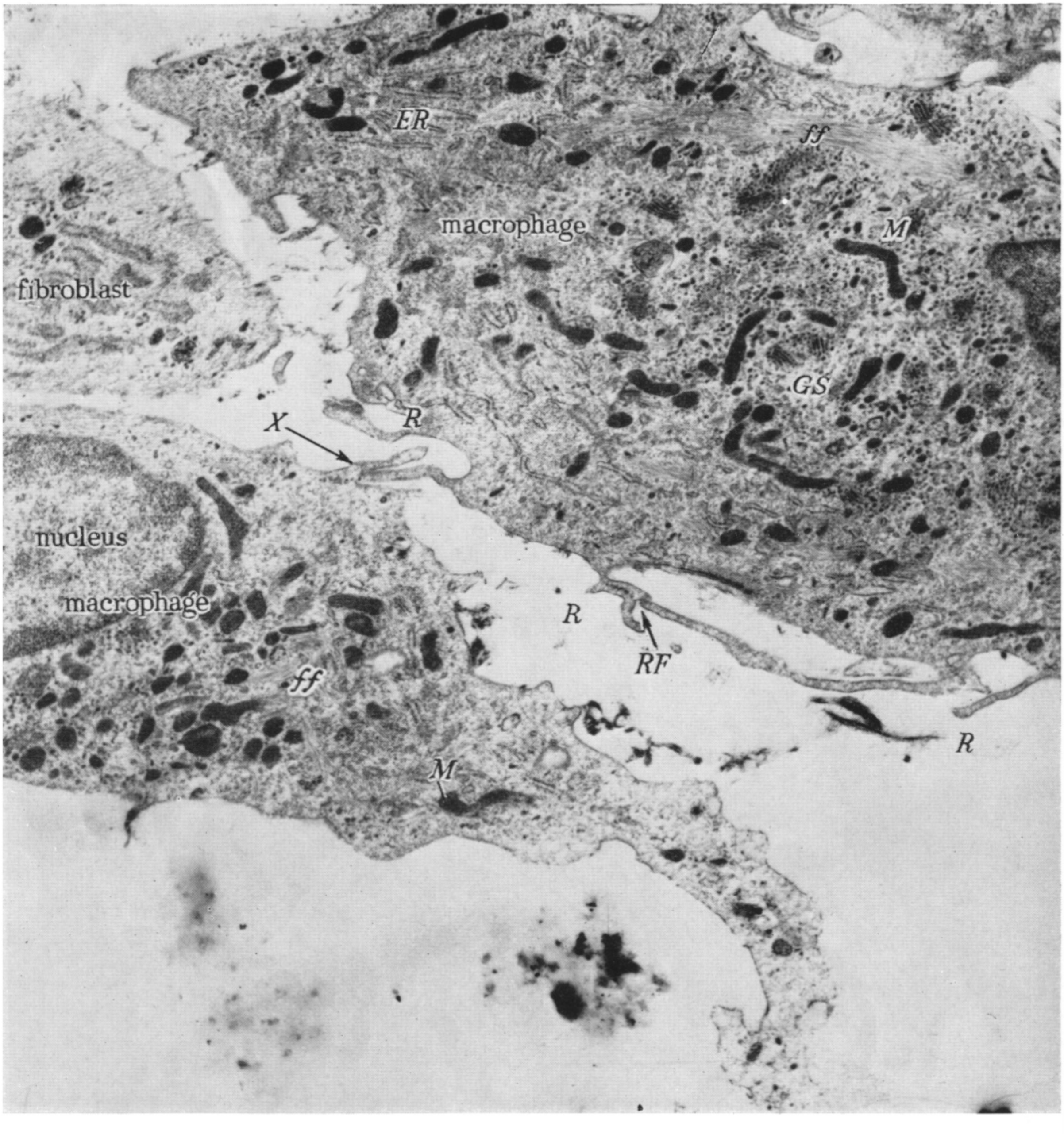

FIGURE 45. Parts of 2 macrophages and 1 fibroblast. The surfaces of the macrophages are thrown into a complex series of folds or 'ruffles' (*R*). Two elements of the ruffled border show fusion of their apposed surfaces at *RF*. At *X* ruffles belonging to the two different macrophages are in extremely close proximity and are almost joined. Highly fibrillary tracts (*ff*) curve through the cytoplasm; they measure up to 0·4 μm in width, and therefore may correspond to optically visible regions of the cells. The endoplasmic reticulum of the macrophages shows signs of orientation (e.g. at *ER*). *GS*, Golgi substance; *M*, mitochondria. Phosphotungstic acid; Araldite ($\times$ 11 000).

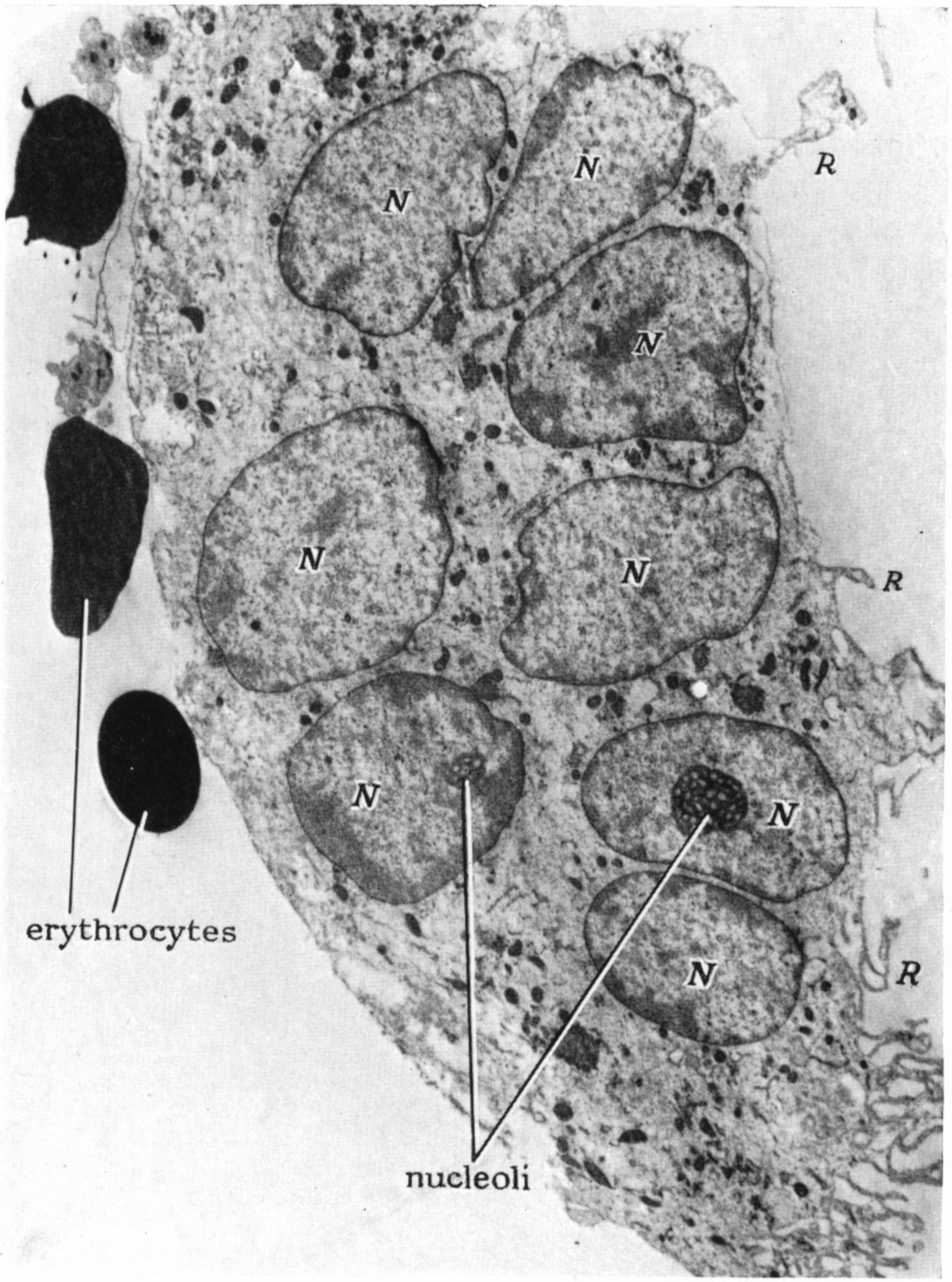

FIGURE 46. A multinucleate giant cell, with adjacent erythrocytes. The giant cell has 8 polygonal nuclei (*N*) in this section. Nucleoli are identified in two of the nuclei and are well-developed mesh-like structures. The diameter of the larger nucleolar profile is 1·5 μm. The surface of the giant cell is thrown into a complex series of ruffles (*R*). Phosphotungstic acid; Araldite ($\times$ 5500).

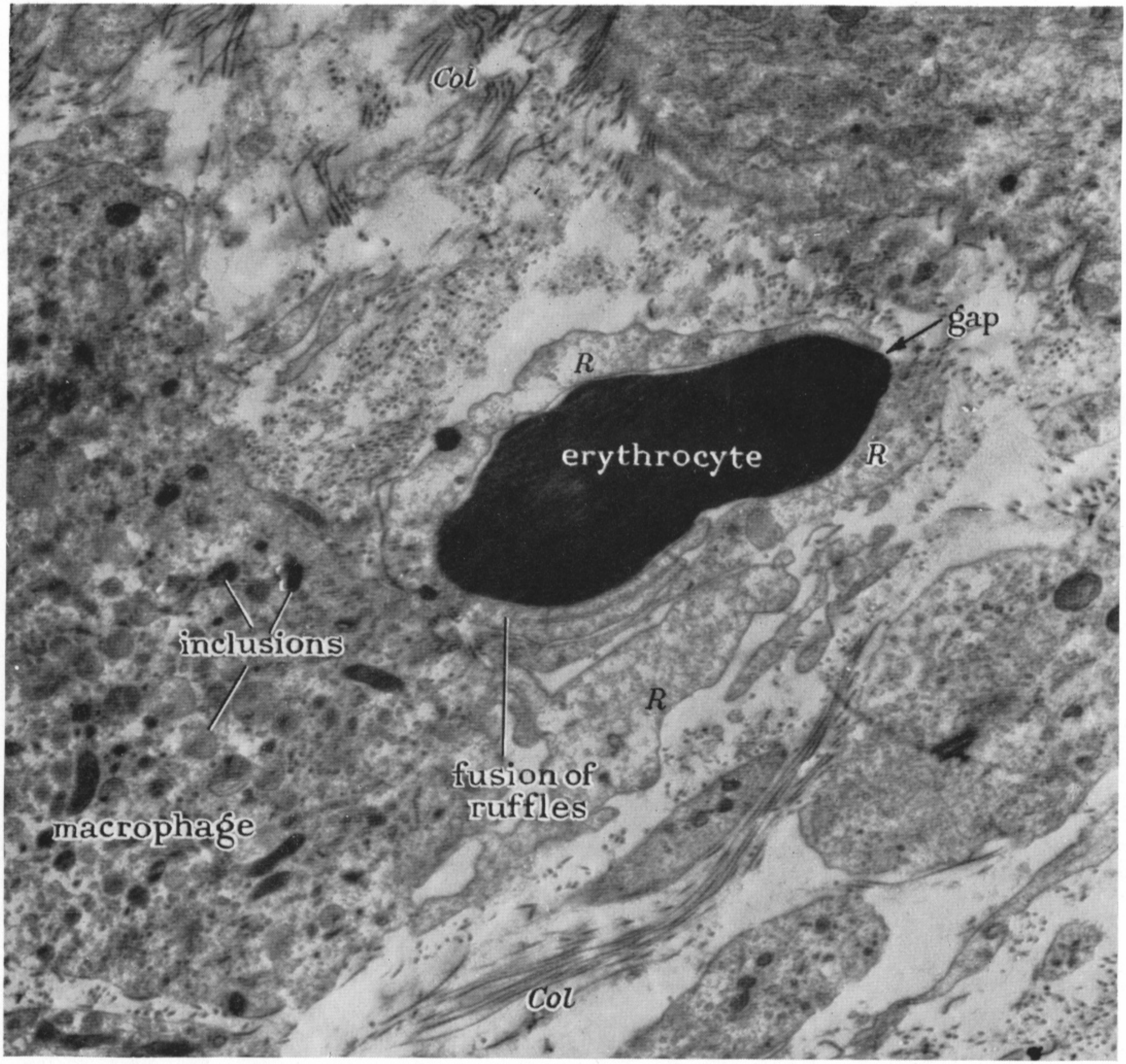

FIGURE 47. A macrophage which contains numerous pleomorphic inclusions and the cytoplasm of which extends into a number of ruffled pseudopodia (*R*). An erythrocyte is enclosed by several of these ruffles except for a small gap. The ruffles enclosing the erythrocyte show evidence of fusion of apposed surfaces. The end of the process would be fusion of the tips of the ruffles across the gap, and the erythrocyte would then be contained in a membrane-bounded cavity within the macrophage. *Col*, Collagen. Phosphotungstic acid; Araldite (× 13 500).

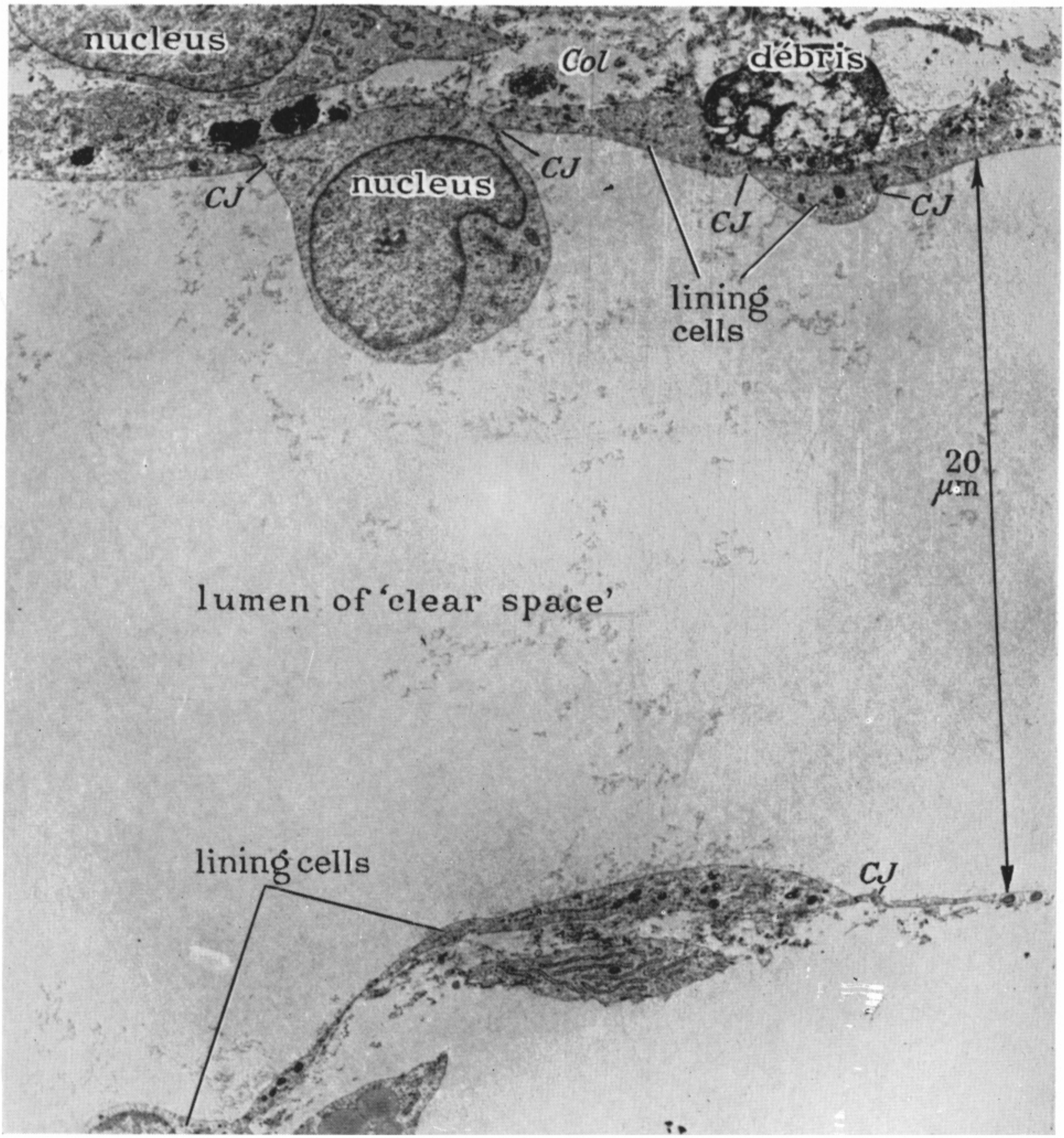

FIGURE 48. Section through part of a 'clear space' in advance of the growing fringe of vessels (see figure 10, plate 29). Collagen fibres (*Col*) and cell débris are present in relation to the wall of the 'clear space', which is lined by a continuous pavement of flattened cells closely abutting edge to edge (*CJ*). There is no related basement membrane. The smallest dimension of this structure (between arrows), measured in the same direction as the depth of the ear chamber is 20 μm. Phosphotungstic acid; Araldite ($\times 4000$).